Classical and quantum aspects of topological solitons: (using numerical methods)

Weidig, Tom

Classical and Quantum Aspects of Topological Solitons

(using numerical methods)

Tom Weidig

Centre for Particle Theory

Department of Mathematical Sciences

Thesis presented for the Degree of Doctor of Philosophy

at the University of Durham

August 1999

To the memory of my grandparents

Preface

After 23 years of formal education, I hereby present my PhD thesis. I cannot deny that it took me a rather long time to get close to the forefront of knowledge and research. When I was very, very young, I thought my parents knew everything. When I was very young, my primary school teachers knew everything. When I was young, my secondary school teachers knew everything. Not long ago, doctors and professors knew everything. Now, I think no-one knows everything–a frightening but liberating thought.

Let me take the opportunity to thank some people. First of all, I want to thank my parents, Gilles, Revel, Monni Paul, Boma Olga and the rest of the family for their moral and financial support. Without their help, everything would have been much harder. Of course, I am grateful to my supervisor Wojtek Zakrzewski for his encouragement and efforts. Many thanks also go to Bernard Piette for computer code and answering my questions in a very Belgian way. I thank all the people who attended the Tuesday seminars, the people from the CPT group in Physics and Maths and the Mathematical Sciences for making my stay an enjoyable one. And I am grateful to my former supervisors Lewis Ryder and Chris Isham for guidance and inspiration.

I acknowledge the receipt of a Durham Research Award, financial support from the department to attend summer schools and a 'bourse universitaire' from the government of Luxembourg.

Last but certainly not least, I thank all my fellow PhD students in Physics and Maths. I

hope I don't forget someone, in no order of preference: Ricardo for many New Inn lunches and for telling me that Luxembourg will soon be a province of Portugal, Matt C. for letting me save your plant, Karate Kid Matt S., John C. pardon Bierhoff, John O., Mark for his collaboration and his computer enthusiasm, Laur for being a true intellectual theoretical physicist in the continental sense, Sabine, Clare L. for inviting me and Kelly to her wedding, Matthias for being a nice guy, Anja for good disco dancing, Steve for being a cheeky bastard, Alan for 'wasting' our time chatting, Imran for his curiosity, Lars for insulting my country and winning 6-0 6-0 in tennis, Sharry for his X-mas party performance, Patrick, David B., Clare for being very nice, Linda, Stuart, Vinay, Medina, Filipe, Owen for showing off his finger, Justin, Iannis and his combat trousers, Wajdi from Libya, Gavin, Pete M., David for being very Cambridge-like, Nuno for extraordinary paintballing skills, Michael, Caroline, Georgios, Billie for winning one chess game (out of 10), Jeppe, Ramòn and Pete for being Pete and many others.

Declaration

This thesis builds on the course taken by the author in elementary particle physics from October 1996 to April 1997 and summarises the research work undertaken from May 1997 to July 1999; both at the Centre for Particle Theory at the department of Mathematical Sciences at the University of Durham, England. No part of this work has been previously submitted for any degree at any university.

Chapter 1 and 2 are reviews on solitons and numerical methods. Most of the computer codes have been written by the author and I acknowledge the use of some routines written by Bernard Piette. Chapter 3 and 4 is believed to be orginal work, unless stated. The research work on the structure of multi-skyrmions orginates from a paper submitted and accepted for publication in *Nonlinearity*. The implementation of the Simulated Annealing scheme has been done in cooperation with Mark Hale.

We adopted the convention to write names with a capital letter and words derived from names with lower letters e.g. the Skyrme model and skyrmions or the Lagrange multiplier and the lagrangian.

Abstract

Classical and Quantum Aspects of Topological Solitons
PhD thesis by Tom Weidig, August 1999

In *Introduction*, we review integrable and topological solitons. In *Numerical Methods*, we describe how to minimise functionals, time-integrate configurations and solve eigenvalue problems. We also present the Simulated Annealing scheme for minimisation in solitonic systems.

In *Classical Aspects*, we analyse the effect of the potential term on the structure of minimal-energy solutions for any topological charge n. The simplest holomorphic baby Skyrme model has no known stable minimal-energy solution for $n > 1$. The one-vacuum baby Skyrme model possesses non-radially symmetric multi-skyrmions that look like 'skyrmion lattices' formed by skyrmions with $n = 2$. The two-vacua baby Skyrme model has radially symmetric multi-skyrmions. We implement Simulated Annealing and it works well for higher order terms. We find that the spatial part of the six-derivative term is zero.

In *Quantum Aspects*, we find the first order quantum mass correction for the ϕ^4 kink using the semi-classical expansion. We derive a trace formula which gives the mass correction by using the eigenmodes and values of the soliton and vacuum perturbations. We show that the zero mode is the most important contribution. We compute the mass correction of ϕ^4 kink and Sine-Gordon numerically by solving the eigenvalue equations and substituting into the trace formula.

Contents

Chapter 1

Introduction

> "Today I looked out of my window: someone was watering the lawn. He was pulling a garden hose behind him. This created a rather strange impression. It was very bright outside and the green hose, moving through the green grass like a snake, wasn't visible at times. But then, at times, I did see it: I saw the knots in the hose that were moving like balls along the grass following an invisible, mysterious force. I found this rather curious. These knots were behaving like independent particles. Could it be that elementary particles are knots in some medium which we don't see???"
>
> *(diary entry, July 1992)*

It does not quite match J. Scott Russell's heroical horse ride along the Edinburgh-Glasgow canal and his subsequent discovery of solitary waves. Nevertheless, my diary entry dating back to 1992 comes amazingly close to the main leitmotiv of my PhD thesis seven years later: the study of objects arising from a non-trivial topology and their application to particle physics. We call these objects topological solitons. They are solutions of non-linear partial differential equations (PDEs) which are derived from a lagrangian system with non-trivial topology. The

literature defines a solitary wave as a localised finite-energy field configuration (a lump of energy) that travels without dispersion. And, solitons are those solitary waves that can pass through each other and retain their shape. Strictly speaking, our topological 'solitons' do not possess this property, rather they scatter at 90 degrees or form more complicated configurations. Thus, they are solitons in the sense that they keep to a localised configuration(s) after collisions; apart from annihilation processes. Most of these non-linear PDEs prove impossible to solve explicitly; especially in more than one space dimension. Therefore, we use numerical methods to study the *classical aspects of solitons*. Any application to particle physics needs an adaptation of the model to the quantum regime. For topological solitons in two or three space dimensions, this task is conceptually and technically very involved. Therefore, our strategy for the study of *quantum aspects of solitons* again resorts to numerical techniques.

Every introduction to solitons starts with the first known study of solitary waves by J. Scott Russell; and so will ours. His work inspired many researchers. The discovery of the Korteweg-de Vries (KdV), the Burgers equations and much more followed. Usually, solitonic systems are classified into two groups: the integrable models and the topological models. Integrable solitons owe their existence to the finely tuned balanced action of non-linear and dispersive or dissipative terms. This is intimately linked to an infinite number of conservation laws and the integrability of the system. Explicit solutions come from various techniques e.g. Lax pair, inverse scattering etc. We move on to construct solitonic systems whose stability is imposed by its topology. Unlike for integrable models, few mathematical tools are available. Field configurations are classified via a topological charge and an appropriate lagrangian ensures stability. The sine-Gordon model is special due to its integrability and its non-trivial topology. The non-linear $O(N)$ model and its stabilised version, the Skyrme model are good examples of topological solitons.

We discuss the application of solitons to particle physics. t'Hooft and Witten's work on

Large-N expansion and low-energy QCD established the nuclear Skyrme model as the candidate theory for the description of nuclei. Adkins, Nappi and Witten's quantization paper have partially confirmed this hope. We discuss the problems involved and recent attempts to improve the predictive power.

We give a brief summary of this thesis. In 'Numerical Methods', we present the numerical techniques used for our study of classical and quantum aspects of solitons. The finite difference is the core ingredient of these standard numerical methods. We also introduce the Metropolis–Simulated Annealing principle. This technique should prove to be an interesting and efficient alternative way to find minimal energy solutions. The implementation of this method to solitonic systems was done by the author and Mark Hale. 'Classical Aspects of Baby Skyrme models' analyses baby Skyrme models. We explore the structure of minimal-energy skyrmion solutions of topological charge greater than one for the different baby Skyrme models. On the way, we review the holomorphic and the old baby Skyrme model and confirm previous work. We find that the new baby Skyrme model has a completely different multi-skyrmion structure. This leads us to the conclusion that the structure is heavily potential dependent. In the 'Quantum Aspects of Solitons', we show how to extract quantum mass corrections via numerical methods. We review the method by Barnes & Turok and confirm the validity of their technique. First, we compute the mass correction for the ϕ^4 kink model explicitly. Then we derive a simple trace formula and redo the calculations explicitly and numerically. We apply it to another model in 1+1 dimensions, namely the Sine-Gordon model.

1.1 How it all started...

Imagine you throw a stone in a lake. The resulting water wave undergoes dispersion and, to a lesser degree, dissipation. It is a superposition of waves at different frequencies which travel

at different speeds: the water wave disperses i.e. becomes delocalised. Dissipative effects lead to a gradual decrease of the amplitude of these travelling waves. The concept of a solitary wave comes from the observation of water waves that do not follow this pattern. Indeed, these water waves are single localised entities. J. Scott Russell seems to be the first to have studied the fundamentally different dynamics underlying solitary waves. In 1844, Russell reported on his observation of 'great waves of translation' in the Edinburgh-Glasgow canal that led to his subsequent studies of such phenomena and started off research on solitons as such [Rus45]:

> I was observing the motion of a boat which was rapidly drawn along a narrow channel by a pair of horses, when the boat suddenly stopped – not so the mass of the water in the channel which it had put in motion; it accumulated round the prow of the vessel in a state of violent agitation, then suddenly leaving it behind, rolled forward with great velocity, assuming the form of a large solitary elevation, a rounded, smooth and well-defined heap of water, which continued its course along the channel apparently without change of form or diminution of speed. I followed it on horseback ... Its height gradually diminished, and after a chase of one or two miles I lost it in the windings of the channel. Such, in the month of August 1834, was my first chance interview with that singular and beautiful phenomenon...

He succeeded in re-creating solitary waves in his laboratory. Simulating the boat in the canal, Russell dropped weights at one end of a water channel. The mass of water displaced formed a solitary wave: the volume of water displaced by the weight was exactly equal to the volume of water in the wave. Further, Russell found an empirical formula relating the speed v and the amplitude a of the wave, the undisturbed depth h of water and the acceleration g of gravity:

$$v^2 = g(h + a). \tag{1.1}$$

The form of the solitary wave depends on the properties of the physical system rather than the circumstances of its creation. Another important observation shed light on the fundamentally different dynamics underlying solitary waves. Russell described how a large wave *'immediately breaks down by spontaneous analysis into two, the greater moving faster and altogether leaving the smaller'*. The concept of a soliton as the solitary wave conserved in collisions is emerging. Subsequent research by Boussinesq (1871), by Lord Rayleigh (1876) and by Korteweg and de Vries (1895) showed that the solitary wave in shallow water can be well described by the KdV equation: see [DJ96, pages 7-15] for example. At a much later stage, numerical experiments by Fermi, Pasta and Ulam [FPU55], by Perring and Skyrme [PS62] and by Zabusky and Kruskal [ZK65] clarified the concept of a soliton and its stability throughout interactions. It's Zabusky and Kruskal who came up with the name 'soliton' and clearly stated in [ZK65]:

> Shortly after the interaction, they reappear virtually unaffected in size or shape. In other words, solitons "pass through" one another without losing their identity. Here we have a nonlinear physical process in which interacting localised pulses do not scatter irreversibly.

1.2 Integrable solitons

Solitons are solitary waves that keep their identity after collisions. Generally, solitons can be classified into integrable solitons and topological solitons. Unfortunately, there is no general agreement over the definition of an integrable system: see [AC91, pages438-439]. Since integrable solitons are not the subject of this thesis, we restrict ourselves to a brief survey of the key concepts and techniques available. This will provide us with a good starting point for the introduction of topological solitons. Their lack of mathematical tools to produce solutions is in stark contrast to integrable systems and requires numerical studies. Useful references on

integrable models are [Bow], [DJ96], [AC91], [RS84].

Integrability of a system is related to the existence of a Lax pair and the Painlevé property. Various techniques can be used to find explicit solutions or the time-evolution of configurations, to name a few: travelling wave solution, inverse scattering, Bäcklund transformation, Lax pair. The stability of the solitons arises from the existence of an infinite number of conservation laws. These laws are often a result of the finely balanced action of a non-linear term and a dispersive or dissipative term. However, the integrability of such systems can be destroyed very easily by a perturbation on the equation e.g. a change of the potential. Unfortunately, in general, integrable solitons do not annihilate each other. Further, integrable systems are usually not Lorentz invariant and are known to exist mainly in (1+1)D. Thus a comparison with real particles is flawed from the start. However, models like the Sine-Gordon are integrable and topological and provide us, as we will see later, with excellent toy models to simulate particle physics properties.

1.2.1 KdV and Burgers equation

We start out with the simple wave equation in one dimension,

$$u_{xx} = u_{tt}; \tag{1.2}$$

we let $c = 1$ and u_{tt} stands for the second partial derivative with respect to time. The differential equation is linear i.e. we can construct new solutions by superposition of known solutions. The general solution known as d'Alembert's solution is given in terms of two functions of variables $x \pm t$:

$$u(x,t) = f(x-t) + g(x+t). \tag{1.3}$$

Given an initial configuration, the wave will split into a right-moving and a left-moving wave. These waves will not change their shape; there is no dispersive or dissipative term present. In

effect, we have two non-interacting waves that travel forever. If we just concentrate on the right-moving wave, the corresponding differential equation simplifies to

$$u_t + u_x = 0. \tag{1.4}$$

There are three modifications one can do to the wave equation (1.4).

The addition of odd derivative terms leads to dispersion of the wave. For example,

$$u_t + u_x + u_{xxx} = 0 \tag{1.5}$$

leads to the general solution

$$u(x,t) = \int_{-\infty}^{\infty} dk A(k) e^{i(kx-\omega(k)t)} \tag{1.6}$$

with some given $A(k)$ fixed by initial conditions. Further, the frequency ω of a wave depends on its wave number k; the dispersion relation

$$\omega(k) = k - k^3. \tag{1.7}$$

This leads to the de-localisation of an initial wave packet as its underlying waves travel at different speeds according to their wave number k.

The addition of even derivative terms leads to dissipation i.e. a decay of the amplitude of the wave. The dispersion relation $\omega(k)$ becomes complex and we end up with an exponentially decaying term. For example,

$$u_t + u_x - u_{xx} = 0 \tag{1.8}$$

leads to a complex dispersion relation

$$\omega(k) = k - ik^2 \tag{1.9}$$

and the general solution gives

$$u(x,t) = \int_{-\infty}^{\infty} dk A(k) e^{-k^2 t} e^{ik(x-t)}. \tag{1.10}$$

The amplitude $A(k)\exp(-k^2t)$ decreases with time and the underlying waves vanish.

Another modification to the wave equation is the addition of a non-linear term, for example

$$u_t + u_x + uu_x = 0. \tag{1.11}$$

The differential equation is non-linear and we cannot construct new solutions by the superposition principle. Further, a time-evolved initial configuration only generates a single-valued solution for a finite amount of time. (see [DJ96, page 5])

What happens if a dissipative or dispersive and a non-linear term is added to the wave equation (1.4)? If we add a dispersive and a non-linear term, we get the *KdV equation* that controls the dynamics of a solitary water wave (see above):

$$u_t + (1+u)u_x + u_{xxx} = 0. \tag{1.12}$$

Transforming $1 + u \to 6u$, we get the most commonly used form of the KdV equation:

$$u_t + 6uu_x + u_{xxx} = 0. \tag{1.13}$$

Replacing the dispersive term with a dissipative term, we end up with the *Burgers equation.*

Surprisingly, there exists an infinite number of conserved quantities of the KdV equation. In addition to the conservation of momentum and energy, many other conserved quantities were found and the existence of infinitely many was conjectured. In 1968 Miura [Miu68] discovered an important transformation that links the KdV equation to the modified KdV equation;

$$v_t - 6v^2v_x + v_{xxx} = 0. \tag{1.14}$$

If v is a solution of the mKdV equation, then necessarily, via the Muira transformation

$$u = -v^2 - v_x, \tag{1.15}$$

u is a solution of the KdV equation, because the expression

$$-(2v + \partial_x)(v_t - 6v^2 v_x + v_{xxx}) = 0 \tag{1.16}$$

equals the KdV equation. This fact led Miura, Gardner and Kruskal [MGK68] to a proof of the conservation of an infinite number of conserved quantities. They generalised Muira's transformation and defined w to be

$$u = w - \epsilon w_x - \epsilon^2 w^2, \tag{1.17}$$

where ϵ is an arbitrary constant. Again, u will be a solution to the KdV equation if and only if w satisfies a differential equation, here

$$w_t + 6(w - \epsilon^2 w^2)w_x + w_{xxx} = 0. \tag{1.18}$$

This equation can be written in a conservation form;

$$(w)_t + (3w^2 - 2\epsilon^2 w^3 + w_{xx})_x = 0 \tag{1.19}$$

and

$$\int_{-\infty}^{\infty} w(x, t; \epsilon)dx = \text{constant}. \tag{1.20}$$

w depends on ϵ, but the KdV equation does not. Thus they expressed the solution in terms of a power series expansion of the form

$$w(x, t; \epsilon) = \sum_{n=0}^{\infty} w_n(x, t)\epsilon^n \tag{1.21}$$

and every w_n, an infinite number of them, represents a conserved quantity

$$\int_{-\infty}^{\infty} w_n(x, t)dx = \text{constant}. \tag{1.22}$$

The conserved quantities and conservation laws are found by substituting (1.21) into (1.17) and equating the coefficients of increasing power of ϵ. See [AC91, pages 23-24] and [DJ96, section 5.1] for a complete proof.

1.2.2 Searching for solutions: various techniques

Unlike for topological solitons, there are various techniques to find solutions to integrable systems. Generally, the problem of solving the corresponding non-linear PDE is divided up into simpler problems like ODEs and integral equations. And one can rely on a vast amount of standard techniques and knowledge in these fields.

Travelling Wave Solution

This is the simplest and oldest technique available. The travelling wave ansatz assumes that the solution is travelling with a constant speed v;

$$u(x,t) = f(x - vt). \tag{1.23}$$

Let us take the KdV equation (1.12) as our example. Using the ansatz, we obtain the following differential equation with respect to f,

$$-vf' + 6ff' + f''' = 0.$$

Integrating twice using appropriate boundary conditions and separating variables, we end up with an integral on both sides,

$$\int \frac{df}{\sqrt{f^2(v-2f)}} = \int d(x - vt),$$

which gives us the travelling wave solution for the KdV equation:

$$f(x - vt) = \frac{v}{2}\text{sech}^2(\frac{\sqrt{v}}{2}(x - x_0 - vt)). \tag{1.24}$$

Inverse Scattering

The inverse scattering method (ISM) is very effective for the time-evolution of an initial solution $u(x,0)$ that falls off sufficiently fast as it approaches spatial infinity. Effectively, the non-linear

PDE problem is reduced to solving two second order ODEs and an integral equation. We will briefly underline the main ideas: see [AC91, section 1.7] and [DJ96, chapter 3 and 4] for detailed discussions. Fourier transforms are similar: a problem is solved in Fourier space and transformed back.

Let us consider the KdV equation. Solving the KdV equation with an initial condition $u(x,0)$ will give us the time-evolution of the initial configuration. Unfortunately, it is not possible to solve the non-linear PDE directly. The main idea of the inverse scattering is to re-formulate the problem into a scattering and inverse scattering problem of the time-independent Schrödinger equation with the potential $u(x,0)$. The Miura relation (1.15) allows us to translate every solution of the mKdV equation (1.14) into a KdV solution (1.12). Actually, this relation is a Riccati equation which can be linearised using the relation

$$v = \frac{\Psi_x}{\Psi}. \tag{1.25}$$

We treat time as a parameter from now onwards. At a given time t, here it is $t = 0$, using the linearisation in (1.15) and the Galilean invariance $u \to -\lambda + u(x + 6\lambda t, t)$ of the KdV equation, we obtain the time-independent Schrödinger equation:

$$\left(-\frac{d^2}{dx^2} + u\right)\Psi = \lambda\Psi.$$

Finding the eigenvalues and eigenfrequencies for the potential $u(x;t)$ is a well-explored area known as the Sturm-Louiville problem. The continuous spectrum is described by

$$\Psi(x) \sim \quad e^{-ikx} + r(k)e^{ikx} \quad \text{as } x \longrightarrow \infty \tag{1.26}$$

$$\Psi(x) \sim \qquad a(k)e^{-ikx} \qquad \text{as } x \longrightarrow -\infty \tag{1.27}$$

$r(k)$ is the reflexion coefficient and $a(k)$ the transmission coefficient. The discrete spectrum is described by

$$\Psi_n(x) \sim c_n e^{-\sqrt{\lambda_n}x}, \tag{1.28}$$

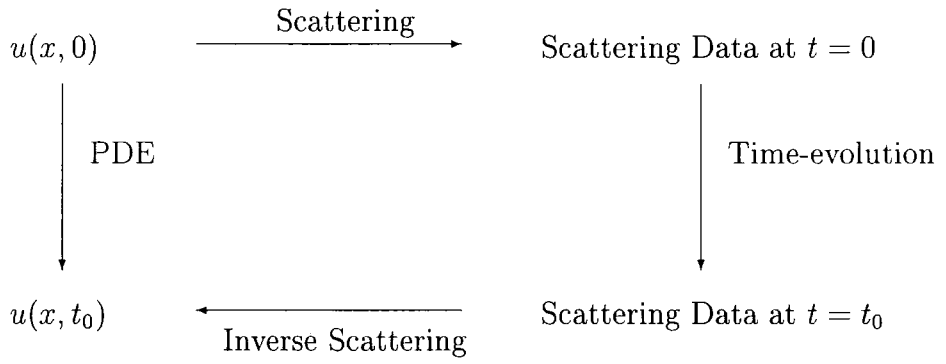

Figure 1.1: Inverse Scattering Method

where λ_n is the nth discrete eigenvalue. This represents all information on the scattering data. Now, the scattering data is time-evolved. Only the reflection coefficient $r(k)$ and c_n are changing with time. We would like to know the potential i.e. $u(x;t)$ that corresponds to the scattering data at time t. Therefore, we have to use the inverse scattering method which corresponds to solving an integral equation called the Gel'fand-Levitan-Marchenko equation. Finally, we end up with $u(x,t)$. However, solving the scattering and inverse scattering problem is not an easy task. A visual representation of the inverse scattering method is given in figure 1.1.

Lax Pair, Painlevé test and Bäcklund Transformation

The inverse scattering method plays a crucial rôle in solving non-linear PDEs of integrable systems. There are several properties or techniques closely related to the ISM. Unfortunately, there is no definite framework unifying all of them together. Rather, one has to prove the relations within the framework of a specific system. For example in the KdV model, we proved

the existence of an infinite number of conserved quantities. We briefly describe three more techniques. For more details, please consult [DJ96], [AC91] and [RS84].

The *compatibility of linear operators* or existence of a *Lax pair* is crucial to the integrability of a system. A model described by $u(x,t)$ is integrable if the set of two N first-order coupled linear DEs with the Lax pair $U(u(x,t);\lambda)$ and $V(u(x,t);\lambda)$,

$$F_x = U(u(x,t);\lambda)F \tag{1.29}$$

$$F_t = V(u(x,t);\lambda)F, \tag{1.30}$$

exists such that the differential equation of the model in terms of $u(x,t)$ satisfies the form

$$U_t - V_x + [U,V] = 0. \tag{1.31}$$

The Lax pair U and V are $N \times N$ matrices and depend on u and its derivatives, F is a N-dimensional vector and that the equations must be satisfied for all complex λ. The spectral problem (see Schrödinger equation in ISM) is effectively encoded in the first of the two DEs (1.29) and time is treated as a parameter. The second DE can be viewed as the auxiliary spectral equation where space is treated as a parameter. If a Lax pair can be found, then one only needs to find the solution to the two linear DEs. For example, Lax pairs exist for the KdV equation and the Sine-Gordon model.

Every evolution equation solvable by ISM seems to have a corresponding Bäcklund transformation. The transformation is very useful for generating N-soliton solutions as its effect on a solution is to add or subtract a soliton. Essentially, the Bäcklund transformation changes a pair of coupled first order equations (u,v) into a pair of uncoupled second order equations in u and v. See [DJ96, section 5.4] and [AC91, section 2.6.6] for details. We will give an example of a Bäcklund transformation during our discussion of the Sine-Gordon model.

Which equations are solvable by ISM? The *Painlevé conjecture* states: "A nonlinear PDE is solvable by the inverse scattering transform if every ordinary differential equation derived from

it (by exact reduction) satisfies the Painlevé property." For the equation to have the Painlevé property, it should not have any movable critical points i.e a movable singularity which is not a pole. In 1884, Fuchs showed that first order equations of the Painlevé type have to satisfy the form

$$\frac{dw}{dz} = a(z)w^2 + b(z)w + c(z) \tag{1.32}$$

where a, b, c are analytic functions of the complex variable z. Painlevé and Gambier generalised the method to second order equations. They found 50 different cases; all but six equations are solvable by elementary functions. The six equations known as Painlevé transcendents are irreducible, but their solutions are known. The KdV equation, for example, reduces to the Painlevé Type II equation. Thus, if one can put a non-linear PDE in the Painlevé form, it is solvable.

1.3 Topological Soliton

Are there integrable systems that are Lorentz invariant? Do solitons exist in higher dimensions? Integrable models are very convenient, because we can find explicit solutions and do a detailed analysis of their dynamics. Unfortunately, integrable models are very rare. Additional constraints like Lorentz invariance and an extension to (3+1)D physical space destroy their integrability. There are no known integrable systems satisfying these conditions. Here comes the topology of a system into play. Integrable systems have solitons due to their conservation laws. Topological solitons exist due to a non-trivial mapping between physical space and field space. We can think of a string with knots in it. You fix your boundary conditions by holding onto both ends of a string. The string with one knot can never be deformed into the string with two or no knots. A more accurate visualisation of topological solitons is a twist in the string. You fix your boundary conditions again and then twist one end of the string around once. If

you hold both ends of the string, there is no way, you can undo the twist without violating the boundary conditions. Further, if you now anti-twist one end, i.e. twist in the opposite direction, you 'annihilate' the first twist. We can imagine topological solitons modelling real elementary particles. The non-trivial mapping gives rise to a twisted field configuration that carries a charge; very much like the baryon number conservation. In addition to non-trivial topology, we need to ensure that the dynamics generated by the lagrangian allows stable solitons. This means the soliton should not shrink to a point or expand to nothing: it must have a stable scale. Often, it has a preferred scale.

To summarise, topological solitons possess all the desired properties like Lorentz invariance by construction and higher dimensions that integrable models do not have. And, integrable models are completely solvable whereas solutions to topological soliton equations are rarely known and have to be explored numerically. In a sense, integrable and topological systems are antagonists with the notable exception of special systems in one space dimension. The prime example is the Sine-Gordon model, a good toy model that has exact solutions which can be compared to numerical results.

1.3.1 The Topology

We can look at a field theory as the mapping $\mathcal{M}$ at time t of a base space X, our physical space $\mathbf{R}^n$, into a target space Φ, the field space. We write:

$$\mathcal{M} \text{ at t}: \quad \mathbf{R}^n \longrightarrow \Phi \tag{1.33}$$

$$x \longrightarrow \phi(x) \tag{1.34}$$

which means that, to every element x in physical space, we associate an element $\phi(x)$ in field space. We impose a physical restriction on our map $\mathcal{M}(X, \Phi)$. For the field theory to be a

'physically good' theory that describes finite, localised objects, we require that

$$\phi(x) \longrightarrow \phi_V \text{ as } |x| \longrightarrow \infty; \tag{1.35}$$

ϕ_V is an element of field space which we call the vacuum field value. Note that this condition is not valid for gauge models, for the additional gauge freedom allows extra freedom in defining the vacuum: see e.g. the abelian Higgs model [Ryd94, last chapter]. In other words, the field of our theory should approach the vacuum at spatial infinity in all directions. Note that the field 'must converge sufficiently fast' to the vacuum field value to ensure energy finiteness, for example. In terms of mapping, all elements 'representing spatial infinity' in physical space are mapped into one single element, namely ϕ_V, in field space. The structure of such a physical space corresponds exactly to the stereographic projection of a circle S^1, a sphere S^2 and so on onto a flat space; depending on how many space dimensions we have. So, effectively, we might as well describe the physical space as S^n as this automatically includes the property of a 'physically good' theory: we say that space is compactified. The map changes to

$$\begin{aligned} \mathcal{M} \text{ at t}: \quad \mathbf{S}^n &\longrightarrow \Phi \\ x &\longrightarrow \phi(x) \end{aligned} \tag{1.36}$$

In the introduction to topological solitons, we talk about how a configuration with one twist cannot be changed into a configuration with two twists, for example. We need to ensure that there is no way that a given field configuration in one class, say the class of one-twist configurations, can dynamically evolve into a field configuration of a different class i.e. a class of configurations with the number of twists different from one. A non-trivial topology of a mapping arises if it is possible to non-trivially classify all maps, representing the field configurations, in terms of the following equivalence relationship: two maps in different equivalence classes cannot deform into each other. Therefore, each equivalence class is characterised by a unique conserved quantity: the topological charge or winding number. Now, these classes form the group elements

of a homotopy group whose group action is the addition of two field configurations. The secret to constructing topological solitons is to choose the manifold of the field space in such a way that it gives rise to non-trivial mapping. [MRS93, Appendix B] provides a good introduction to homotopy groups. The homotopy group we are interested in is the nth homotopy group $\pi_n(\Phi)$ such that the group is isomorphic to the addition group $\mathbf{Z}$. In general, any non-trivial homotopy group will lead to a non-trivial classification of field configurations. For example, this means that we can add together two configurations with one twist each and get a configuration with two twists. The group action of $\mathbf{Z}$ effectively adds up the topological charge of both configurations. Thus, annihilations are possible: we can think of a configuration with one twist added to one with one anti-twist that gives a configuration with no twist. There are standard tables like [MRS93, Table B.1, page 226] which list the nth homotopy group for a given Φ manifold. The common choice is S^n as the nth homotopy group of S^n,

$$\pi_n(S^n) = \mathbf{Z}. \tag{1.37}$$

One can think of many other choices. For example, for S^3 i.e. compactified 3 dimensional space, the 3th homotopy group of the manifold of the Lie group $SU(n)$ is also equal to the addition group $\mathbf{Z}$.

The most interesting feature is the emergence of a conserved quantity: the topological charge. This is due to the fact that an equivalence relation exists which can classify the mappings into equivalence classes. And, by definition, an equivalence class can be classified by a unique quantity. Thus, this leaves us with the interesting option to define a conserved quantity not via Noether's theorem, but purely out of the non-trivial mapping of a field theory satisfying the compactification property of physical space.

We give an explicit example: the topological charge of the map $S^2 \longrightarrow S^2$. The topological charge or winding number must give the number of times an element of the S^2 field space is mapped to or, in other words, the number of times the map winds around the S^2 field sphere.

Consider S^2 a sphere of unit radius. Its surface can be described by a three dimensional vector $\vec{\phi} = (\phi_1, \phi_2, \phi_3)$ with $\vec{\phi} \cdot \vec{\phi} = 1$ or an unconstrained coordinate system (σ_1, σ_2) e.g. polar coordinates. The expression of an infinitesimal surface area pointing in the ϕ_a direction is

$$dS_a = \frac{1}{2}\epsilon^{ij}\epsilon^{abc}\frac{\partial\phi_b}{\partial\sigma_i}\frac{\partial\phi_c}{\partial\sigma_j}d^2\sigma. \tag{1.38}$$

This is valid for all unconstrained two-dimensional coordinates: a change in the coordinates is absorbed by the Jacobian. The integral over the map $\vec{\phi}(\sigma_1, \sigma_2)$ gives

$$I = \int dS_a \cdot \phi_a = \int dS = 4\pi N. \tag{1.39}$$

The surface of the unit sphere is 4π and we take into account the number of times N the sphere is mapped to. Therefore, we use this integral to construct the topological charge which is given by

$$Q = \frac{1}{8\pi}\int \phi_a\epsilon^{ij}\epsilon^{abc}\frac{\partial\phi_b}{\partial x_i}\frac{\partial\phi_c}{\partial x_j}dxdy = \frac{1}{4\pi}\int dxdy(\partial_x\vec{\phi} \times \partial_y\vec{\phi}) \cdot \vec{\phi} \tag{1.40}$$

There is a general method for constructing topological charges of a given field theory: Isham's construction of topological charges (see [MRS93, section 2.1-2.3]).

1.3.2 The Lagrangian and Hobart-Derrick theorem

A non-trivial topology is a necessary but not sufficient condition for the existence of stable topological solitons. The dynamics generated by the lagrangian must lead to a stable field configuration: the stability condition. A stable configuration has a stable scale i.e. any change of scale by a perturbation is energetically unfavourable. Further, a physical theory needs to be Lorentz invariant and sometimes satisfy further constraints like chiral invariance. Special relativity i.e. Lorentz invariance restricts the choice of terms in the lagrangian. For example, the Lorentz indices need to be contracted i.e. each term of the lagrangian needs to have an even number of derivatives. We discuss the various options later.

The Hobart-Derrick theorem provides a useful check on the stability of a minimal-energy solution. It checks whether a solution can be stable under scaling transformations. It is a necessary but not sufficient condition for stability: we can rule out certain lagrangians due to the instability of the static solution under scale transformations. Let $\phi_{ST}(x)$ be the static solution of the Euler-Lagrange equation with the principle of least action

$$\delta E[\phi_{ST}] = 0, \tag{1.41}$$

where E is the energy functional. Let x undergo a scale transformation

$$x \longrightarrow \tilde{x} = \lambda x \tag{1.42}$$

and

$$\phi_{ST}(x) \longrightarrow \phi_\lambda = \tilde{\phi}_{ST}(\lambda x). \tag{1.43}$$

We re-write the principle of least action (1.41 as

$$\delta E[\phi_{ST}] = \left.\frac{\partial E[\phi_{ST}(\lambda x)]}{\partial \lambda}\right|_{\lambda=1} \delta\lambda = 0. \tag{1.44}$$

This equation should be invariant for any scale transformation of λ. We end up with the condition that

$$\left.\frac{\partial E[\phi_{ST}(\lambda x)]}{\partial \lambda}\right|_{\lambda=1} = 0. \tag{1.45}$$

For a stable solution, the second derivative with respect to the energy functional should be positive:

$$\left.\frac{\partial^2 E[\phi_{ST}(\lambda x)]}{\partial \lambda^2}\right|_{\lambda=1} > 0. \tag{1.46}$$

1.3.3 $O(3)\sigma$-model (or Non-linear σ model)

Consider a field theory in (2+1) dimensions with a mapping

$$S^2 \longrightarrow S^2. \tag{1.47}$$

This gives rise to a non-trivial homotopy group $\pi_2(S^2)$ and the topological charge has been derived above:

$$Q = \frac{1}{4\pi} \int dxdy(\partial_x \vec{\phi} \times \partial_y \vec{\phi}) \cdot \vec{\phi}. \tag{1.48}$$

The expression is valid for any finite-energy field configuration of any lagrangian and tells us the topological sector the configuration belongs to i.e. which topological charge it has. The S^2 space can be described by a three-dimensional field vector $\vec{\phi}(t, x, y)$ constructed out of three real scalar fields with the constraint

$$\vec{\phi}(t, x, y) \cdot \vec{\phi}(t, x, y) = 1.$$

This also implies

$$\partial_\mu \vec{\phi} \cdot \vec{\phi} = 0$$

and

$$\partial_\mu \partial^\mu \vec{\phi} \cdot \vec{\phi} = -\partial^\mu \vec{\phi} \cdot \partial_\mu \vec{\phi}.$$

The field vector describes a point on the sphere S^2. A choice of an unconstrained coordinate system for S^2 is a complex field vector $W(t, x, y)$ which is the stereographic projection of the field vector $\vec{\phi}$. The disadvantage of this coordinate system is its singularity at infinity i.e. the north pole is mapped to infinity. This problem is overcome by choosing two coordinate sets: W maps the north pole to infinity and the inverse map $U = \frac{1}{W}$ maps the south pole to infinity. Another choice is the use of two angles to describe a point on the sphere S^2. Again, two coordinate sets are needed to completely map out every point.

The lagrangian density of the $O(3)$ σ-model consists of one term called the σ term:

$$\mathcal{L} = \partial_\mu \vec{\phi} \cdot \partial^\mu \vec{\phi}. \tag{1.49}$$

The coordinates are x_μ with $\mu = 0 \ldots 2$. The coordinate x_0 is the time and x_i labels the space coordinates with $x_1 = x$ and $x_2 = y$. The contracted covariant derivatives enforce Lorentz

invariance. The rule consists of putting all Lorentz indices μ down or up according to the transformation $\partial^0 = -\partial_0$ and $\partial^i = \partial_i$. The dot product i.e. summing over the field components ensures the $O(3)$ symmetry of the lagrangian. We have to remember to include the constraint on the field vector $\vec{\phi}$. A Lagrange multiplier has to be included and the full action has the form:

$$S[\vec{\phi}(t,x,y)] = \int dt \int dxdy[\partial_\mu \vec{\phi} \cdot \partial^\mu \vec{\phi} + \lambda(t,x,y)(\vec{\phi} \cdot \vec{\phi} - 1)]. \tag{1.50}$$

The action is invariant under an $O(3)$ transformation of the field vector. This corresponds to a $O(3)$ symmetry of the action; hence the name $O(3)$ σ model. However, we might as well call it S^2 σ model as the invariant subspace of an unconstrained field vector $\vec{\phi}$ is precisely the sphere S^2. The Euler-Lagrange equation

$$\partial_\mu \frac{\partial \mathcal{L}}{\partial(\partial_\mu \phi_a)} - \frac{\partial \mathcal{L}}{\partial \phi_a} = 0 \tag{1.51}$$

with respect to the field component ϕ_a gives the field equations

$$2\partial_\mu \partial^\mu \vec{\phi} - \lambda \vec{\phi} = 0.$$

Using the constraint $\vec{\phi} \cdot \vec{\phi} = 1$, λ takes the form $2\partial_\mu \partial^\mu \vec{\phi} \cdot \vec{\phi}$. The final version of the field equations is

$$\partial_\mu \partial^\mu \vec{\phi} + (\partial_\mu \vec{\phi} \cdot \partial^\mu \vec{\phi})\vec{\phi} = 0. \tag{1.52}$$

An important aspect of topological solitons is the existence of a lower bound on the minimal-energy solution in a given topological sector: the Bogomolnyi bound. We start out with the identity

$$\int dxdy(\partial_i \vec{\phi} \pm \epsilon_{ij} \vec{\phi} \times \partial_j \vec{\phi})^2 \geq 0 \tag{1.53}$$

Expanding the expression and using the constraints (1.3.3), we end up with

$$\int dxdy(\partial_i \vec{\phi} \cdot \partial^i \vec{\phi}) \geq \pm \int dxdy(\partial_x \vec{\phi} \times \partial_y \vec{\phi}) \cdot \vec{\phi}. \tag{1.54}$$

This is nothing else than a lower bound on the energy in a given topological sector,

$$E \geq 4\pi|Q|. \tag{1.55}$$

If the field configuration for a given charge satisfies the Bogomolnyi bound exactly, it is a minimal-energy solution. Thus $E = 4\pi|Q|$. This also means that the identity (1.53) is zero and the field has to satisfy the *Bogomolnyi equation*

$$\partial_i\vec{\phi} \pm \epsilon_{ij}\vec{\phi} \times \partial_j\vec{\phi} = 0. \tag{1.56}$$

One can show that this first-order equation satisfies the second-order field equation (1.52). Hence, the existence of the Bogomolnyi equation simplifies the search for minimal-energy solutions. Note that this is only the case if there exists a minimal-energy solution that satisfies the bound.[1]

We switch to the stereographic coordinate system $W(t, x, y)$. The complex field W is given by

$$W = \frac{1 - \phi_3}{\phi_1 + i\phi_2}. \tag{1.57}$$

in terms of the field vector $\vec{\phi}$ components. The inverse transformation relates W to $\vec{\phi}$ with

$$\phi_1 = \frac{W + W^*}{1 + |W|^2} \qquad \phi_2 = i\frac{W - W^*}{1 + |W|^2} \qquad \phi_3 = \frac{1 - |W|^2}{1 + |W|^2}. \tag{1.58}$$

The form of the energy density changes to

$$\mathcal{L} = \frac{\partial_\mu W \partial^\mu W^*}{(1 + |W|^2)^2} \tag{1.59}$$

and the equation of motion becomes

$$(W_{xx} + W_{yy} - W_{tt})(1 + |W|^2) + 2W^*\left((W_t)^2 - (W_x)^2 - (W_y)^2\right) = 0. \tag{1.60}$$

[1]The derivation of the equation is often called 'completing the square'.

The Bogomolnyi equation (1.56) re-written in terms of the complex field is exactly the Cauchy-Riemann equation: see [Raj96, page56-57]. Thus, any analytic function actually satisfies the equation and is a minimal-energy solution. A simple solution for a given charge n is

$$W(z) = [\lambda(z - z_0)]^n \tag{1.61}$$

where $z = x + iy$. We can easily check that this solution has indeed topological charge n. This is done by using the Bogomolnyi bound and the expression of the energy density (1.59).

The charge does not depend on the scaling factor λ and nor does the energy. Performing the integral, one notices that λ can be scaled away. This turns our attention to Derrick's theorem for an explanation. How does the σ term (1.49) scale? Which effect does it have on the energy density? The condition for stability (1.45) is not fulfilled, because

$$E[\tilde{\phi}(\lambda x)] = E[\phi(x)]$$

is independent of λ and the second derivative will be zero. The energy functional is scale invariant. The soliton can contract or expand without changing its energy. Therefore, it does not have a preferred scale. It is unstable in the sense that a small perturbation will change its size. The model is not very reliable in numerical simulations due to the very small but unavoidable perturbations induced by numerical errors. We can also see that in more or less dimensions, λ is present and the condition of stability cannot be fulfilled either. The stability can only be retained by adding extra terms with different scaling behaviours. This concludes our discussion on this model. In the next section, we analyse modified versions with the crucial help of Derrick's theorem.

1.3.4 Other topological models

We have seen that the $O(3)\sigma$-model is scale invariant. A generalisation of the σ term to n dimensions shows that the energy functional scales as

$$E[\tilde{\phi}(\lambda x)] = \lambda^{2-d} E[\phi(x)]. \tag{1.62}$$

In one dimension, the energy scales as λ. Decreasing λ the coordinate grid shrinks and the soliton spreads out and vice versa. A decrease in λ leads to a decrease in energy. Therefore, the dynamics will expand the soliton and decrease the energy. There is no counterbalance and the soliton spreads out more and more and the energy goes to zero. In two dimensions, it is scale invariant. In three dimensions, the energy scales as λ^{-1}. Then, the soliton will shrink to zero and the energy goes to zero, too. Clearly, if we want to have stable solitons, we need to add appropriate terms to the lagrangian i.e. terms with different scaling behaviour.

Consider the general energy term T_α with 2α second order derivatives in n dimensions:

$$T_\alpha = E[\phi(x)] = \int (dx)^d (\partial_i \phi)^{2\alpha}. \tag{1.63}$$

Note that the number of derivatives is even due to Lorentz invariance. The mixing of the Lorentz indices also gives rise to many different derivative terms but with the same scaling behaviour. The term with $\alpha = 0$ is the potential term: a function of $\vec{\phi}$ does not scale i.e. we set it to 1. A scale transformation induces the following changes:

$$x \longrightarrow \tilde{x} = \lambda x$$

$$\partial_i \longrightarrow \tilde{\partial}_i = \lambda^{-1} \partial_i$$

$$\phi(x) \longrightarrow \tilde{\phi}(\tilde{x}) \equiv \phi(x)$$

Using these transformations, we obtain

$$E[\tilde{\phi}(\lambda x)] = \lambda^{d-2\alpha} E[\phi(x)]. \tag{1.64}$$

Applying Derrick's theorem, the conditions for stability (1.45) for a general energy functional containing all terms T_α up to Nth order in n dimensions are

$$\sum_{\alpha=0}^{N}(d-2\alpha)T_\alpha = 0 \tag{1.65}$$

and

$$\sum_{\alpha=0}^{N}(d-2\alpha)(d-2\alpha-1)T_\alpha > 0. \tag{1.66}$$

We are now able to select out the models which satisfy the conditions for stability. However, Derrick's theorem is just a necessary but not sufficient conditions. Thus, rather than proving stability, we discard the models that are unstable.

Topological Solitons in 1D

The simplest stable lagrangian is

$$\mathcal{L} = (\partial_t\phi)^2 - (\partial_x\phi)^2 - V(\phi). \tag{1.67}$$

There exist different models according to the potential e.g.

$$V(\phi) = (1-\phi^2)^2 \quad \phi^4 \text{ theory} \tag{1.68}$$

$$V(\phi) = 1-\cos\phi \quad \text{Sine-Gordon model} \tag{1.69}$$

'Completing the square' leads to the Bogomolnyi equation

$$\left(\frac{d\phi}{dx}\right)^2 = V(\phi). \tag{1.70}$$

The static minimal-energy solutions are solutions of

$$\int \frac{d\phi}{\sqrt{V(\phi)}} = x + x_0. \tag{1.71}$$

We will discuss the Sine-Gordon model in the next section as the 1D toy model for particle physics.

Topological Solitons in 2D

The lagrangian of the $O(3)\sigma$ model is unstable in two dimensions, because the σ term is scale invariant. We need to add a higher order term e.g. with four derivatives and a potential term. The common choice is the Skyrme term

$$\mathcal{L}_{SK} = (\partial_\mu \vec{\phi} \cdot \partial^\mu \vec{\phi})^2 - (\partial_\mu \vec{\phi} \cdot \partial_\nu \vec{\phi})(\partial^\mu \vec{\phi} \cdot \partial^\nu \vec{\phi}) \tag{1.72}$$

where $\vec{\phi}$ is the three dimensional field vector. The term is a combination of the two possible terms with four derivatives. It was originally proposed by Skyrme and is designed in such the way that the time derivatives in the field equation is maximally of second power and the energy functional is positive. The two-derivative term is scale invariant. And the potential term scales as λ^{-2} and will balance out the λ^2 behaviour of the Skyrme term. We end up with the baby Skyrme model:

$$\mathcal{L} = \mathcal{L}_\sigma - \mathcal{L}_{SK} - V(\phi). \tag{1.73}$$

The choice of potential is largely arbitrary. This model will be the focus of our study of classical aspects of topological solitons and has first been explored by Zakrzewski et al.: see [LPZ90]. Another possibility is the abelian Higgs vortices. The lagrangian contains a magnetic field and a charged scalar field: see [Ryd94].

Topological Solitons in 3D

In three dimensions, the potential term is optional: the σ term scales as λ^{-1} and the Skyrme term as λ^1. The nuclear Skyrme model first proposed by Skyrme has the form:

$$\mathcal{L} = \mathcal{L}_\sigma - \mathcal{L}_{SK}. \tag{1.74}$$

The Skyrme model is a popular candidate for the description of low energy QCD: it is an effective theory. We will discuss the model in detail later. Other topological solitons in three dimensions are the Yang-Mills Higgs monopoles: see [Ryd94].

1.3.5 The Sine-Gordon model: 1D toy model

As mentioned above, the Sine-Gordon model is a very useful toy model for particle physics and clarifies the concepts used in higher dimensional models. Explicit solutions can be found using the techniques associated to the integrability of the model. The Sine-Gordon solitons are also topological solitons and mimic various properties in particle physics e.g. particle annihilation. The Sine-Gordon energy density in terms of an angular variable $\phi(t,x)$ is

$$\mathcal{E} = \frac{1}{2}(\partial_t\phi)^2 + \frac{1}{2}(\partial_x\phi)^2 + (1-\cos\phi). \tag{1.75}$$

For fixed t, the mapping of the field goes from $S^1 \longrightarrow S^1$. One-dimensional space is compactified to S^1, for we require the field $\phi(t,x)$ to be the same (up to multiples of 2π) at $x=\infty$ and $x=-\infty$. And, the energy has to go to zero ergo $\phi(\infty)$ and $\phi(-\infty)$ are multiples of 2π. Of course, the angular variable $\phi(x)$ describes S^1 field space. Consider $\phi(-\infty)$ to be fixed to zero without loss of generality due to the $\phi \to \phi + 2\pi$ symmetry. The boundary condition at $x=\infty$ is $\phi = 2\pi n$ and we analyse the various configurations:

$n=0$: The minimal energy solution is $\phi = 0$ which satisfies the boundary condition and the energy is zero and minimal; as ϕ is a constant.

$n>0$: The minimal energy solutions are non-trivial and have topological charge n. The field maps n times over the field space S^1 i.e. the circle: it starts at $\phi = 0$ and ends up at $\phi = 2\pi n$. The solutions are the topological solitons.

$n<0$: These configurations have negative topological charge and represent the anti-solitons. The field maps n times over the field space S^1 i.e. the circle: it starts at $\phi = 0$ and ends up at $\phi = -2\pi|n|$.

We can see that, by adding a soliton and anti-soliton solution, the boundary condition at $x=\infty$ changes to zero and the solitons are annihilated i.e. the topological charge is zero. We

now derive the minimal-energy solution of topological charge one via the Bogomolnyi equation (1.56):

$$\int \frac{d\phi}{\sqrt{2(1-\cos\phi)}} = x + x_0. \tag{1.76}$$

We re-write it in terms of $\sin(\phi/2)$, integrate, invert and get

$$\phi_{st}(x) = 4\arctan[\exp(x + x_0)]. \tag{1.77}$$

We can obtain a moving solution by performing a Lorentz boost. The static minimal-energy solution satisfies the boundary condition $\phi(-\infty) = 0$ and $\phi(\infty) = 2\pi$: the field winds around the field sphere S^2 once. The expression of the energy density is

$$\epsilon(x) = 4\sin^2[\phi_{st}(x)]. \tag{1.78}$$

The energy goes to zero at spatial infinity and the integral is finite. Note that if we write the potential as $V = 1 - \cos(\lambda\phi)$, λ plays the rôle of coupling constant. The total energy or mass is now proportional to λ^{-1}. Clearly, we could not have obtained a good approximation via a perturbative expansion. Our 1-kink solution is non-perturbative.

The Sine-Gordon model is an integrable system and we can use the Bäcklund transformation to generate solutions. We re-write the Sine-Gordon equation in terms of the light-cone coordinates:

$$\partial_+\partial_-\phi - \sin\phi = 0.$$

The corresponding Bäcklund equations are defined as

$$\frac{1}{2}\partial_+(\phi_1 - \phi_0) = a\sin\left[\frac{1}{2}(\phi_1 + \phi_0)\right]$$

and

$$\frac{1}{2}\partial_-(\phi_1 + \phi_0) = a^{-1}\sin\left[\frac{1}{2}(\phi_1 - \phi_0)\right].$$

where a is a non-zero arbitrary constant that becomes a parameter for the new solution. We differentiate the first equation by ∂_-, substitute this expression in the second equation and use trigonometric identities to obtain

$$\partial_+\partial_-(\phi_1 - \phi_0) = \sin\phi_1 - \sin\phi_0. \tag{1.79}$$

Clearly, if ϕ_0 is a solution to the Sine-Gordon equation, then so is ϕ_1. Thus we can use a solution ϕ_0 to generate another solution ϕ_1. Note that we only have to solve two first order equations instead of second order! If $\phi_0 = 0$, we get the Bogomolnyi equation for the 1-kink solution. If we use this 1-kink solution as our ϕ_0, we get the 2-kink solution. It turns out that ϕ_1 is the $n+1$-kink solution for an initial n-kink input for ϕ_0. Note that the constant a is related to the speed when you construct a single soliton from the vacuum, but it is a more general parameter otherwise.

The quantum theory is discussed in *Quantum Aspects*. The beauty of the Sine-Gordon model and ϕ^4 kink model is that we can get exact results which can be compared to our numerical methods.

1.4 The nuclear Skyrme model

The nuclear Skyrme model is one of the 'raison d'être' of the study of topological solitons in theoretical particle physics. In the early 60's, Skyrme came up with a theory to describe the hadronic spectrum i.e. a theory of mesons and baryons [Sky61]. He had the ingenious idea to construct an effective field theory of mesons where the baryons are the topological solitons of the theory. Baryon conservation is equivalent to the conservation of the topological charge. His ideas were put aside by the success of QCD in the description of hadrons in terms of quarks. The QED lagrangian is invariant under the $U(1)$ gauge transformations; the gauge field being the photon. The QCD lagrangian is of the Yangs-Mills type. It is invariant under the non-abelian

$SU(3)$ gauge transformation; the gauge fields called gluons being the adjoint representation of the $SU(3)$ colour group. The QCD lagrangian is given by

$$\mathcal{L}_{QCD} = \sum_{\mu,\nu,\alpha,a} \overline{q}_a^\alpha (i\gamma^\mu D_\mu - m_\alpha) q_a^\alpha - \frac{1}{4} \sum_{\mu,\nu,i} G^i_{\mu\nu} G^{\mu\nu,i}. \tag{1.80}$$

D_μ is the covariant derivative and $G_{\mu\nu}$ the gluon field strength components. We will not go into any details. Basically, the lagrangian terms include the propagation of the massive quarks (q_a^α with the flavour index a and the colour index α and mass m_α), the massless gluon field and the interaction term with the coupling constant. Both the gluon fields and the interaction are hidden away in the covariant derivative and field strength. A crucial step forward in the understanding of QCD is the emergence of the idea of confinement. In QED, the running coupling constant decreases with distance of interaction and a perturbation expansion is very effective. In QCD, the inverse is true: only at small distance ergo high energy does the coupling become small and the quarks are free particles. At low energies, people believe that the quarks form colourless colour-singlet states: the hadrons. This must be true as there is no experimental evidence to the contrary. Sofar, no-one has come up with a decent way of deriving the confinement in QCD. This is due to the rising coupling constant i.e. perturbation techniques are useless. This energy region of QCD is called non-perturbative region. Clearly, the lack of a small parameter to do a perturbation expansion is evident. In the mid 70's, t'Hooft [tH74][tH73] generalised QCD to be invariant under a $SU(N_C)$ gauge group. He realised that the quantum treatment of QCD simplified considerably and it is possible to derive some qualitative statements in the large N_C and low energy limit. This comes from the fact that non-planar diagrams and internal quark loops are suppressed by a factor of N_C^{-2} respectively N_C^{-1}. For large N_C, QCD is a weakly interacting theory of mesons with the meson-meson interaction of order N_C^{-1}. For $N_C \to \infty$, QCD is therefore a theory of mesons which are free and non-interacting. Witten [Wit79] realised that weakly coupled theories may exhibit non-perturbative states like solitons or monopoles. A typical example is the Polyakov-'t Hooft monopole whose mass diverges for

vanishing coupling.[2] He showed that baryons behave as if they are solitons in a large-N_C meson theory. The derivation of effective actions from the QCD lagrangian is an unsolved problem. The Skyrme model is the simplest of a candidate theory for the low-energy effective lagrangian of QCD. Of course, one may add some higher order correction terms. See [MRS93, chapter 9] for a simple review on the relation between QCD and the Skyrme model.

Let us give a brief description of the Skyrme lagrangian and its features: see [HS86] and [MRS93] for more details. The lagrangian has already been described above in terms of the $\vec{\phi}$ notation. In effect, the most commonly used notation is in terms of a coordinate set on the $SU(3)$ group manifold. The lagrangian has the following form

$$\mathcal{L} = tr\left[\partial_\mu U \partial^\mu U^\dagger\right] + \theta\ tr\left[\left[(\partial_\mu U)U^\dagger, (\partial_\nu U)U^\dagger\right]^2\right] \tag{1.81}$$

where U is a SU(2) matrix and θ is fitted to experiments. We can re-write the nuclear Skyrme lagrangian (1.74) in the $\vec{\phi}$ notation as follows:

$$\mathcal{L} = \sum_{a,b} \dot{\phi}_a K_{ab}(\partial\vec{\phi})\dot{\phi}_b - V(\partial\vec{\phi}). \tag{1.82}$$

If we think about K_{ab} being a constant, the quantization procedure is greatly simplified. The lagrangian just looks like a generalised harmonic oscillator type. In 1981, Adkins, Nappi and Witten [ANW83] realised that a slowly rotating radially symmetric skyrmion solution satisfies this condition; K being the rotational inertia matrix and a constant of motion. Then they quantise the model as a spinning top and are able to extract all the important quantum properties of the proton i.e. the skyrmion with topological charge one. However, this quantisation procedure does not take into account the centrifugal deformation of a fast rotating skyrmion and is restricted to topological charge one. All skyrmions with topological charge greater than one have a discrete symmetry and the procedure fails. A more rigorous description of the problems

[2] see the Sine-Gordon model for diverging mass at vanishing coupling.

associated with the quantisation of the Skyrme model is given in [MRS93, chapter 8]. Let us just briefly note that the quantisation is ambiguous, because the theory is not renormalisable. One can do a renormalisation to a given order, but it will depend on the scheme. Therefore, it is essential to compare the scheme-dependent results with experimental data.

We will discuss quantisation issues in the chapter on quantum aspects of solitons. We are using the semi-classical approximation: quantisation around the minimal-energy solution in a given topological sector. The quantum corrections e.g. for the mass are given by the normal modes of the static solution.

Chapter 2

Numerical Methods

"Should we call in an expert or screw it up ourselves?"
(on an expert's office door)

The success of our study of classical and quantum aspects of solitons crucially depends on our ability to solve the differential and eigenvalue equations of the associated systems. Many such problems do not have a known explicit solution. In general, only (1+1) dimensional integrable models e.g. the Sine-Gordon model are solvable. They provide a very useful check on the numerical techniques we have used in (2+1) dimensions. We have compared our numerical results with the exact explicit solutions and find acceptable agreement between both. Higher dimensional solitonic field theories like the (2+1) dimensional baby Skyrme model pose a challenge. They are non-integrable systems and only in a few, rather special, occasions can we find explicit solutions to their resulting differential equations. Numerical methods are the only way forward in (2+1) dimensions, but we are faced with the need for more memory allocation and computational power. The advent of fast computers makes this task manageable and not too time-consuming.

We are using the method of finite differences. The continuous system is approximated on

a discrete lattice and the derivatives become finite differences. In this chapter, we will discuss all the numerical techniques that have been used for our studies:

- the minimisation of functionals: to find minimal energy solutions e.g. of the baby Skyrme model in the hedgehog ansatz.
- the time-evolution of an initial configuration: to study scattering behaviour in the baby Skyrme model and to get static non-radially symmetric minimal energy solutions by adding a damping term.
- the eigenvalue problem: to find the vibrational modes of a static solution around which we quantise.

We always try to point out alternative approaches. Some of our C programs use modified versions of Bernard Piette's routines and general data structure as described in [Pie96]. The implementation of the Metropolis-Simulated Annealing method to solitonic field theories is thought to be original work by Mark Hale and the author. Useful references of numerical techniques are: [PTVF92], [Pie96], [PZ98], [Ame77]. Boyd gives a refreshingly different viewpoint in [Boy89].

2.1 Discretisation Procedure

2.1.1 Discrete Lattice

A field value is associated to each point in continuum space and time. Discretising space means approximating this space as a discrete lattice in terms of N lattice points e.g. with a constant lattice spacing ϵ. A field value is associated to each lattice point:

$$\phi(x) \longrightarrow \phi_i$$

with $i = 1 \ldots N$. On a lattice, derivatives are replaced by finite differences. There are many ways of discretising derivatives; however all versions have to approach the continuum derivative for the limit of the lattice spacing ϵ going to zero. The explicit form also depends on the nature of the problem studied, particularly for non-linear PDEs and the Metropolis algorithm. The first derivative, for example, can be discretised as a forward difference

$$\frac{d\phi(x)}{dx} \longrightarrow \frac{\phi_i - \phi_{i+1}}{\epsilon}, \tag{2.1}$$

a backward difference

$$\frac{d\phi(x)}{dx} \longrightarrow \frac{\phi_{i-1} - \phi_i}{\epsilon} \tag{2.2}$$

or a combination of the two, the central difference

$$\frac{d\phi(x)}{dx} \longrightarrow \frac{\phi_{i-1} - \phi_{i+1}}{2\epsilon}. \tag{2.3}$$

Usually, we use the central differences for the PDEs. This excludes the Metropolis algorithm and the boundaries where we have to use the forward or backward difference. The discretised version of other derivatives, including in higher dimensions i.e. partial derivatives, are obtained by straightforward generalisation. The discretisation of the second derivative has the form

$$\frac{d^2\phi(x)}{dx^2} \longrightarrow \frac{\phi_{i-1} - 2\phi_i + \phi_{i+1}}{\epsilon^2}. \tag{2.4}$$

Extra care is needed for the the baby Skyrme model in (2+1) dimensions. Here, the form of the laplacian becomes crucial for an accurate numerical integration. Only a good approximation of the continuum laplacian i.e the use of information from more grid points can handle highly non-linear effects. The usual 5-point laplacian is too sensitive towards grid effects and fails to represent these non-linear effects reliably. Its 9-point analogue comes closer to restoring the rotational symmetry of the continuum laplacian. The discretised 2D 9-point laplacian has the general form

$$\nabla^2\phi(x,y) \longrightarrow \frac{1}{6\epsilon^2} \sum_{\alpha,\beta=-1}^{\alpha,\beta=1} W_{\alpha\beta}\ \phi_{\alpha,\beta} \tag{2.5}$$

where α and β are labelling the x and y axis. We are using the following weight distribution W of the lattice points:

1	4	1
4	-20	4
1	4	1

The centre lattice point has the biggest weight. The lattice points at the corners have weight one.

Our discretisation procedure is certainly not 'the last word'. There are many improvements possible: see [PZ98]. The use of a 25-point laplacian is desirable, but 2.5 times slower than the use of a 9-point laplacian. We are using a constant equally-spaced lattice. The use of a hexagonal grid instead of a square one increases accuracy, but more memory allocation is needed per lattice area. Another interesting idea is the multi-grid method. The closer one gets to the centre of the grid, the more lattice points there are. This is particularly useful for scattering of solitons. Nothing much happens outside the centre: two skyrmions do not really interact. Few lattice points are needed to represent this system. However, at the centre, the scattering of two skyrmions is a highly non-linear effect and a larger number of lattice points per area is certainly desirable. The multi-grid method helps at increasing accuracy and lowering memory needs. However, it is harder to implement and specific to the problem studied. Finally, some prefer to discretise the lagrangian and derive an equation of motion via the discretised Euler-Lagrange equations. This procedure leads to an exact discretised system and ensured a very good conservation of energy. We discretise the equation of motion and plug the fields back into the lagrangian. This approach should get closer to the real continuum dynamics, but the correspondence between equation of motion and energy density functional is not exact.

Thus, there is ample opportunity for improvement. Our numerical scheme may not be the most sophisticated one, but it is robust, reasonably fast, easy to implement and accurate

enough for our needs. New methods may improve accuracy, but one needs time to implement them and it probably leads to an increase in CPU time and memory needs.

2.1.2 ODE and PDE as sets of first order DEs

All ordinary differential equations (ODEs) and discretised partial differential equations (PDEs) can be broken down to ordinary first order differential equations. For example, a second order differential equation of the form

$$\frac{d^2 f(x)}{dx^2} = F\left(x, f(x), \frac{df(x)}{dx}\right) \tag{2.6}$$

is equivalent to a set of two first order ODEs

$$\frac{df(x)}{dx} = g(x) \tag{2.7}$$

$$\frac{dg(x)}{dx} = F\left(x, f(x), g(x)\right). \tag{2.8}$$

An ODE of order n can be re-written as a set of n first order ODEs. Similarly, any PDE can be written as a set of coupled first order ODEs. Our example is the wave equation with a damping term; ignoring any coefficients

$$\frac{d^2 u(x,t)}{dt^2} = \frac{d^2 u(x,t)}{dx^2} + \lambda \frac{du(x,t)}{dt}. \tag{2.9}$$

We discretise space as lattice points labelled by i and $u(x)$ becomes u_i. Now, (2.9) turns into an ODE for each lattice point i:

$$\frac{d^2 u_i(t)}{dt^2} = \frac{1}{\epsilon^2}\left(u_{i-1}(t) - 2u_i(t) + u_{i+1}(t)\right) + \lambda \frac{du_i(t)}{dt}. \tag{2.10}$$

Then we write the expression as a set of coupled first order ODEs:

$$\frac{du_i(t)}{dt} = v_i(t) \tag{2.11}$$

$$\frac{dv_i(t)}{dt} = \frac{1}{\epsilon^2}\left(u_{i-1}(t) - 2u_i(t) + u_{i+1}(t)\right) + \lambda v_i(t). \tag{2.12}$$

For every lattice point i, we have to solve a set of first order ODEs.

2.1.3 Integration Techniques

A differential equation is not sufficient description of a system. Additional information in terms of boundary conditions are needed. There are two types of problems: the initial value problem and the boundary value problem. All ODEs can be reduced to sets of first order ODEs.

Therefore, we concentrate on the one dimensional first order differential equation; written as

$$\frac{df}{dx} = F(x, f(x)). \tag{2.13}$$

If we know the value of the function f at $x = x_0$, then the function is uniquely determined. In general, an approximation of a function at $x + \epsilon$ is given in terms of its Taylor expansion

$$f(x + \epsilon) = f(x) + \epsilon \frac{df(x)}{dx} + O(\epsilon^2). \tag{2.14}$$

Thus, up to first order precision in ϵ, the value of the function at $x + \epsilon$ is

$$f(x + \epsilon) = f(x) + \epsilon F(x, f(x)) + O(\epsilon^2). \tag{2.15}$$

where we have used (2.13). We discretise the function on a discrete lattice. The lattice points are equally spaced by ϵ and labelled i with $x_i = x_0 + i\epsilon$. The function at the lattice point i is labelled f_i. We have

$$f_{i+1} = f_i + \epsilon F(x_i, f_i) + O(\epsilon^2). \tag{2.16}$$

Knowing the value of the function at the lattice point $i = 0$, f_0, we know the value of F at this lattice point and we can find f_1 up to first order precision in ϵ. We can repeat this procedure over and over again. Now, we know the value of f_{i+1} and F_{i+1} and we find the approximate value of the function f_{i+2}. This procedure is called the Euler integration method. The integration is only accurate to first order in ϵ. The error may be small for one integration step, but they sum up and become important.

The 2nd order Runge Kutta method is a step forward and gives second order precision. $f(x+\epsilon)$ is calculated via a linear combination of the derivative at the starting point x and a point $x+\alpha\epsilon$ within the integration interval; ergo $\alpha < 1$[1]

$$f_{i+1} = f_i + ak_1 + bk_2 \tag{2.17}$$

$$k_1 = \epsilon F(x_i, f_i) \tag{2.18}$$

$$k_2 = \epsilon F(x_i + \alpha\epsilon, f_i + \alpha k_1) \tag{2.19}$$

We have to find the value of the constants a, b, α that satisfy the Taylor expansion of f up to second order:

$$f_{i+1} = f_i + \epsilon F(x_i, f_i) + \frac{1}{2}\epsilon^2 \frac{dF}{dx}(x_i, f_i) + O(\epsilon^3). \tag{2.20}$$

Expanding (2.17) as a Taylor series, we get

$$f_{i+1} = f_i + (a+b)\epsilon F(x_i, f_i) + b\alpha\epsilon^2 \frac{dF}{dx}(x_i, f_i) + O(\epsilon^3). \tag{2.21}$$

Comparing both expansions, we may choose $a = 0$, $b = 1$ and $\alpha = \frac{1}{2}$. We end up with the following expressions:

$$f_{i+1} = f_i + \epsilon F(x_i + \frac{1}{2}\epsilon, f_i + \frac{1}{2}k_1) \tag{2.22}$$

$$k_1 = F(x_i, f_i) \tag{2.23}$$

We use a more sophisticated version of the Euler method: the 4th order Runge-Kutta method. It is accurate to 4th order in terms of the Taylor series expansion. The idea is to use derivative information from the starting point, two midpoints and the final point. The Runge-Kutta 4th order formula takes the form:

$$f_{i+1} = f_i + \frac{1}{6}(k_1 + 2k_2 + 2k_3 + k_4)$$

[1] following [Pie96]

$$k_1 = \epsilon F(x_i, f_i)$$

$$k_2 = \epsilon F(x_i + 0.5\epsilon, f_i + 0.5k_1)$$

$$k_3 = \epsilon F(x_i + 0.5\epsilon, f_i + 0.5k_2)$$

$$k_4 = \epsilon F(x_i + \epsilon, f_i + k_3)$$

Higher order Runge-Kutta methods are not necessarily more accurate. However, the use of an adaptive step size version of the Runge-Kutta method may be desirable. Often, the integration is done over a very smooth interval and a bigger step size ϵ is sufficient. Or, a smaller step size is needed for regions with a lot of non-linear effects e.g. the region where two solitons scatter. An adaptive step size version would automatically take this into account by making error estimates and adapt the step size accordingly (see [Pie96]). [BFR78] provides supplementary information on the Runge-Kutta-Fehlberg method.

2.2 Minimisation of Functionals

We start out with the minimisation of a functional E; typically the integral of an energy density $\mathcal{E}$ in one dimension over the interval $[a, b]$:

$$E = \int_a^b dx\ \mathcal{E}[x, f(x), f'(x)] \tag{2.24}$$

where $f(a)$ and $f(b)$ are known. This corresponds to searching for the minimal energy solution $f(x)$ of the system. We use three different techniques. Apart from the shooting method, they can be extended to more than one dimension. However, the decrease in the speed of convergence and the increase in memory needs and CPU time is considerable and puts a serious limit on any higher dimensional minimisation.

We can try to find the minimal energy solution directly from the functional: see [PTVF92, chapter 10]. Marc Hale and the author have implemented the Metropolis–Simulated Annealing method as an interesting alternative to the standard techniques (to be discussed later). This brute force method is qualitatively very different from any other technique and builds on physical intuition. However, the standard procedure uses the Euler-Lagrange equation of the functional E with respect to the function $f(x)$ to find the minimal energy solution $f(x)$. The problem turns out to be equivalent to a two point boundary value problem satisfying the following differential equation:

$$\frac{d}{dx}\left(\frac{dE}{df'}\right) - \frac{dE}{df} = 0. \tag{2.25}$$

It is a second order ODE and equivalent to a set of two first order ODEs. There are two standard ways of approaching the problem: see [PTVF92, chapter 17]. The shooting method transforms the two boundary values problem into an initial value problem and adjusts the initial conditions to fit the boundary value. The relaxation method starts out with an initial guess function and the function relaxes to the hopefully global minimum.

2.2.1 Shooting Method (only for 1D)

There are two ways of uniquely determining the DE (2.25): either by specifying the two boundary values or the value of the function and its derivative at one of the two boundaries. For the shooting method, the two boundary value problem is turned into an initial value problem. We adjust the value of the derivative of the function at one boundary in such a way that the function matches the second boundary value. Therefore, we have to integrate the function over and over again from the one boundary to the other; using different values for the derivative to get the right boundary value. In a sense, we shoot a bullet from a certain height $f(a)$ at $x = a$ and have to adjust the angle (the derivative) to hit the target at the height $f(b)$ at $x = b$. In this example, the differential equation would represent the gravitational field and the air

resistance.

The second order ODE (2.25) is a set of two first order ODEs

$$\frac{df(x)}{dx} = g(x) \tag{2.26}$$

$$\frac{dg(x)}{dx} = F(x, f(x), g(x)) \tag{2.27}$$

which satisfy two known boundary values $f(a)$ and $f(b)$. We know $f(a)$ and guess $\alpha = \frac{df(a)}{dx}$. Then we numerically integrate up to the point $x = b$ and try to match the value of the integrated function $f_\alpha(b)$ to $f(b)$. We adjust α accordingly. Our algorithm follows:

1. INPUT a, b, $f(a)$, $f(b)$.
2. INPUT interval $[\alpha_{MIN},\alpha_{MAX}]$ for $\alpha = \frac{df(a)}{dx}$. α_{MIN} should undershoot i.e. $f_\alpha(b) < f(b)$ and α_{MAX} should overshoot i.e. $f_\alpha(b) > f(b)$.
3. COMPUTE $\alpha = \frac{\alpha_{MAX}+\alpha_{MIN}}{2}$.
4. DO a Runge-Kutta integration from $x = a$ to $x = b$.
5. IF $f_\alpha(b) > f(b)$ then PUT $\alpha_{MAX} = \alpha$. IF $f_\alpha(b) < f(b)$ then PUT $\alpha_{MIN} = \alpha$.
6. GO TO 3 unless $f_\alpha(b) \approx f(b)$.
7. DO one more Runge-Kutta integration.
8. SAVE function and COMPUTE energy.

There are certainly other ways of determining α: see [PTVF92, chapter 17].

2.2.2 Relaxation Methods

A numerical relaxation is another way of solving the differential equation. We are using two different approaches.

One might derive the full equation of motion from the lagrangian and add a damping term to the differential equation. The system becomes dissipative and energy decreases with time until a minimum is reached. A configuration close to the real solution is taken as an initial condition. The kinetic energy is gradually taken out of the system by adding the damping factor to the time-evolution equation. In fact, absorbing at the boundaries can have a similar effect: the time-derivatives of the field components are multiplied by a factor that goes smoothly to zero at the boundary. Thus finding a solution is translated into a relaxation of a time-evolved configuration. We describe this technique in more detail during our discussion of the time-evolution of the baby Skyrme model i.e. scattering and our search for multi-skyrmions. Actually, this technique is only useful if one wants to do the time-evolution problem anyway.

A much more efficient way is the Gauss-Seidel over-relaxation technique [PTVF92, chapter 17]. Let us re-write equation (2.25) in the following way:

$$0 = \frac{d^2 f(x)}{dx^2} - F\left(x, f(x), \frac{df(x)}{dx}\right). \tag{2.28}$$

Then we construct a time-dependent DE, basically a diffusion equation,

$$\frac{df(x,t)}{dt} = \frac{d^2 f(x,t)}{dx^2} - F\left(x, f(x,t), \frac{df(x,t)}{dx}\right) \tag{2.29}$$

whose limit, for large time t and $\frac{df}{dt} = 0$, satisfies the original DE. So we may start out with any initial configuration ideally satisfying the two boundary conditions. If the system settles down i.e. $\frac{df}{dt} = 0$, this configuration is the solution to the original DE. We modify the diffusion equation and add a convergence factor ω:

$$\frac{df(x,t)}{dt} = \omega dx^2 \left(\frac{d^2 f(x,t)}{dx^2} - F\left(x, f(x,t), \frac{df(x,t)}{dx}\right)\right) \tag{2.30}$$

The coefficient of the leading term $\frac{d^2f}{dx^2}$ is dimensionless and the factor ω determines the speed of convergence. Obviously, a good initial guess is vital for a fast convergence. There are many ways of time-integrating the DE (2.30). The Euler method proves to be as good as the Runge-Kutta method, for we are only interested in the asymptotic behaviour of the system. ω needs to be smaller than one. Another integration technique is the Crank-Nicholson method. We are using the Gauss-Seidel over-relaxation (SOR) method where ω needs to be smaller than two. The SOR is in effect the Euler method using up-dated information from the already computed field values at lattice points. The subroutine, we are using, computes all even lattice points on the grid and then uses this up-dated information to compute the odd points. This technique ensures better convergence.

There are other ways of using up-dated information. One scheme uses the new data sequentially i.e. compute the first point, compute the second point using the up-dated field value from the first point and so on. Even the SOR may have slow convergence, because the optimal choice of ω can rarely be theoretically determined for a non-linear system. Therefore, the search for the ω giving best convergence is very important. We do it by trial and error. However, one could use a simple algorithm that integrates a few time steps and finds the optimal value. This should be repeated 'after a while', because the optimal value should change in non-linear theories.

2.2.3 Metropolis–Simulated Annealing

We propose to use a more general, flexible and easy-to-implement minimisation technique: *Simulated Annealing*. The standard minimisation techniques solve the corresponding Euler-Lagrange equation of the functional via the shooting method or the relaxation method, for example. Unfortunately, these methods have some drawbacks:

The Euler-Lagrange equation becomes very extensive if we deal with high order lagrangians

and the constraints on the field vector. A good example is the time-evolution of the Skyrme model. Our work was just manageable, but including higher order terms would make our task very difficult.

The shooting method is restricted to one-dimensional problems. The relaxation technique depends on our choice of the initial configuration. It may not converge or we end up in a local minimum (which often turns out to be the global minimum). The method cannot escape a local minimum.

The discretisation of the field equation might be a worse option than the discretisation of the functional.

There are clear limitations on the use of the standard techniques for complicated lagrangians. Nevertheless, for our study of the baby Skyrme model, the methods are sufficient and give satisfactory results.

Unlike the iterative minimisation methods, Simulated Annealing is a randomisation technique. In 1953, Metropolis and al. proposed an algorithm, now called the *Metropolis algorithm*, that describes the evolution of a statistical system to thermal equilibrium. Assume the energy of the system is changed by a random thermal fluctuation that modifies the system configuration C to C_{new}. If the energy of the new configuration C_{new} is lower, the system accepts the change. If the energy is higher, there is a probability of transition

$$\mathcal{P}(C \longrightarrow C_{new}) = e^{\left(\frac{E-E_{new}}{kT}\right)} \tag{2.31}$$

at temperature T; according to the Boltzmann probability distribution. Hence, the system will accept an upward step in energy with a probability $\mathcal{P}$. This is crucial to achieve thermal equilibrium: the system can escape a local minimum. Figure (2.2.3) shows the Metropolis algorithm. Note that $\mathcal{F}$ stands for the functional to be minimised.

Figure 2.1: The Metropolis algorithm: Scheme for thermal equilibrium

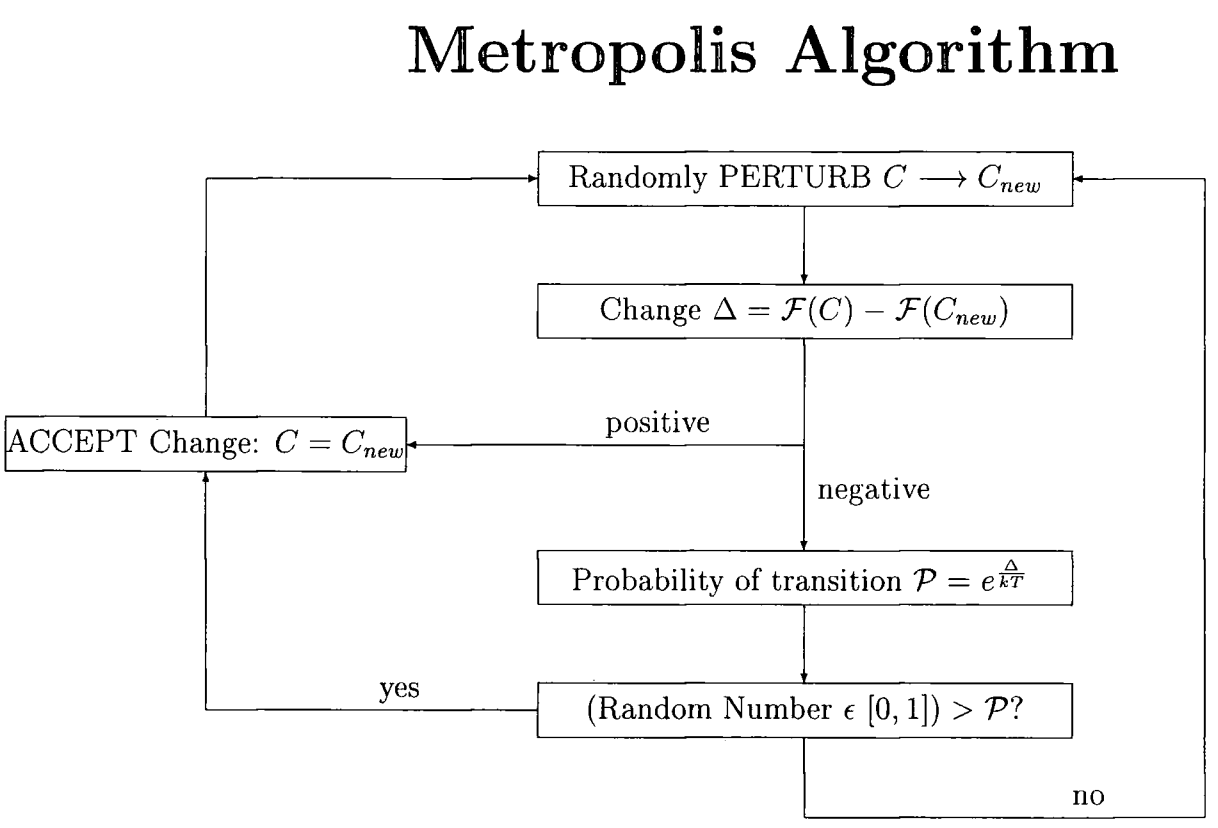

Figure 2.2: Simulated Annealing: Scheme for Minimisation

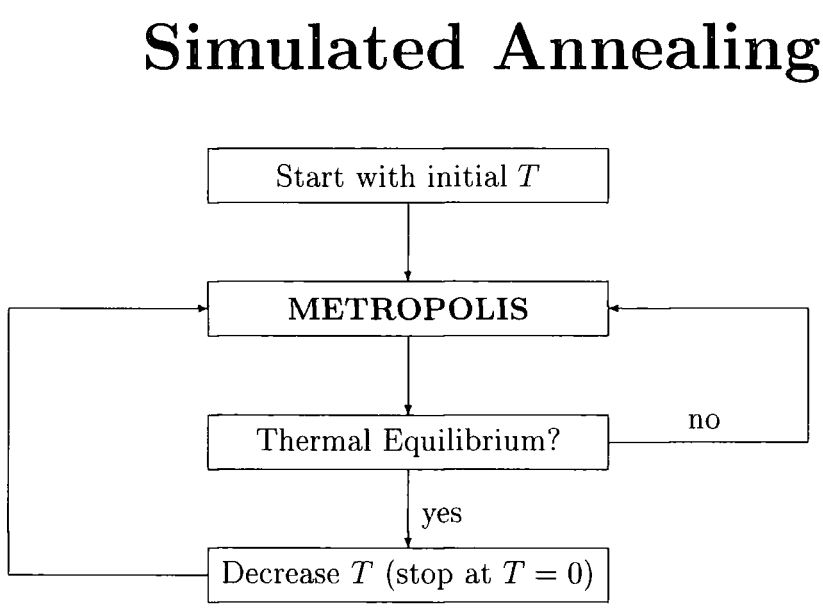

In effect, the algorithm simulates the annealing of a solid. If you cool down the solid sufficiently slow, you reach the ground state of the solid. Here, sufficient slow cooling means thermal equilibrium at each stage of the cooling. Thirty years later, Kirkpatrick and others realised a deep analogy between annealing of solids and the optimisation problem. If we define the energy to be the function to be optimised, we can use the Simulated Annealing method to find the minimum of the function. We start out with an initial temperature T and run the Metropolis algorithm until we reach thermal equilibrium. Then we decrease the temperature and re-do the procedure until $T = 0$. Simulated Annealing is a conceptually easy-to-understand minimisation technique: see figure (2.2.3).

Its implementation in a computer code is straightforward. The method has mainly been used for discrete problems e.g. the travelling salesman. The application to a continuous minimisation

problem deserves some reflexion on the discretisation of the derivatives. A more general and crucial question is the cooling schedule. There are several issues we had to address in order to implement the technique:

Which initial guess? Unlike for the relaxation method, the initial configuration is not important as the system should be able to jump out of local minima. Of course, an initial guess close to the global minimum solution reduces the running time.

How to randomly perturb C? The perturbation has to depend on the temperature e.g. small changes at low temperature. A smooth random distribution e.g. a Gaussian that scales with T is desirable.

When is equilibrium reached? The correct answer is to do a statistical study on the changes done to the system and compare this statistical distribution with the Boltzmann distribution. However, one can just loop sufficiently long at the same temperature. The number of loops can be determined empirically.

At what initial temperature to start? Conceptually speaking, it corresponds to the temperature of the initial configuration. A too high temperature 'melts' the initial configuration to the liquid phase and the cooling time increases. A too low initial temperature may freeze the system into a local minimum. Hence, better a temperature that is too high than too low.

Decrease T by which step size? This depends on how we determine the equilibrium. If we loop a fixed number of times at a given temperature T, the decrement of T should depend on the evolution. If we loop until equilibrium, the decrement of T should be constant.

Restarting i.e. cooling, re-heating and cooling? Often, the cooling is too fast and we have to repeat the procedure. We use the lowest energy configuration as the initial guess and a

lower initial temperature.

Discretisation of continuous functional $\mathcal{F}$? This is a critical part of the minimisation scheme. It's important NOT to use the central difference, because it does not depend on the function at the centre point. If we randomly change the configuration at a given point, the derivative will not be sensitive to the change at all and not affect the probability of transition.

Use of constraints? Constraints are no problem, because we just use random perturbations that satisfy the constraints.

To summarise, the cooling schedule is very crucial, because it determines the speed of convergence. A simple schedule will do, but it will be much slower than a carefully thought out one. Different schedules are discussed in [vLA87, chapter 5 and 6] and [BFR78, section 10.9]. Our cooling schedule is simple: Budget K total Metropolis moves. Start with temperature T_0. Loop m times at a given temperature T. Reduce T by

$$T = T_0 \left(1 - k/K\right)^{\alpha} \tag{2.32}$$

where k is the total number of moves sofar. α determines how much time is spent at different T i.e. large α means more loops at lower temperature. We set $\alpha = 1$ for computational efficiency. All others parameters are chosen empirically. We implement this technique in *Classical Aspects* and discuss the choice of parameters chosen in more detail.

2.3 Time evolution of initial configuration

In this section, we describe the time evolution of an initial configuration. We need this framework to study the scattering of skyrmions. Another application is the search for static solutions

by adding a damping term. The time-evolution is determined by the equation of motion of the system. We discretise space and do a time integration of an initial configuration via the Runge-Kutta method, for example. The boundary of the lattice can cause problems, for the derivatives cannot be computed. A way around it is to set the derivatives to zero or impose periodic boundary conditions. The choice really depends on which kind of dynamics you are looking at. It is important to monitor the quality of the time-integration by looking at the conserved quantities involved, namely: the topological charge and the Noether quantities like total energy etc. We present a time-evolution of a specific model: the baby Skyrme model. This example is most appropriate, because it is our main tool to analyse classical aspects of the baby Skyrme model in the next chapter. The time-evolution in 1D, for example the Sine-Gordon system, is a straightforward simplification to the one of the baby Skyrme model.

2.3.1 The equation of motion: (2+1)D baby Skyrme model

First, we need to obtain the equation of motion of the baby Skyrme model. Using the $\vec{\phi}$ notation, we have to add a Lagrange multiplier to the baby Skyrme lagrangian (1.73) in order to take care of the constraint $\vec{\phi}\cdot\vec{\phi}=1$. We get the equation of motion for each field component ϕ_a and λ via the Euler-Lagrange equation. Solving for λ, the equation of motion takes the form:

$$\begin{aligned}\partial_\mu\partial^\mu\phi_a-(\vec{\phi}\cdot\partial_\mu\partial^\mu\phi)\phi_a-2\theta_1[(\partial_\nu\vec{\phi}\cdot\partial^\nu\vec{\phi})\partial_\mu\partial^\mu\phi_a+(\partial_\mu\partial^\nu\vec{\phi}\cdot\partial^\mu\vec{\phi})\partial_\nu\phi_a\\-(\partial^\nu\vec{\phi}\cdot\partial^\mu\vec{\phi})\partial_\nu\partial_\mu\phi_a-(\partial_\nu\partial^\nu\vec{\phi}\cdot\partial^\mu\vec{\phi})\partial_\mu\phi_a+(\partial_\mu\vec{\phi}\cdot\partial^\mu\vec{\phi})(\partial_\nu\vec{\phi}\cdot\partial^\nu\vec{\phi})\phi_a\\-(\partial_\nu\vec{\phi}\cdot\partial_\mu\vec{\phi})(\partial^\nu\vec{\phi}\cdot\partial^\mu\vec{\phi})\phi_a]+\frac{1}{2}\theta_2\frac{dV}{d\phi_3}(\delta_{a3}-\phi_a\phi_3)=0\end{aligned}\tag{2.33}$$

The equation of motion can be rewritten as

$$K_{ab}\ddot{\phi}_b=\mathcal{F}_a\left(\vec{\phi},\dot{\vec{\phi}},\partial_i\vec{\phi}\right)$$

with

$$K_{ab} = (1 + 2\theta_1 \partial_i \vec{\phi} \cdot \partial_i \vec{\phi})\delta_{ab} - 2\theta_1 \partial_a \phi \partial_b \phi. \tag{2.34}$$

The inverse matrix of K exists in an analytic, but rather messy form (see appendix A). Now,

$$\ddot{\phi}_a = K^{-1}_{ab} \mathcal{F}_b \left(\vec{\phi}, \dot{\vec{\phi}}, \partial_i \vec{\phi} \right). \tag{2.35}$$

The equation of motion is a 2nd order partial differential equation or a set of two 1st order partial differential equation,

$$\begin{pmatrix} \dot{\phi}_a \\ \dot{\psi}_a \end{pmatrix} = \begin{pmatrix} \psi_a \\ K^{-1}_{ab} \mathcal{F}_b \left(\vec{\phi}, \vec{\psi}, \partial_i \vec{\phi} \right) \end{pmatrix}, \tag{2.36}$$

and we can time integrate it with the Runge-Kutta 4th order.

Initial set-up:

The initial field configuration is a linear superposition of static solutions with or without initial velocity. The superposition is justified, because the profile function decays exponentially. The superposition is done in the complex field formalism W i.e. the stereographic projection of the $\vec{\phi}$ field of S^2 (see [PZ95]). We use the profile function of a static solution (typically of topological charge one) to obtain

$$W = \tan\left(\frac{f(r)}{2}\right) e^{-in\theta}. \tag{2.37}$$

This equation holds in the rest frame of a static skyrmion solution centred around its origin and $\frac{dW}{dt} = 0$. We may introduce moving solutions by switching to a different frame of reference. This can be done by performing a Lorentz boost on the rest frame of a given W, because W is a Lorentz scalar. The time derivative of W becomes

$$\frac{dW}{dt} = e^{-in\theta} \left(\frac{f'(xv_x + yv_y)}{2\sqrt{x^2+y^2}\cos^2\left(\frac{f}{2}\right)} + i\frac{n\tan\left(\frac{f}{2}\right)(xv_x - yv_y)}{x^2+y^2} \right) \tag{2.38}$$

where x undergoes a Lorentz contraction $\gamma(x-v_x t)$ and y $\gamma(y-v_y t)$. Now it is easy to construct a linear superposition of individual, moving or not, baby skyrmion solutions W_α by

$$W(x,y) = \sum_\alpha W_\alpha(x - x_\alpha, y - y_\alpha) \tag{2.39}$$

where (x_α,y_α) is the location of the centre of the αth skyrmion. It is important that the different skyrmions are not too close to each other. Finally, the complex field is re-written in terms of the field $\vec{\phi}$ and its derivative.

Integration Technique on S^2

It is important to make sure that the time-evolution does not introduce significant numerical errors. A integration method, no matter how sophisticated, will always introduce small error. Those should not make a qualitative or even quantitative difference, for they are random to a certain degree. Systematic errors are far more dangerous as they can significantly change the outcome of a simulation; often the system becomes singular–it 'explodes'. The first thing to do is to monitor the conserved quantity required by Noether's theorem and by the topology.

The equation of motion incorporates the O(3) constraint

$$\vec{\phi}\cdot\vec{\phi} = 1 \tag{2.40}$$

because of the added Lagrange multiplier. The field should therefore always lie on the sphere. This fact provides a crucial check of the numerically integrated fields. These numerically computed fields are not exact. They leave the sphere and need to be projected back onto the sphere. The most simplest and sufficient projections are:

$$\phi_a \longrightarrow \frac{\phi_a}{\sqrt{\vec{\phi}\cdot\vec{\phi}}} \tag{2.41}$$

$$\partial_t\phi_a \longrightarrow \partial_t\phi_a - \frac{\partial_t\vec{\phi}\cdot\vec{\phi}}{\vec{\phi}\cdot\vec{\phi}}\phi_a \tag{2.42}$$

Of course, the space derivatives may also be corrected. See [PZ98] for further discussions.

Relaxation technique

We mentioned that it is possible to find static solutions by relaxing a configuration. A damping term in the equation of motion will gradually take the kinetic energy out of the system; the system becomes dissipative. The equation (2.33) changes to

$$\ddot{\phi}_a = K_{ab}^{-1}\mathcal{F}_b\left(\vec{\phi}, \vec{\dot{\phi}}, \partial_i\vec{\phi}\right) - \gamma\dot{\phi}_a. \tag{2.43}$$

where γ is the damping coefficient. We set γ to 0.1, but most values will do as long as they are not too large. Another approach is to absorb the outwards travelling kinetic energy waves in the boundary region.

2.4 Eigenvalue Problem

The eigenvalue problems are very common and important. For example, we will need it to calculate the mass correction in *Quantum Aspects*. *Numerical Recipes* devotes a whole chapter to it: see [PTVF92, chapter 11]. The aim is to solve the eigenvalue equation:

$$\hat{\mathrm{A}}(\mathrm{x})\eta(x) = \lambda\eta(x) \tag{2.44}$$

where $\hat{\mathrm{A}}$ is an operator, η is the eigenvector with eigenvalue λ. We are discretising the system and end up with

$$\mathbf{A}\vec{\eta} = \lambda\vec{\eta} \tag{2.45}$$

where $\mathbf{A}$ is an N x N matrix. The equation (2.45) only holds if and only if

$$\det(\mathbf{A} - \lambda\mathbf{1}) = 0.$$

If we expand out, we get a Nth polynomial in λ which gives N solutions, not necessarily distinct. There are several methods available. We discuss the brute force matrix diagonalisation. It works fine in one dimension, but the computational effort grows like N^3. The shooting method is very good but can only be used in one dimension. We also discuss a diffusion method.

Finally, the eigenvalue problem depends on the system itself; specifically on the structure of the matrix: the sparser it is, the faster the convergence. It is easy in one dimension, but very difficult in two or three.

2.4.1 Brute Force Matrix & Shooting Method

First, we reduce the real and symmetric matrix **A** to a tridiagonal matrix via the Householder reduction. The number of operations grows with $\frac{4}{3}N^3$ (if we want both eigenvalues and eigenvectors). We are using the routine *tred2* from *Numerical Recipes*: see [PTVF92, page 474]. The final step i.e. the diagonalisation is done by the routine *tqli* (see [PTVF92, page 480]) using the QL algorithm with implicit shifts. Again, the number of operations grows with order n^3. The technique works well in one dimension, but it is too slow in two or three dimensions.

Often, the eigenvalue equation is equivalent to the static Schrödinger equation:

$$\left(-\frac{d^2}{dx^2} + V(x)\right)\psi(x) = E\psi(x). \tag{2.46}$$

We can discretise the equation and get a relationship for ψ^{n+1} in terms of the value of ψ^n and ψ^{n-1}. If we further assume that the function ψ goes to zero at spatial infinity, we are able to use the shooting method. We pick a value for large negative x with small $V(x) - E$. Then we set ψ to zero and start integrating using the relationship. If we know the eigenvalue, we can get the eigenfunction up to a factor. This factor depends on our starting point of integration and can be 'normalised away'. If we don't know the eigenvalue, we can do a shooting method and narrow down the energy value for which the function goes to zero at $x = -\infty$. We use the

routine written by Bernard Piette.

2.4.2 Diffusion Method

The idea is equivalent to finding the minimal-energy solution via relaxation. First, we relax an initial configuration down to its minimal energy solution: the lowest mode. We normalise this first mode. Then we create a new initial configuration from which we project out the first mode. We re-do the relaxation projecting out this mode again from time to time. We end up with the second lowest mode which we normalise and orthogonalise with respect to the first mode. Then we project both modes out of the initial configuration and re-do the relaxation. In this way, we build up an archive of the lowest orthonormal modes. This technique has been used by Barnes and Turok in [BT97]. However, we use the Runge-Kutta integration scheme instead of the Crank-Nicholson integration technique. A crucial drawback of the diffusion technique is the accumulation of numerical errors for higher modes, because a higher mode is computed by using information from already computed lower modes.

Chapter 3

Classical Aspects of Solitons

"Mein Busen fühlt sich jugendlich erschüttert,
vom Zauberhauch, der Euren Zug umwittert."
(from Goethe's Faust and dedicated to my beloved baby skyrmions)

In this chapter, we discuss classical aspects of solitons using the numerical methods discussed in the previous chapter. We want to emphasise that numerical methods are the only possible way of studying non-integrable solitons in a general framework. The main part of the work repeated in this chapter consists of the study of the multi-skyrmion structure of the baby Skyrme models. This work will soon to be published in *Non-linearity*. We find that the structure of multi-skyrmions depends on the potential of the baby Skyrme models. We also include other relevant information and numerical results which we have excluded from the to-be-published version. Then, we present our foundation work on the use of Simulated Annealing in one dimension. We show that Simulated Annealing works well for known results. Further, we emphasise the ease with which we can include higher order terms. The work on Simulated Annealing has been done in co-operation with Mark Hale. Finally, we briefly discuss how to include a higher order term i.e. six-derivatives term into the lagrangian and suggest further

research on this topic.

3.1 Baby Skyrme Models and Their Multi-Skyrmions

First, we analyse the structure of minimal-energy solutions of the baby Skyrme model for any topological charge n; the baby multi-skyrmions. Unlike in the (3+1)D nuclear Skyrme model, a potential term must be present in the (2+1)D baby Skyrme model to ensure stability of skyrmions. The form of this potential term has a crucial effect on the existence and structure of baby multi-skyrmions. The simplest holomorphic baby Skyrme model has no known stable minimal-energy solution for n greater than one. The other baby Skyrme model studied in the literature possesses non-radially symmetric minimal-energy configurations that look like 'skyrmion lattices' formed by skyrmions with $n = 2$. We discuss a baby Skyrme model with a potential that has two vacua. Surprisingly, the minimal-energy solution for every n is radially-symmetric and the energy grows linearly for large n. Further, these multi-skyrmions are tighter bound, have less energy and the same large r behaviour than in the model with one vacuum. We rely on numerical studies and approximations to test and verify this observation.

3.1.1 Introduction

The baby Skyrme model is a modified version of the (2+1)D S^2 sigma model. The addition of a potential and a Skyrme term to the lagrangian ensures stable solitonic solutions. The Skyrme term has its origin from the nuclear Skyrme model proposed in [Sky61] and the baby Skyrme model can therefore be viewed as its (2+1)D analogue. However, in (2+1) dimensions, a potential term is necessary in the baby Skyrme models to ensure stability of skyrmions; this term is optional in the (3+1)D nuclear Skyrme model. The multi-skyrmion structure of the nuclear Skyrme model has been studied numerically by Braaten et al. [BTC90] and by Battye

and Sutcliffe [BS97].

The form of the potential term is largely arbitrary and gives rise to a multitude of possible baby Skyrme models. In the literature, two specific models have been studied in great detail (see [PZ95],[PSZ95b]). The simplest holomorphic model does not seem to admit stable n-skyrmions where n is greater than one. (We define an n-skyrmion to be the minimal-energy solution with topological charge n.) And the 'baby Skyrme model'[1] with a very simple potential possesses rather beautiful, non-radially symmetric multi-skyrmions. A new[2] slightly modified potential gives rise to a remarkably different structure for multi-skyrmions: we call it the new baby Skyrme model. In fact, we show that the energy density of all n-skyrmions turns out to be radially symmetric configurations, namely rings of larger and larger radii. Clearly, the choice of the potential term has a major impact on the formation of multi-skyrmions and their shape.

We start with a short introduction to the baby Skyrme models. The earlier results for the two baby Skyrme models are re-calculated and reviewed in the light of their multi-skyrmion structure. We present a numerical and theoretical study of the new baby Skyrme model. We create n-skyrmions by putting n 1-skyrmions in an attractive channel. They form a bound state which we relax to the minimal-energy state. We find radially-symmetric new baby multi-skyrmions solutions. Therefore, we are led to look for static hedgehog solutions. Finally, we make some general comments about the existence and structure of multi-skyrmions depending on the choice of the potential term.

[1] it is called baby Skyrme model!... we call it old baby Skyrme model to avoid confusion.

[2] first used in [KPZ98].

3.1.2 Baby Skyrme models

Non-trivial Topology & 'Stable' Lagrangian

Baby Skyrme models[3] admit stable field configurations of finite energy and solitonic nature. These baby skyrmions are topological solitons. Their existence is a consequence of the non-trivial topology of the mapping of physical space into field space at a given time t:

$$\mathcal{M} : \mathcal{S}^2 \longrightarrow \mathcal{S}^2. \tag{3.1}$$

Here, physical space $\mathcal{R}^2$ is compactified to $\mathcal{S}^2$ by requiring spatial infinity to be equivalent in each direction. This one-point compactification is necessary to ensure a non-trivial mapping. The target manifold (or internal space) is described by a three-dimensional vector $\vec{\phi}$ with $\vec{\phi} \cdot \vec{\phi} = 1$. The non-trivial topology allows to classify maps into equivalence classes; each of which has a unique conserved quantity: the topological charge

$$Q = \frac{1}{4\pi} \epsilon^{abc} \int dxdy \phi_a \left(\partial_x \phi_b\right) \left(\partial_y \phi_c\right) \tag{3.2}$$

given in integer units. See chapter *Introduction.*

Further, stability is ensured by an appropriate choice of lagrangian terms of field derivatives and a potential. The lagrangian has the form

$$L = \partial_\mu \vec{\phi} \cdot \partial^\mu \vec{\phi} - \theta_S \left[(\partial_\mu \vec{\phi} \cdot \partial^\mu \vec{\phi})^2 - (\partial_\mu \vec{\phi} \cdot \partial_\nu \vec{\phi})(\partial^\mu \vec{\phi} \cdot \partial^\nu \vec{\phi}) \right] - \theta_V V(\vec{\phi}) \tag{3.3}$$

and consists of three terms; from left to right: the sigma model, the Skyrme and the potential term. At a classical level, the coefficient of the sigma model term can always be set to one by re-defining θ_S and θ_V. Thus, there are two free parameters in the model. Each term has a different scaling behaviour and, together, they ensure stability according to Derrick's theorem[Raj96, pages 47-48]. We require that the potential vanishes at infinity for a given

[3] see review [PZ95]

vacuum field value; for example $\vec{\phi} = (0, 0, 1)$. Care should be taken that the potential term is invariant under the $SO(2)$ group transformation of ϕ; this becomes vital for the use of the hedgehog ansatz. There is a further possibility that the potential is also zero for other values of the field. Actually, the fact that the potential vanishes at infinity makes the energy finite and justifies the one-point compactification of physical space discussed above.

Hedgehog Static Solutions

The static energy functional density of the baby Skyrme model is

$$\mathcal{E} = \left(\partial_i\vec{\phi}\cdot\partial_i\vec{\phi}\right) + \theta_S\left[\left(\partial_i\vec{\phi}\cdot\partial_i\vec{\phi}\right)^2 - \left(\partial_i\vec{\phi}\cdot\partial_j\vec{\phi}\right)\left(\partial_i\vec{\phi}\cdot\partial_j\vec{\phi}\right)\right] + \theta_V V(\vec{\phi}). \tag{3.4}$$

We look for solutions of the corresponding Euler-Lagrange equation. This is a very difficult task. The hedgehog ansatz provides a starting point of our search for static solutions; in polar coordinates

$$\vec{\phi} = \begin{pmatrix} \sin[f(r)]\cos(n\theta - \chi) \\ \sin[f(r)]\sin(n\theta - \chi) \\ \cos[f(r)] \end{pmatrix}. \tag{3.5}$$

Note that n is a non-zero integer (it is the topological charge as we will discover later), θ the polar angle, χ a phase shift and $f(r)$ the profile function satisfying certain boundary conditions. The hedgehog field (3.5) is chosen, because it is invariant under the maximal group of symmetry that leaves the energy functional invariant for non-zero topological charge (see [PSZ95b, page 167]). According to the 'Principle of Symmetric Criticality' or 'Coleman-Palais theorem'([MRS93, pages 72-76]), we can search for static solutions invariant under any symmetry by solving the variational problem for the invariant field.

The integrated energy density takes the form

$$E = (4\pi)\frac{1}{2}\int_0^\infty r dr\left(f'^2 + n^2\frac{\sin^2 f}{r^2}(1 + 2\theta_S f'^2) + \theta_V\tilde{\mathrm{V}}(f)\right). \tag{3.6}$$

The energy density depends only on the profile function $f(r)$: the invariant field. It is independent of the polar angle and has a radial symmetry. Then, the corresponding Euler-Lagrange equation with respect to the invariant field $f(r)$ leads to a second-order ODE,

$$\left(r + \frac{2\theta_S n^2 \sin^2 f}{r}\right) f'' + \left(1 - \frac{2\theta_S n^2 \sin^2 f}{r^2} + \frac{2\theta_S n^2 \sin f \cos f f'}{r}\right) f' - \frac{n^2 \sin f \cos f}{r} - r\frac{\theta_V}{2}\frac{d\tilde{V}(f)}{df} = 0, \tag{3.7}$$

which we re-write in terms of the second derivative of the profile function:

$$f'' = \mathcal{F}(f, f', r). \tag{3.8}$$

The profile function $f(r)$ is a static solution of the baby Skyrme model. These static solutions are certainly critical points, but not necessarily global minima. However, it has been proven that the hedgehog solution of the nuclear Skyrme model is the minimal-energy solution for topological charge one (see [MRS93, pages 80-88]). Further, an explicit hedgehog solution with the topological charge one exists for the holomorphic baby Skyrme model and has the lowest energy. Therefore, it is reasonable, but not proven here, that the hedgehog solution for topological charge one is the minimal-energy solution.

The topological charge takes the form

$$T = -\frac{n}{2}\int_0^\infty r dr \left(\frac{f' \sin f}{r}\right) = \frac{n}{2}[\cos f(\infty) - \cos f(0)]. \tag{3.9}$$

The boundary conditions for the profile function need to be fixed. Our value of the vacuum at infinity is $\vec{\phi} = (0, 0, 1)$ and we may choose

$$\lim_{r\to\infty} f(r) = 0. \tag{3.10}$$

Then the value of the profile function at the origin needs to be

$$f(0) = m\pi \tag{3.11}$$

where m is an odd integer. The topological charge is n in integer units. From now on, we write all other quantities in 4π units. All $m \neq 1$ solutions are expected to decay into $m = 1$ solutions. Thus, in this paper, we concentrate our attention on solutions corresponding to $m = 1$.

The Equation of Motion

A Lagrange multiplier term $\lambda(\vec{\phi} \cdot \vec{\phi} - 1)$ needs to be included in the lagrangian (3.3) to take care of the S^2 constraint (see [Raj96, pages 48-58]). The equations of motion for each field component ϕ_a and λ are obtained via the Euler-Lagrange equation. Solving for λ, the equation of motion takes the form

$$\begin{aligned}\partial_\mu\partial^\mu\phi_a - (\vec{\phi}\cdot\partial_\mu\partial^\mu\phi)\phi_a - 2\theta_S[(\partial_\nu\vec{\phi}\cdot\partial^\nu\vec{\phi})\partial_\mu\partial^\mu\phi_a + (\partial_\mu\partial^\nu\vec{\phi}\cdot\partial^\mu\vec{\phi})\partial_\nu\phi_a \\ -(\partial^\nu\vec{\phi}\cdot\partial^\mu\vec{\phi})\partial_\nu\partial_\mu\phi_a - (\partial_\nu\partial^\nu\vec{\phi}\cdot\partial^\mu\vec{\phi})\partial_\mu\phi_a + (\partial_\mu\vec{\phi}\cdot\partial^\mu\vec{\phi})(\partial_\nu\vec{\phi}\cdot\partial^\nu\vec{\phi})\phi_a \\ -(\partial_\nu\vec{\phi}\cdot\partial_\mu\vec{\phi})(\partial^\nu\vec{\phi}\cdot\partial^\mu\vec{\phi})\phi_a] + \frac{1}{2}\theta_V\frac{dV}{d\phi_3}(\delta_{a3} - \phi_a\phi_3) = 0 \end{aligned} \tag{3.12}$$

which we re-write in terms of the acceleration of the field ϕ_a:

$$\partial_{tt}\phi_a = K^{-1}_{ab}\mathcal{F}_b\left(\vec{\phi}, \partial_t\vec{\phi}, \partial_i\vec{\phi}\right) \tag{3.13}$$

with

$$K_{ab} = (1 + 2\theta_S\partial_i\vec{\phi}\cdot\partial_i\vec{\phi})\delta_{ab} - 2\theta_S\partial_i\phi_a\partial_i\phi_b. \tag{3.14}$$

We find that the inverse matrix of K exists in an explicit, but rather messy form. The equation of motion is a second order PDE.

3.1.3 Theoretical Prediction

Is it possible to predict the general features of the multi-skyrmions? The main obstacle is the non-linearity of the DEs even in a simpler form like in the hedgehog ansatz. Nevertheless,

at special points i.e. the boundaries, approximations can be made which simplify the DEs. Derrick's theorem allows us to give further quantitative predictions. Both serve as consistency checks for our numerical work and help our understanding of the models.

The value of the field is known at two space locations. Those special points are $r = 0$ and $r = \infty$. In the hedgehog ansatz, the ODE can be approximated around these points.

- At the origin, the profile function is approximated as

$$f \simeq \pi + C_n r^n \tag{3.15}$$

and so

$$f' \simeq n C_n r^{n-1} \tag{3.16}$$

as long as $\frac{dV(f)}{df}$ tends to zero at this point. We need this approximation for the shooting method [PMKTZ94]. Further, the energy density at the origin is

$$\begin{aligned} \mathcal{E}(0) = &\quad C_1^2(1 + \theta_S C_1^2) + \tfrac{1}{2}\theta_V \tilde{\mathrm{V}}[\pi] \quad (n = 1) \\ \mathcal{E}(0) = &\quad \tfrac{1}{2}\theta_V \tilde{\mathrm{V}}[\pi] \qquad\qquad (n \geq 2). \end{aligned} \tag{3.17}$$

As one would expect, the energy density of the new baby Skyrme model at the origin is zero, because there is a further vacuum at the origin;$\tilde{\mathrm{V}}[\pi] = 0$. It is non-zero only in the topological sector one. Clearly, if the hedgehog solutions are the minimal-energy solutions, the new baby n-skyrmions are ring configurations. However, in the case of the old or holomorphic baby Skyrme model, the energy density is always non-zero for any static hedgehog solution. These hedgehog solutions do not seem to minimise the energy as well as in the new baby model. Our numerical results confirm this.

- At large r, the ODE reduces to

$$f'' + \frac{1}{r}f' - \frac{n^2}{r^2}f - \frac{\theta_V}{2}\left.\frac{d\tilde{\mathrm{V}}(f)}{df}\right|_{\text{small f}} = 0. \tag{3.18}$$

The last term, arising from the potential, can be neglected for some potentials in a consistent way, because it is small compared to the other terms. This is the case for the holomorphic model where this term is of order f^7. However, the term has to be included for the old and new baby Skyrme model and gives $-\frac{\theta_V}{2}f$ or $-\theta_V f$ respectively. Looking at large r, the old and the new baby skyrmions behave in the same way[4]. Actually, the DE is that of a static Klein-Gordon field with a radially symmetric form where θ_V plays the role of the meson mass. As discussed above, the real difference lies in the small r and medium r region. For the new baby Skyrme model, the equation (3.18) gives

$$f'' + \frac{1}{r}f' - f(\frac{n^2}{r^2} + \theta_V) = 0. \tag{3.19}$$

The coefficient of the potential term is present here. The potential localises the skyrmion exponentially. Solving for appropriate boundary conditions, the profile function decays exponentially

$$f(r) \longrightarrow \frac{1}{\sqrt{\theta_V r}} \exp(-\theta_V r). \tag{3.20}$$

Derrick's theorem[5] (see [MRS93, pages 52-54]) provides a necessary but not sufficient condition for the existence of stable solutions. Under a simple scale transformation $r \to \lambda r$, the total energy changes to a function of λ and the non-scaled energies of the three terms:

$$E[\tilde{f}(\lambda r)] = E_\sigma + \lambda^2 \theta_S E_s + \lambda^{-2} \theta_V E_V. \tag{3.21}$$

The sigma term is scale invariant. The derivative of the energy with respect to λ at $\lambda = 1$ has to be zero if a stable solution exists. This implies

$$\theta_S E_s = \theta_V E_V. \tag{3.22}$$

[4] we just re-define θ_V for one of the models.

[5] it is also known as the Hobart-Derrick theorem

Our numerical results have to fulfill this condition. Further (3.21) suggests that the scaling effect can be un-done by redefining θ_S to $\lambda^2\theta_S$ and θ_V to $\lambda^{-2}\theta_V$. In fact, writing the DE (3.8) in terms of $\tilde{f}(\tilde{r}, \tilde{\theta}_S, \tilde{\theta}_V)$ and using $\tilde{r} = \lambda r$, we find

$$\tilde{f}(\lambda r, \lambda^{-2}\theta_S, \lambda^2\theta_V) = f(r, \theta_S, \theta_V). \tag{3.23}$$

Substituting $\tilde{f}$ into the energy functional gives exactly the same energy as f does. If two models with coefficients θ_S and θ_V, respectively $\tilde{\theta}_S$ and $\tilde{\theta}_V$, satisfy

$$\theta_S\theta_V = \tilde{\theta}_S\tilde{\theta}_V, \tag{3.24}$$

then their stable solutions have the same energy. This is a further consistency check.

3.1.4 Numerical Techniques

The baby Skyrme model is a non-integrable system and explicit solutions to its resulting differential equations are nearly impossible to find. Numerical methods are the only way forward. We need (2.33) for the time-evolution and relaxation of an initial configuration and use (3.8) to find static hedgehog solutions. These DEs are re-written as sets of two first order DEs. We discretise DEs by restricting our function to values at lattice points and by reducing the derivatives to finite differences.[6](as explained in [PZ98], see also [PTVF92]). We take the time step to be half the lattice spacing: $\delta t = \frac{1}{2}\delta x$. We use fixed boundary conditions i.e. we set the time derivatives to zero at the boundary. We check our numerical results via quantities conserved in the continuum limit and by changing lattice spacing and number of points. Moreover, we compare them with theoretical predictions.

Looking for static hedgehog solutions The static hedgehog solutions of (3.8) are found by the shooting method using the 4th order Runge-Kutta integration and the boundary conditions

[6]we use the 9-point laplacian

(3.10) and (3.11). Alternatively, one can use a relaxation technique like the Gauss-Seidel over-relaxation ([PTVF92]) applied to an initial configuration with the same boundary conditions.

Looking for multi-skyrmions We construct n-skyrmions by relaxing an initial set-up of n 1-skyrmions with relative phase shift of $\frac{2\pi}{n}$. Using the dipole picture developed by Piette et al. [PSZ95b], two old (or new) baby 1-skyrmions attract each other for a non-zero value of the relative phase; phase shift of π for maximal attraction. A circular set-up is crucial as they maximally attract each other and 1-skyrmions do not form several states that repel each other. One possible objection to a circular set-up is its apparent discrete symmetry, the cyclic group Z_n. However, the discretised PDE on a finite square lattice is not invariant under Z_n as we impose boundary conditions. Further, the linear superposition is only an approximate solution of the model and the 1-skyrmions used are produced from the hedgehog ansatz. In this sense, lattice effects and small integration errors even provide useful small perturbations. We have run simulations for non-circular set-ups, but either the 1-skyrmions take longer to fuse together or they fuse into many bound-states and repel each other. We run our simulations on grids with 200^2 or 300^2 lattice points and the lattice was $\delta x = 0.1$ or 0.05. However, for large topological charge, we need larger grids and the relaxation takes a long time. The corresponding hedgehog solution as an initial set-up usually works well and is faster, but biased due to its large symmetry group. The time-evolution of an initial configuration is determined by the equation of motion (2.33). We are using the 4th order Runge-Kutta method to evolve the initial set-up and correction techniques to keep the errors small. We relax i.e. take out kinetic energy by using a damping (or friction) term.

Initial set-up: see numerical methods chapter.

Correction techniques: see numerical methods chapter.

Relaxation technique: see numerical methods chapter.

3.1.5 The Different Models

So far, the literature on baby skyrmions reports work on the holomorphic model with $V = (1 + \phi_3)^4$ and the old baby Skyrme model with $V = 1 - \phi_3$. There are no stable multi-skyrmions found in the holomorphic model. However, the old baby Skyrme model possesses non-radially symmetric minimal-energy solutions. We will show that the new baby Skyrme model with $V = 1 - \phi_3^2$ has radially symmetric multi-skyrmions.

Holomorphic Model

The simplest holomorphic model has the potential $V = (1 + \phi_3)^4$ and is the first baby Skyrme model studied in the literature. ([LPZ90], [Sut91], [PZ95]). We have re-done the calculations and agree with the literature. This agreement provides a check on our numerical methods.

The holomorphic potential is unique in the sense that its model admits an explicit solution for a skyrmion with topological charge one (we call it a 1-skyrmion). To leading order, the asymptotic behaviour does not depend on the potential. The skyrmion is polynomially localised. The force between two holomorphic skyrmions is always repulsive. This repulsion can be overcome by sending the two 1-skyrmions against each other at a sufficiently high speed. Above a critical value, they overlap and form a intermediate state. However, this state is not stable and the two 1-skyrmions scatter at 90 degrees. No multi-skyrmions are known to exist in this model.

Exact static solutions The form of the potential seems arbitrary, but it is not. It emerges out of the most simplest ansatz. In the W-formulation, the equation of the static solutions has the form

$$\begin{aligned} -W_{xx} - W_{yy} \;+\; & 2\frac{W^*}{1+|W|^2}(W_x^2 + W_y^2) \\ & +4\frac{\theta_1}{(1+|W|^2)^2}(-2W_{xy}^* W_x W_y + W_{xx}^* W_y^2 + W_{yy}^* W_x^2 \\ & -W_{xx}^*|W_y|^2 - W_{yy}^*|W_x|^2 + W_{xy}(W_x^* W_y + W_y^* W_x)) \\ & -8\frac{\theta_1 W}{(1+|W|^2)^3}(W_x^* W_y - W_y^* W_x)^2 - 2\theta_2(1+|W|^2)^2\frac{dV}{dW^*} \\ =\; & 0 \end{aligned} \tag{3.25}$$

plus its complex conjugate. W_x stands for the partial derivative of W with respect to x. An explicit solution can be found using the most simplest ansatz for a static solution,

$$W = \lambda r \exp(i\theta) = \lambda(x + iy) = \lambda z. \tag{3.26}$$

Note that λ takes the role of scaling the radius r and thus determines the size of the skyrmion. Now, the PDE in this ansatz reduces to

$$\frac{dV}{dW^*} = \frac{2^7\theta_1\lambda^4 W}{\theta_2(1+|W|^2)^5}. \tag{3.27}$$

This equation is satisfied for $V = (1+\phi_3)^4$ and

$$\lambda = \sqrt[4]{\frac{\theta_2}{2\theta_1}}. \tag{3.28}$$

Note that another choice of ansatz leads to a different potential and model. For example, it is possible to find exact multi-skyrmion solutions for any charge n of the simple form

$$W = \lambda^n z^n \tag{3.29}$$

by using an appropriate potential that satisfies (3.27). Coming back to our 1-skyrmion solution, the energy density gives

$$E(r) = \frac{2\lambda^2}{(1+\lambda^2 r^2)^2} + \frac{8\theta_1\lambda^4 + 4\theta_2}{(1+\lambda^2 r^2)^4}. \tag{3.30}$$

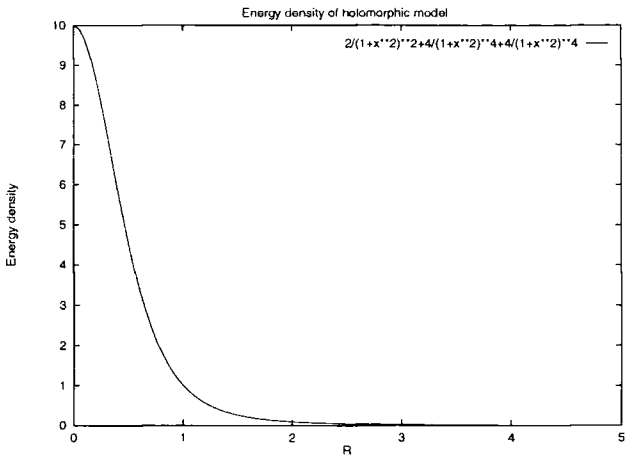

Figure 3.1: The profile function of the holomorphic skyrmion

The energy density is clearly decaying polynomially for large r. Or, in the hedgehog ansatz equation (3.18) gives

$$f'' + \frac{1}{r}f' - \frac{n^2}{r^2}f = 0 \tag{3.31}$$

for large r. The potential term with θ_2 drops out; f^7 is neglected compared to $\frac{f}{r^2}$. An appropriate choice of boundary conditions gives the asymptotic form of the profile function,

$$f(r) \longrightarrow \frac{1}{r}. \tag{3.32}$$

Again, the profile function and hence energy density is decaying polynomially. The exact energy density is shown in figure 3.1. λ is set to 1 and the parameters are chosen accordingly; $\theta_1 = 0.5$ and $\theta_2 = 1$. The total energy in terms of λ clearly shows the stabilising effect of the differently scaling lagrangian terms;

$$E = 2\pi(1 + \frac{4}{3}\theta_1\lambda^2 + \frac{2}{3}\theta_2\lambda^{-2}) = 2\pi(1 + \frac{4}{3}\sqrt{2\theta_1\theta_2}). \tag{3.33}$$

Time-evolution So far, no-one has found an exact explicit expression for a time-dependent configuration. A good way to check the stability of the skyrmion and the computer code is to

perturb the exact static solution. Figure 3.2 shows the time-evolution of the perturbed static solution $W = \lambda z$ with $\lambda \to 2\lambda$. The initial configuration has twice the size of the static solution (plot 1). The skyrmion 'shakes' off its extra energy (plot 2) and radiates out kinetic energy waves (plot 3 & 4). The stable skyrmion remains; the stability of the 1-skyrmion is fine.

As mentioned before, the common technique to create multi-skyrmions is as follows: use an approximate ansatz of n skyrmions apart from each other at rest at relative phase angles, they attract and form a bound state, take out the kinetic energy of the bound-state by relaxation. This does not work for the holomorphic model as there is a repulsive force between two skyrmions.

The exact two-soliton configuration of the σ model,

$$W = \lambda \frac{(z-a)(z+a)}{2a}, \tag{3.34}$$

is good enough for two skyrmions $2a$ units apart in the rest frame.

The result of the simulation is shown in figure 3.3. Two 1-skyrmions at rest repel each other after adjusting to the lattice and the presence of the other skyrmion. The repulsive force is overcome by giving both skyrmions an initial velocity towards each other (plot 1). In fact, there is a critical velocity at which they come on top of each other (see the paper by Sutcliffe [Sut91]). They form a ring-like bound state (plot 2) and scatter at 90 degrees (plot 3). However they escape to infinity (plot 4). There does not seem to be a stable bound-state due to the repulsion. For further information, see the references on the holomorphic model above.

Old Baby Skyrme Model

The old baby Skyrme model has been extensively studied in [PSZ95b] and [PSZ95a]. The potential $V = 1 - \phi_3$ gives rise to very structured multi-skyrmions. The configurations are crystal-like in the sense that its building block is a 2-skyrmion. We have re-done Piette et al.'s

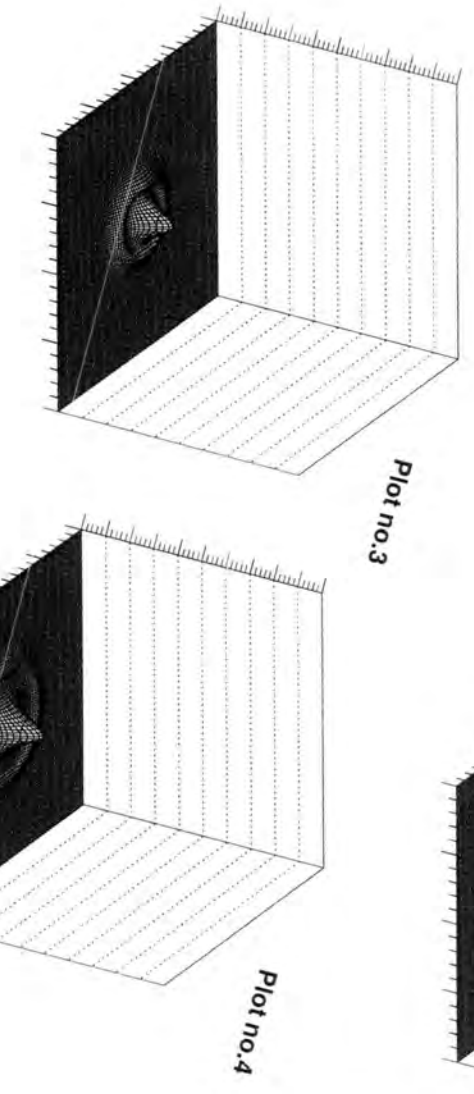

Figure 3.2: The perturbed static skyrmion emits a kinetic wave

Figure 3.3: Two holomorphic skyrmions don't form a bound-state after 90 degrees scattering

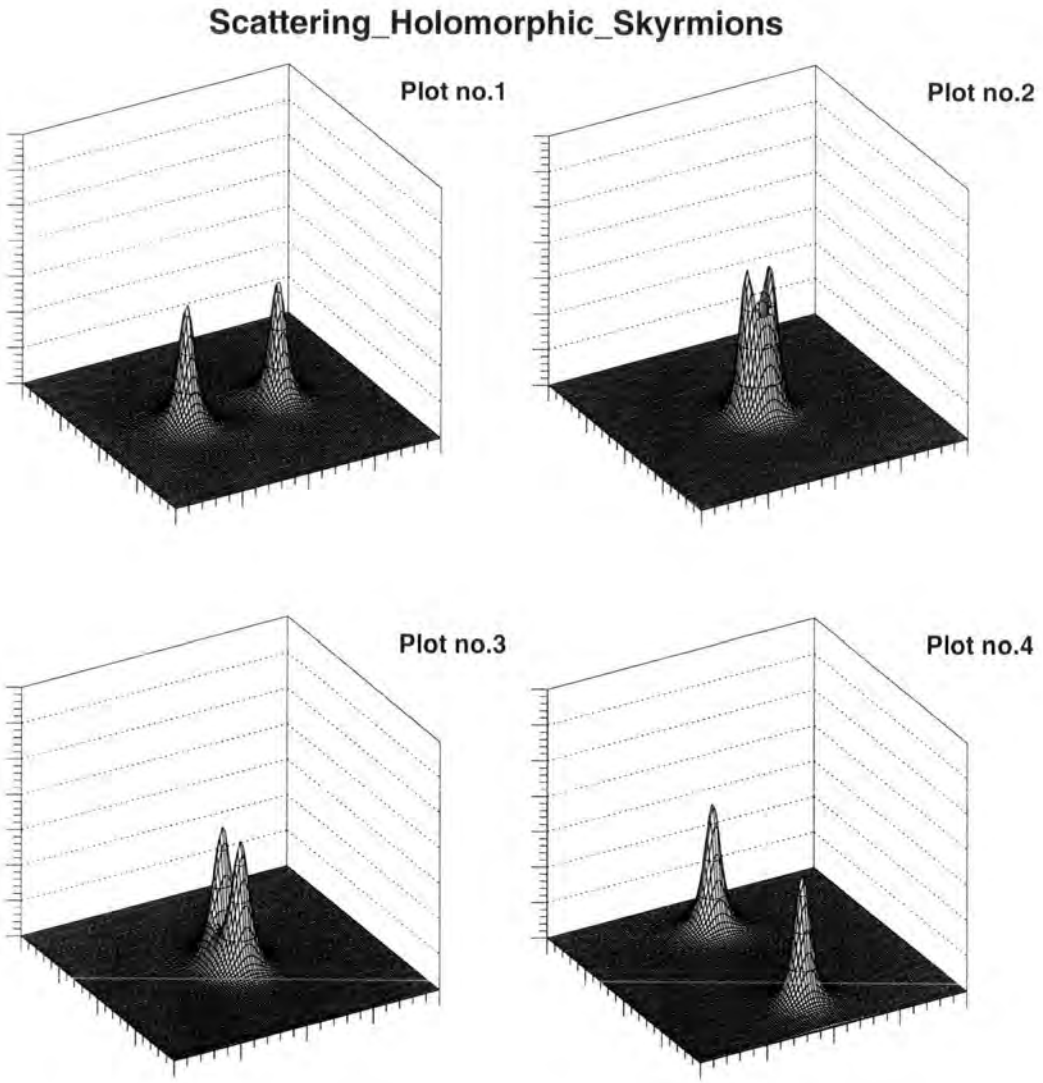

computations for multi-skyrmions and confirm their results. We use their coefficients i.e. add a factor $\frac{1}{2}$ to the sigma model term, $\theta_S = 0.25$ and $\theta_V = 0.1$ [see (3.3)].

Multi-skyrmions We construct a 2-skyrmion by sending two 1-skyrmions against each other. Put close to each other, they merge into an oscillating bound-state (see next section for picture) which leads to the stable radially symmetric 2-skyrmion by numerical relaxation. We have checked its stability by evolving it in time without relaxation. We repeat the procedure and find that all higher n-skyrmions are not radially symmetric. We extend Piette et al.'s work to $n = 7$, $n = 8$ and $n = 9$ to make sure that the n-skyrmions are 'skyrmion crystals' formed by 2-skyrmions. In this work, we only present the formation of an 8-skyrmion (see figure 3.4). We put eight 1-skyrmions on a circle with a phase shift of $\frac{2\pi}{n}$ between neighbouring 1-skyrmions. The initial configuration of eight 1-skyrmions is time-evolved and relaxed. The system starts moving to four 2-skyrmions which re-arrange themselves. Slowly, the system moves towards a stable configuration, the 8-skyrmion. The building block of this crystal-like structure is the 2-skyrmion. Figure 3.6 shows the 7 and 9-skyrmion.

Hedgehog Ansatz Solutions of the hedgehog ansatz can be found numerically by solving equation (3.8) via the shooting method. As seen above, only the $n = 1$ and $n = 2$ hedgehog configurations are global minima. The 1-skyrmion has a hill shape and is exponentially localised. Unlike in the holomorphic model, the asymptotic behaviour of the profile function does depend on the potential term to leading order. The 2-skyrmion is a ring-like configuration. A $n = 3$ static hedgehog solution exists, but does not have the lowest energy in its topological sector. A time-evolution shows that it is unstable and relaxes to the non-radially symmetric 3-skyrmion.

Figure 3.4: Contour plots of energy density: Eight 1-skyrmions merge together (pictures 1-4)

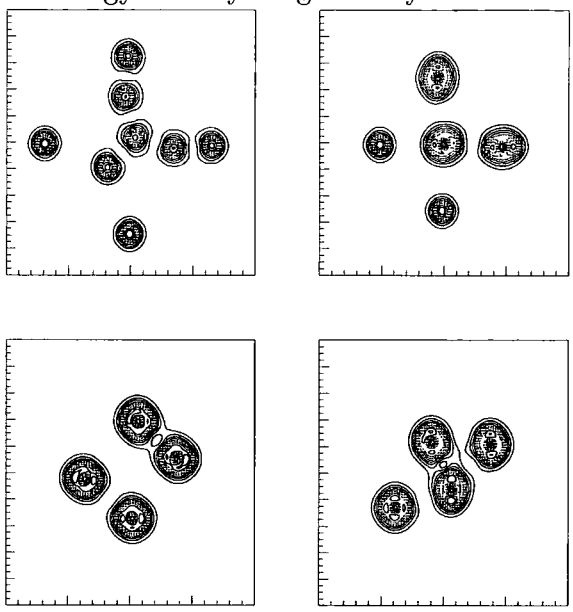

Figure 3.5: Contour plots of energy density: Bound state relaxes into an 8-skyrmion (pictures 5-8)

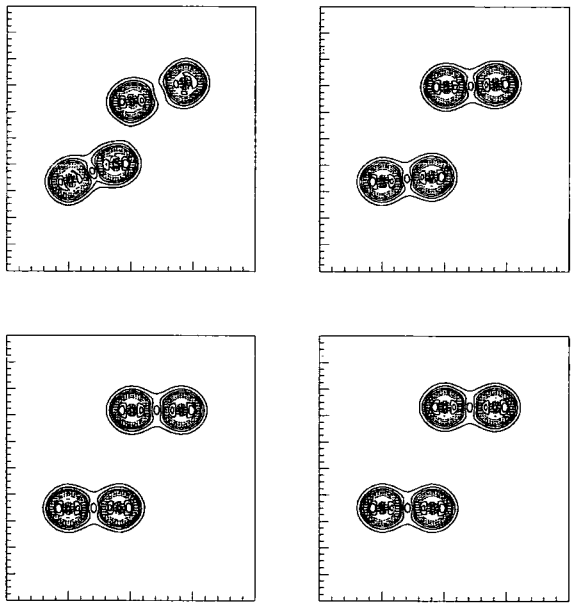

Figure 3.6: Energy density of a 7-skyrmion

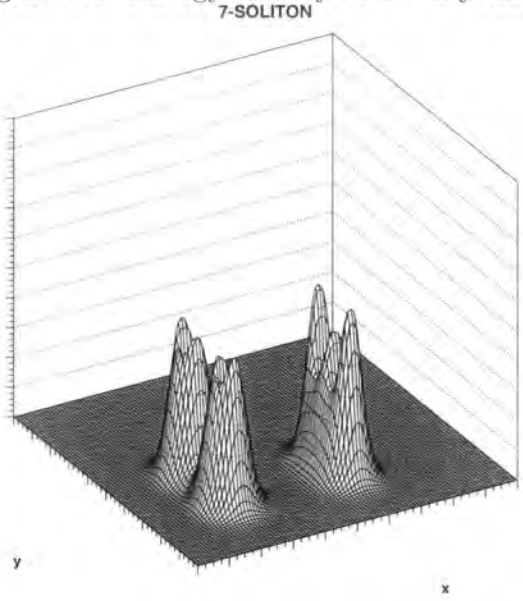

Figure 3.7: Energy density of a 9-skyrmion

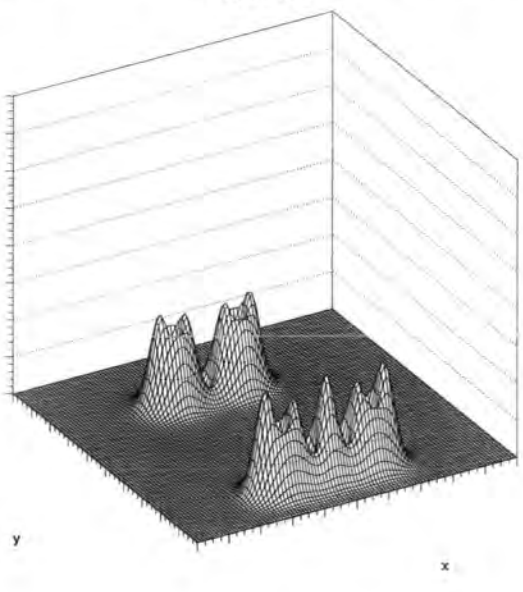

Charge	Energy	Energy per skyrmion	Break-up modes	Ionisation Energy
1	1.549	1.549	-	-
2	2.907	1.454	$1+1$	0.191
3	4.379	1.460	$2+1$	0.077
4	5.800	1.450	$2+2$	0.014
			$3+1$	0.128
5	7.282	1.456	$3+2$	0.005
			$4+1$	0.068
6	8.693	1.449	$4+2$	0.015
			$3+3$	0.066
			$5+1$	0.138

Table 3.1: Multi-skyrmions of the old baby Skyrme model

Energies Table 1 reproduces Piette et al.'s results and we will compare them to the new baby model's. The ionisation energy E_{kl} is defined as the energy you have to add to a n-skyrmion to break it up into a k-skyrmion and a l-skyrmion:

$$E_{kl} = E_n - (E_k + E_l). \tag{3.35}$$

As n increases, the ionisation energy decreases (but not continuously) and the n-skyrmions become less bound. The 2-skyrmion emission is the energetically most favourable break-up mode. An emission of a 2-skyrmion takes the smallest amount of kinetic energy to break up an 8-skyrmion. Thus, it is justified to think about a n-skyrmion as a collection of 2-skyrmions bound together.

Note that the data comes from the full time-evolution. Using the hedgehog ansatz leads to slightly different, more accurate, values. There the energy of a 1-skyrmion is 1.564 and the energy of a 2-skyrmion is 2.936. This effect is due to the finite lattice and the fact that we can use more lattice points in the hedgehog ansatz.

New Baby Skyrme Model

The new baby Skyrme model[7] exhibits a completely different structure for multi-skyrmions. In fact, the multi-skyrmions are ring-like configurations; their radii being proportional to their topological charge. The form of the potential is

$$V = 1 - \phi_3^2 = (1 - \phi_3)(1 + \phi_3). \tag{3.36}$$

The potential has two vacua; for $\phi_3 = 1$ and $\phi_3 = -1$. At infinity, the old and the new baby Skyrme models have the same vacuum $\phi_3 = 1$ and behave in the same way. They only differ for small r. Another important fact is that the lagrangian of the new baby Skyrme model is invariant under $\vec{\phi} \longrightarrow -\vec{\phi}$.

[7] see also [KPZ98]

Figure 3.8: Contour plot of energy density: Formation of 2-skyrmion

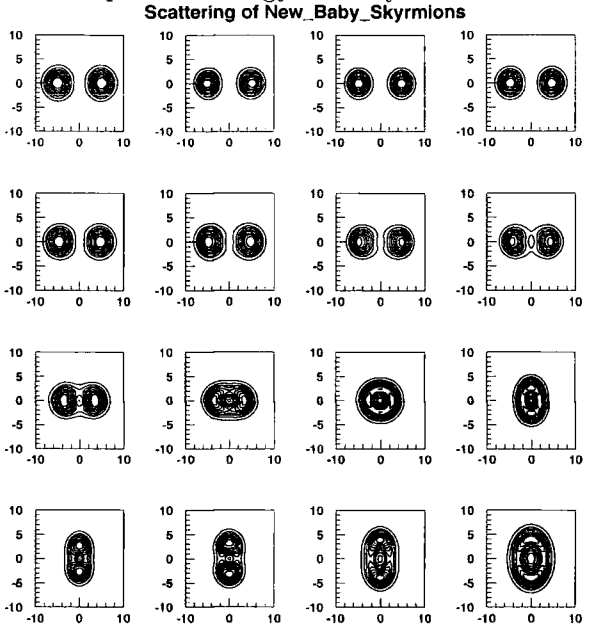

Looking for multi-skyrmions First, two new baby 1-skyrmions scatter in the same way as the old baby skyrmions do. Figure 3.8 shows how the two 1-skyrmions attract each other, form a bound-state, scatter away at 90 degrees, get slowed down by their mutual attraction, attract each other again and so on. This oscillating but stable bound-state is an excited state of the 2-skyrmion solution. Taking out the kinetic energy, the bound-state relaxes to the 2-skyrmion; a ring.

We have looked at all higher n-skyrmions. Figure 3.9 presents the results of some of our simulations: the formation of a 5, 7 and 10-skyrmion. The skyrmions attract each other and merge into intermediate states. Relaxation takes out the kinetic energy and the unstable intermediate states merge together. They form an irregular ring configuration that moves like a vibrating closed string. Slowly, the configuration settles down to a radially symmetric form due to the loss of kinetic energy. Figure 3.12 shows the final configuration of multi-skyrmions

Figure 3.9: Contour Plot of Energy Density: Formation of 5-skyrmion

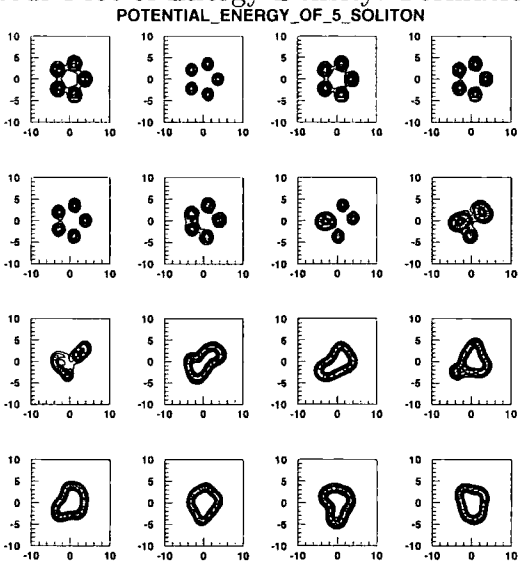

from charge two to five. Actually, the larger rings are slightly deformed. This effect is due to boundary effects and reduced by using larger grids. Thus, we have convinced ourself of the radial symmetry of n-skyrmions.

In the hedgehog ansatz The n-skyrmions are radially symmetric and we can study them in the hedgehog ansatz. Numerically speaking, the problem is reduced to one dimension and, effectively, we can take as many lattice points as we want. We want to compare the multi-skyrmions to those of the old baby Skyrme model. We add a factor of $\frac{1}{2}$ to the sigma term. The coefficient θ_V is set to half of the value of θ_V in the old baby Skyrme model: $\theta_V = 0.05$. Now, the old baby Skyrme model has exactly the same large r behaviour i.e same pion mass. Then, we set θ_S so that the energy of the new baby 1-skyrmion is now approximately the same as the old baby 1-skyrmion in the hedgehog ansatz: $\theta_S = 0.44365$. This convention puts both models on an equal footing. Note that there is a certain ambiguity about the choice of the

Figure 3.10: Contour Plot of Energy Density: Formation of 7-skyrmion

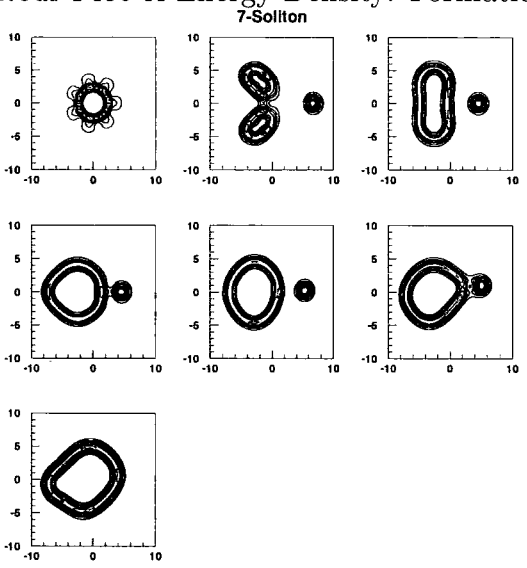

Figure 3.11: Contour Plot of Energy Density: Formation of 10-skyrmion

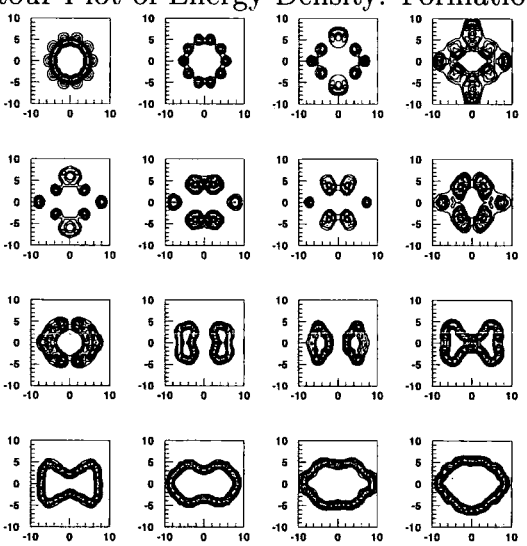

Figure 3.12: Contour Plot of Energy Density: Rings of multi-skyrmions from n=2 to n=5

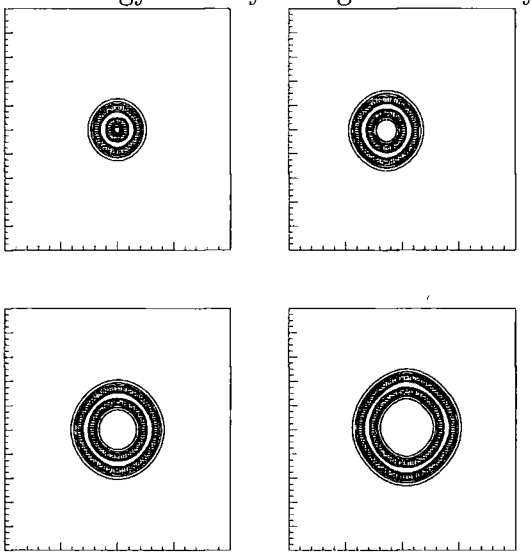

coefficients. The energy is a function of $\theta_S\theta_V$ and a compensating change of both coefficients gives the same energy.

Again, we find the hedgehog solutions by solving (3.8) using the shooting method. Figure 3.13 shows all solutions up to topological charge 10. The higher the charge the more difficult it becomes to find solutions numerically. The shooting method becomes more and more sensitive to the numerically determined value of its derivative at the origin i.e. $C_{10} \approx 10^{-10}$(see 3.15). The numerical results are very interesting. The peaks of the energy density of rings converge to an asymptotic height and their position shifts by an asymptotically constant amount. This observation deserves some further understanding.

Relation between energy peak and its location Our numerical results show that the profile function f at the position of the energy density peak, $r = d(n)$, approaches the value $\frac{\pi}{2}$

Figure 3.13: The energy density of new baby skyrmions up to charge 10

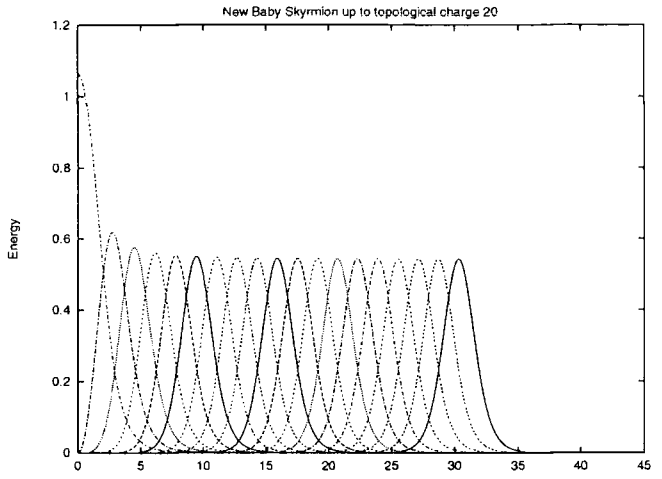

for large n. The energy density at this point reduces to

$$\mathcal{E}[d(n), n] = f_d'^2 + \frac{n^2}{d^2}(1 + 2\theta_S f_d'^2) + \theta_V. \tag{3.37}$$

Its value depends on the derivative of the profile function at $d(n)$ and the ratio between n and $d(n)$. Now, figure 3.13 shows that the height of the energy density of the peak is approximately a constant for large n i.e.

$$\lim_{n\to\infty} \mathcal{E}[d(n), n] = constant. \tag{3.38}$$

The larger the topological charge the more the multi-skyrmion approaches the peak and shape of the 'asymptotic multi-skyrmion'. Using this empirical knowledge leads us to conclude that, in the large n limit,

$$\lim_{n\to\infty} f_d'^2 = \alpha^2 \tag{3.39}$$

and

$$\lim_{n\to\infty} \frac{n^2}{d(n)^2} = \beta^2, \tag{3.40}$$

where α and β are constants. And, the peak of the ring shifts by a fixed amount from a skyrmion of charge n to one of charge $n+1$ i.e.

$$d(n) = \beta^{-1} n. \tag{3.41}$$

This relation agrees with our numerical work and provides a good consistency check. The energy density becomes

$$\mathcal{E}[d(\infty)] = \alpha^2 + \beta^2(1 + 2\theta_S\alpha^2) + \theta_V; \tag{3.42}$$

taking (3.24) into account. The shape of the n-skyrmions approaches that of the 'asymptotic multi-skyrmion'. We can approximate the configurations by a finite box of height $\mathcal{E}_d$ around the point $r = d(n)$. This gives us the dependence of the total energy on the topological charge i.e.

$$E = \int_{d(n)-a}^{d(n)+a} dr r \mathcal{E}_d = 2\mathcal{E}_d a d(n) = (2\mathcal{E}_d a\beta^2)n \tag{3.43}$$

using (3.41). Asymptotically, the total energy grows linearly with n.

Energies Table 2 shows our numerical results for the energies of the multi-skyrmions up to $n = 6$. First, the 2-skyrmion has a lower energy than an old baby 2-skyrmion, but looks exactly the same at large r. The multi-skyrmions do not break up via a 2-skyrmion emission (see last section) but into two similar configurations ie. $5 \to 3 + 2$ or $6 \to 3 + 3$. This can be seen from the ionisation energy.

Further the ionisation energy and the energy per skyrmion decreases to an asymptotic value for large n (unlike the old baby multi-skyrmions). The monotonic decrease of the ionisation energy shows that the large n-skyrmions become less stable: a smaller addition of kinetic energy can break them apart. Nevertheless, they are much tighter bound and more stable than their old baby analogues.

Charge	Energy	Energy per skyrmion	Break-up modes	Ionisation Energy
1	1.564	1.564	-	-
2	2.809	1.405	$1+1$	0.319
3	4.112	1.371	$2+1$	0.262
			$1+1+1$	0.580
4	5.433	1.358	$2+2$	0.186
			$3+1$	0.243
5	6.761	1.352	$3+2$	0.160
			$4+1$	0.235
6	8.094	1.349	$3+3$	0.130
			$4+2$	0.148

Table 3.2: Multi-skyrmions of the new baby Skyrme model

3.1.6 Summary and Open Questions

Clearly, the choice of the potential term has a crucial effect on the structure of multi-skyrmions. The comparison between the new and the old baby Skyrme model has proved to be very interesting. Both models have the same asymptotic behaviour, but possess completely different multi-skyrmion structures. The new baby Skyrme model has radially symmetric minimal-energy solutions for all topological charges whereas the old baby multi-skyrmions are 'skyrmion lattices' formed by 2-skyrmions. New baby multi-skyrmions are tighter bound and have less energy than their old baby analogues.

We have backed up our numerical results by monitoring conserved quantities (like energy, topological charge, S^2 constraints), comparing with approximations for small and large r, checking the relation between energy peaks and their position and verifying conditions imposed by Derrick's theorem.

Obviously, a general framework that predicts the structure of multi-skyrmions for a given potential is desirable. However, we have not been able to achieve this goal. Rather, we state some empirical laws derived from our numerical experiments.

Existence of multi-skyrmions. The new and old baby Skyrme models admit stable multi-skyrmions. When 2 1-skyrmions are put at rest at a finite distance, they attract, move towards each other, form an intermediate state and scatter at 90 degrees. After the scattering, they move away from each other, slow down, stop and eventually move towards each other again and scatter one more time. This process is repeated many times, and as the skyrmions radiate some energy during each scattering they progressively form a bound state. This is not true for the holomorphic model, for the two 1-skyrmions repel each other. A related observation leads us to the conjecture that if the asymptotic behaviour does not depend on the potential coefficient, the force between two 1-skyrmions is repulsive; see the holomorphic model.

Structure of multi-skyrmions. The potential shapes the structure of multi-skyrmions. Unfortunately, we can only show the fact by our numerical results. The existence of more than one vacuum seems to be crucial to the radial symmetric shape of the new baby n-skyrmions. It might well be possible to prove that potentials with more than one vacuum lead to radially symmetric multi-skyrmions. However, we were not able to back such claims by a theoretical study.

To conclude, some interesting questions arise from the study of multi-skyrmions in the baby Skyrme models and are worth investigating further.

- The choice for potential terms is largely arbitrary. The study of other potentials and in particular those with multiple vacua could help to clarify the issues surrounding the existence and structure of multi-skyrmions. Further, on one hand, potentials with multiple vacua can still have the same large distance behaviour like old baby skyrmions. On the other hand, their multi-skyrmion solutions should have rather exotic shapes, because the dynamics tries to have multiple vacua. Unlike the conventional smooth lump of the 1-skyrmion, their 1-skyrmion lumps may have riddles in them. Or, one might like to rephrase our question and ask whether multi-vacua models have circular domain walls, too.

- The application of the baby Skyrme model in the quantum regime requires an appropriate quantization scheme. The radially symmetric new baby multi-skyrmion solutions could simplify this task. The mass correction of *all multi-skyrmions* i.e. the eigenvalue equation in the harmonic approximation (see next chapter) can be calculated numerically without excessive computer power. This is not true for the old baby Skyrme model, for higher multi-skyrmions do not have a continuous symmetry.

- Are there any applications? If there are 90 degrees scattering phenomena observed in experiments, then the analysis of bound-states can lead to the determination of the potential responsible for these phenomena.

- The choice of the potential crucially shapes the structure of multi-skyrmions. This is probably not true in the nuclear Skyrme model, because the sigma term is not scale invariant. Often, an 'old baby Skyrme'-type potential is included to have a pion mass and exponential decay. There is no argument why the potential term used cannot have two vacua. What happens in a nuclear Skyrme model with a 'new baby Skyrme potential'? Is the energy of the n-skyrmions lower?

It is also possible to interpret the ring-like multi-skyrmions of the new baby Skyrme model as circular domain walls separating the two vacua. This is an interesting and conceptually clearer viewpoint. Indeed, at the location of the peak of the energy density, the field switches from one vacuum value to the other. These domain walls also have a topological charge.

3.2 Using Simulated Annealing for 1D minimisation...

In this section, we present the results of our implementation of the Simulated Annealing minimisation scheme described in detail in the last chapter. We show that it works well in one dimension and is easy to implement. There is no need to derive the Euler-Lagrange equation and higher order terms can be easily added to the energy functional. First, we reproduce some known results: exact one for the Sine-Gordon model and numerical ones for the Skyrme-type models. Secondly, we revisit the radially symmetric new baby multi-skyrmion solutions and get much clearer results than with the shooting method used in our earlier study. Finally, we include a higher order term to the nuclear Skyrme model and show the relationship between the value of its coefficient and its minimal energy.

We include our computer code in appendix B. Three parameters are crucial for a successful cooling. The initial temperature must be high enough to avoid the system getting frozen in a local minimum. The 'Boltzmann constant' K defines the probability of acceptance of upwards moves i.e. moves which have a higher energy: we typically use $K = 10^{-6}$. The condition for thermal equilibrium is crucial for a well-minimised result. If the number of upwards and downwards steps is roughly the same after X changes, the system is in thermal equilibrium. How big is X i.e. how long should a monitored chain of changes be until we are confident the system has reached thermal equilibrium? We typically take 100N or 1000N changes where N is the number of lattice points. The longer the chain the better and the slower the cooling. We have to emphasise that we only get the same answer for a re-run if the configuration is the minimal-energy solution. If the answer is slightly different, we need to increase the chain. We usually start with a small chain and increase it until the result does not change anymore. This procedure ensures that the schedule really did allow for thermal equilibrium at each temperature. To conclude, a 'paramaterology' does not exist for Simulated Annealing , we find the best values by trial and error. For more details, please see the last chapter.

3.2.1 The Sine-Gordon and Skyrme models

Comparison with theoretical value We start out with the integrable sine-Gordon model. Its energy functional is given in (1.75). Its minimal-energy solution is $\phi_{st}(x) = 4\arctan[\exp x]$ whose total energy is exactly 8. Our initial configuration is a straight line from one boundary value, $\phi = 0$, to the other, $\phi = \pi$. The parameters of our cooling schedule are: $T_{initial} = 1000$, $K = 10^{-6}$, 500 cooling iterations and our condition for thermal equilibrium is $100N$. For $N = 600$ points with box-size $L = 30$, we obtain 7.999837: see cooling in figure (3.14). The plot clearly shows that the decrease in energy of the configuration is not monotonically: upwards step are allowed. We re-run the code and get slightly different result in the last three digits.

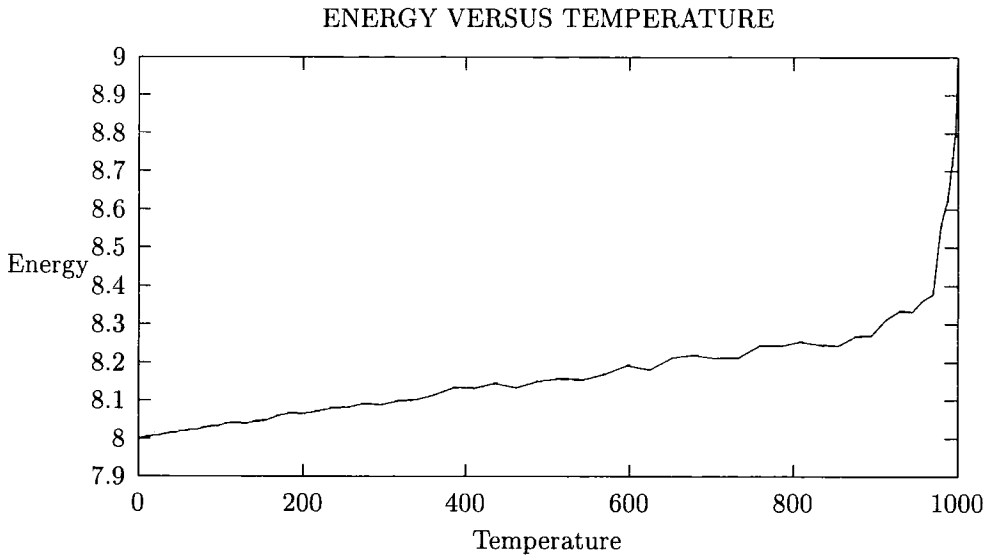

Figure 3.14: Cooling of initial configuration to minimal-energy solution

Hence, we increase the chain to 1000N. We obtain 7.999367. We re-run it and obtain the same energy. As a general guide, maximum accuracy is not attainable due to discretisation and finite box effects. We trust our numerical values to three-digit precision: thus 7.999.

Comparison with published numerical results We run our computer code for the 1 and 2-skyrmion solutions of the old and new baby Skyrme model. We use 401 lattice points and the box size is 15. The cooling schedule is $T_{initial} = 500$, $K = 10^{-6}$ and the chain is $500N$. Our results are identical up to three-digits precision to the results in the previous section: see also [PSZ95a]. We use the coefficients of the papers. The computed energies of the old baby Skyrme model are $E_1 = 1.5644$ and $E_2 = 2.9363$. And those of the new baby Skyrme model are $E_1 = 1.5642$ and $E_2 = 2.8094$. We also evaluate the energy of the 1-skyrmion of the nuclear Skyrme model. Using the expression given in [MRS93], the energy functional of the nuclear

Skyrme model is

$$E[f(r)] = \pi \int_0^\infty dr \left[f'^2 \left(\frac{r^2}{2} + 4\sin^2 f \right) + \sin^2 f + 2\frac{\sin^4 f}{r^2} \right]. \tag{3.44}$$

in units of $\frac{F_\pi}{e}$. We obtain the minimal-energy profile function with the correct polynomial decay and a total energy value of $E = 36.566\frac{F_\pi}{e}$; compared to 36.5 in Nappi et al. [ANW83]

3.2.2 Domain Walls in new baby Skyrme model

In our earlier study of multi-skyrmions, we have looked at the minimal-energy solution of the new baby Skyrme model for any topological charge. We found that the solutions are radially symmetric energy configurations. However, the shooting method did not produce reliable results for higher charges. The value of the derivative has to be adjusted so that the function falls off to zero at infinity. In our case, the correct derivative at the origin is very small for a large charge and the Runge-Kutta numerical integration method could not handle such small values and became very sensitive to the number of lattice points used and the finite size of the box. The Simulated Annealing method has no such problems and works fine. Let us note that the relaxation method described in the last chapter works fine, too.

We use the same coefficients as in the last section. Table 3.3 shows the energies of multi-skyrmions from charge one to twenty. Figure 3.15 shows that the energy-per-charge density of a multi-skyrmion decreases to an asymptotic value of around 1.35. We also look at the location of the peak of the energy density of each multi-skyrmion. Again, the relationship is asymptotically linear (see figure 3.16) i.e. the location of the peak divided by the charge goes to a constant. However, due to the discretisation of space, we only know the peak location approximately. Thus, our obtained values are not very accurate; the value of the 'constant' is roughly 1.38. Figure 3.17 shows the profile function of the 1, 5, 10, 15 and 20-skyrmion. The higher the topological charge, the more distinct the transition between one vacuum to the other becomes.

Charge	Energy	E/C	Peak Location	Charge	Energy	E/C	Peak Location
1	1.564	1.564	0.00	11	14.782	1.344	15.20
2	2.809	1.404	2.82	12	16.122	1.343	16.56
3	4.112	1.371	4.16	13	17.461	1.343	17.96
4	5.433	1.358	5.56	14	18.802	1.343	19.36
5	6.761	1.352	6.92	15	20.142	1.343	20.75
6	8.094	1.349	8.32	16	21.482	1.343	22.12
7	9.430	1.347	9.68	17	22.823	1.343	23.44
8	10.767	1.346	11.08	18	24.164	1.342	24.80
9	12.105	1.345	12.40	19	25.504	1.342	26.24
10	13.443	1.344	13.84	20	26.845	1.342	27.60

Table 3.3: Multi-skyrmions of the new baby Skyrme model

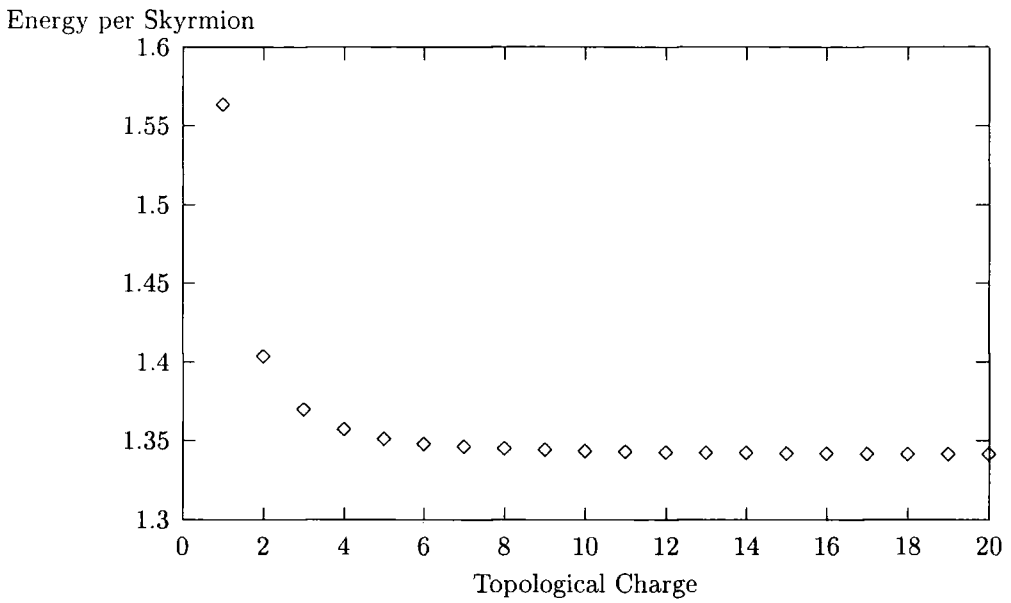

Figure 3.15: Asymptotic decrease of the energy per skyrmion of a multi-skyrmion

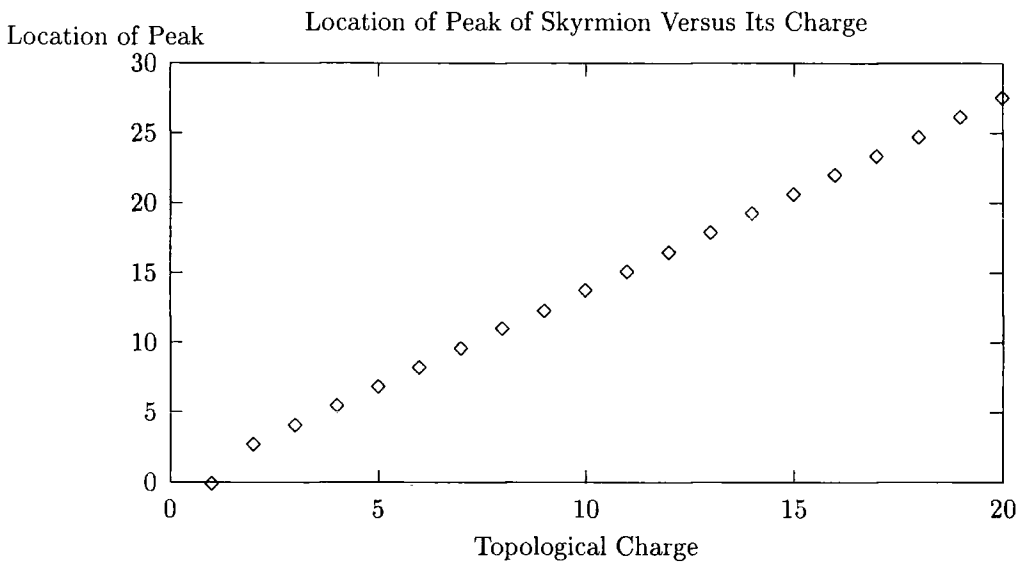

Figure 3.16: Linear dependence of the location of the energy peak vs. its charge

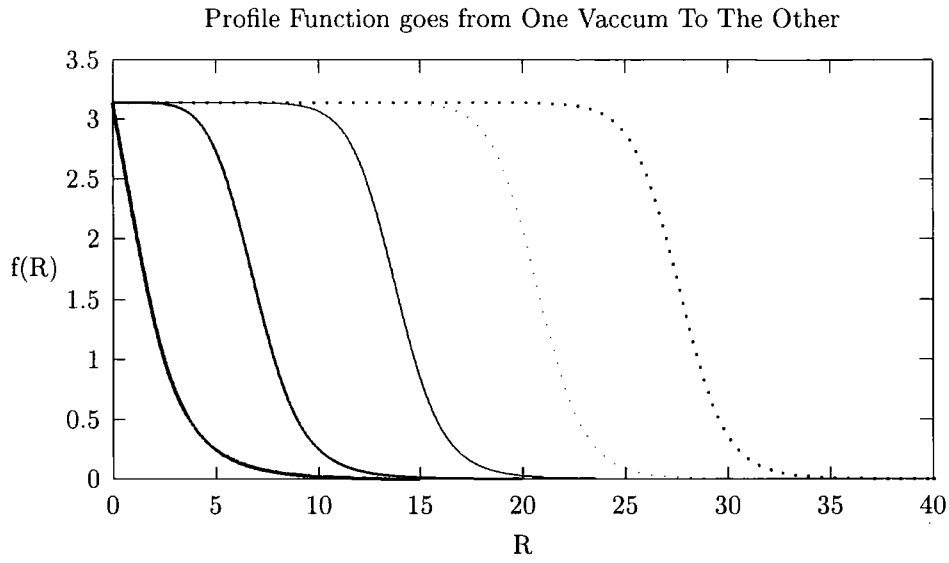

Figure 3.17: Profile function of 1, 5, 10, 15 and 20-skyrmion

Therefore, we might as well view our multi-skyrmion solutions as charged domain walls; the location of the peak of the energy being the transition from one vacuum to the other. We conclude that Simulated Annealing is very useful for studying classical aspects of skyrmions. The multi-skyrmion solutions are intriguingly simple and a further study of the behaviour of such charged circular domain walls might be worthwhile. Further, does the inclusion of a higher order Skyrme term change the structure of the multi-skyrmions?

3.2.3 Higher Order Term in nuclear Skyrme model

In this section, we include a higher order term in the lagrangian of the nuclear Skyrme model and find the energy of the 1-skyrmion using the hedgehog ansatz. From Marleau [Mar90] and

Jackson et al. [JJGB85], we must add the term

$$\theta \int_0^\infty dr \; f'^2 \frac{\sin^4 f(r)}{r^2} \tag{3.45}$$

in the hedgehog ansatz; θ being the coefficient of the higher order term. This six-derivatives term is the most physical one, for it is positive and only first order in time derivatives. Note that it is also possible to replace the Skyrme term with the six-derivatives term.

The θ coefficient should really be positive otherwise the model would have configurations with an arbitrary large negative energy. Indeed, if we assume that θ is negative, we can think of a configuration in the form of a delta function. Then the negative six-order term will always 'win', i.e. lead to a negative energy, if we take the derivative sufficiently large. Nevertheless, we will explore the full range of θ for which we obtain positive energy solutions.

Derrick's theorem and the topological bound give us necessary but not sufficient conditions on the minimal-energy solution of the functional. From Derrick's theorem, the Skyrme term in 2+1 or 3+1 dimensions tries to expand the skyrmion. Intuitively, its derivatives have to be small to minimise a functional. The same is true for the six-derivatives term. Using the condition of stability (1.45), the 'shrinking' σ term balances the 'expanding' Skyrme and six-derivatives term:

$$E_\sigma = E_{Sk} + 3\theta E_6; \tag{3.46}$$

the coefficients of the σ and Skyrme term are treated as constants. Further, there is a topological bound on the energy functional

$$E \geq 3\pi^2 \approx 29.6; \tag{3.47}$$

the same as for the nuclear Skyrme model. This bound arises from Bogomulyni's bound on the σ term, $1.5\pi^2$, and the relation (3.46).

We compute the energy of the minimal-energy solutions for various values of θ. It is easy to add one or more higher order terms to the functional in the Simulated Annealing scheme,

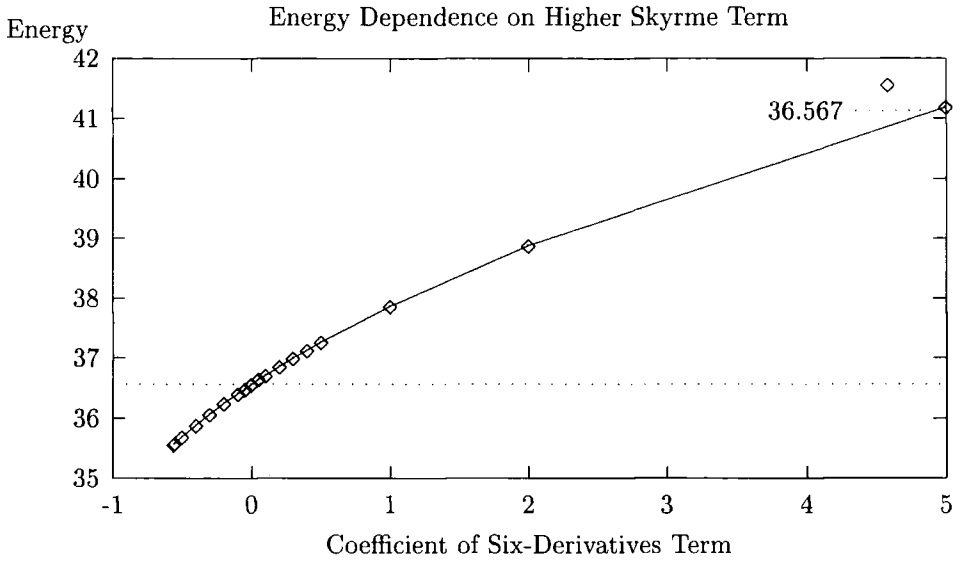

Figure 3.18: Logarithmic dependence of the energy on θ

because we do not have to derive the Euler-Lagrange equation. We use 301 lattice points and lattice spacing $\delta x = 0.05$. The cooling schedule is similar to previous ones. We find a roughly logarithmic dependence of the energy on θ: see figure 3.18. The computed energy of the 1-skyrmion in the nuclear Skyrme model i.e. $\theta = 0$ is $E = 36.566$ which is approximately 1.23 times the topological bound. As expected a positive θ leads to a higher energy and a small negative one to a lower energy. The lowest energy we get is 35.571 for $\theta = -0.56$ and it is roughly 1.20 times the bound. For a value slightly above the critical $\theta = -0.56$, the minimisation technique gives us a negative value for the energy. If we double the number of points and increase the box to 20, we can push the critical value that leads to a positive energy to -0.57. Conceivably, even more lattice points and a wider box might give us a solution of slightly lower energy. Still, we believe that this is, apart from numerical precision, a real cut-off in the theory above the theoretical bound.

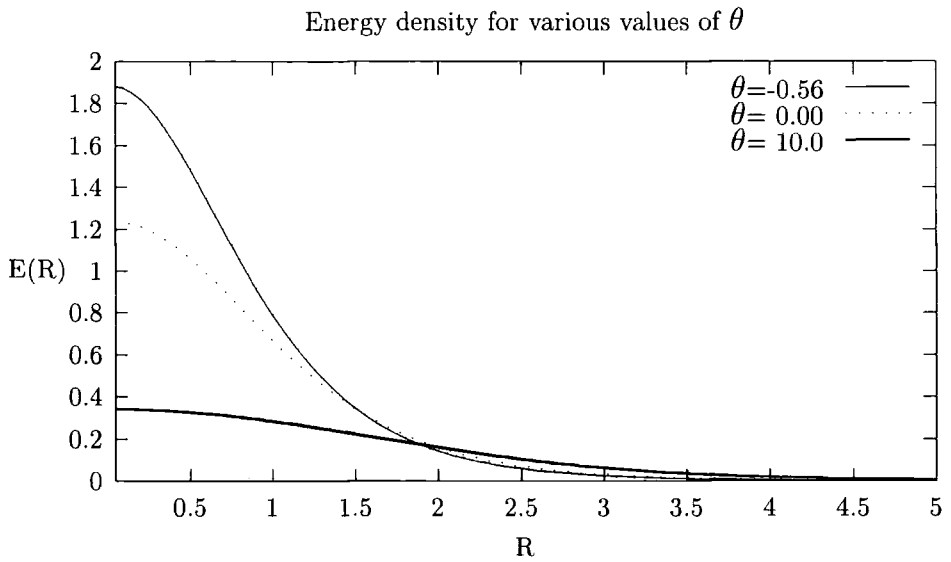

Figure 3.19: Energy density of 1-skyrmion with coefficient -0.56, 0 and 10

In figure 3.19, we present the energy densities for different θ values. The higher the value of θ, the more dominant the higher order term becomes. Using Derrick's theorem, the relation (3.46) helps us to explain figure 3.19. For large $\theta = 10$, the skyrmion is more spread out. For negative θ, the effect of the two 'expanding' terms is partially cancelled and the soliton shrinks.

Finally, there are plenty of interesting research ideas. Why is there a cut-off and at what value? What is the structure of the multi-skyrmions? We have used the hedgehog ansatz. What about the general case? Work is on progress on the implementation of a 2D minimisation scheme using Simulated Annealing.

3.3 Adding a six-derivatives term...

We want to know what happens if we add a higher order term to the baby Skyrme lagrangian. The Skyrme term is just the trivial 2-space dimensional analogue of the (3+1) Skyrme term. We do the same for the higher order term and translate it to (2+1) dimensions.

The non-linear σ model, a model of pions, is the simplest approximation to an effective field theory of QCD. However, the soliton is not stable and shrinks to zero-size. The lagrangian does not satisfy the condition of stability (1.45) according to Derrick's theorem. Therefore, a higher derivative term e.g. four-derivatives term was added to insure stability. The addition of the Skyrme term in the lagrangian is a reasonable and simplest choice of a low-energy effective field theory. And the model is unambiguous, because the Skyrme term is the only four-derivatives term which leads to a positive and first-order in time hamiltonian. Adkins et al. point out that 'the Skyrme model is only a rough description, since it omits the other mesons and interactions that are present in the large-N limit.' Jackson et al. [JJGB85] look at the possibility to simulate ω-mesons physics by adding (or replacing the Skyrme term) by a six-derivatives term. Marleau [Mar90] attempts to derive a generalised Skyrme lagrangian of second order in time and obeying constraints from vector meson physics. In both approaches, the researchers are restricted to the hedgehog ansatz to manage the calculations.

The six-derivatives term that they propose has the form

$$L_6 = \left(\partial_\mu\vec{\phi}\cdot\partial^\mu\vec{\phi}\right)^3 - 3\left(\partial_\mu\vec{\phi}\cdot\partial^\mu\vec{\phi}\right)\left(\partial_\nu\vec{\phi}\cdot\partial_\rho\vec{\phi}\right)\left(\partial^\nu\vec{\phi}\cdot\partial^\rho\vec{\phi}\right) + 2\left(\partial_\mu\vec{\phi}\cdot\partial_\nu\vec{\phi}\right)\left(\partial_\rho\vec{\phi}\cdot\partial^\mu\vec{\phi}\right)\left(\partial^\nu\vec{\phi}\cdot\partial^\rho\vec{\phi}\right) \tag{3.48}$$

where we sum over μ, ν and ρ. We split the time derivative from the space derivative terms and get

$$\begin{aligned} L_6 = {} & 3(\dot{\phi}\cdot\dot{\phi})\left[(\phi_i\cdot\phi_i)^2 - (\phi_i\cdot\phi_j)^2\right] - 6(\dot{\phi}\cdot\phi_i)^2(\phi_j\cdot\phi_j) + 6(\dot{\phi}\cdot\phi_i)(\dot{\phi}\cdot\phi_j)(\phi_i\cdot\phi_j) \\ & -(\phi_i\cdot\phi_i)^3 + 3(\phi_i\cdot\phi_j)^2(\phi_k\cdot\phi_k) - 2(\phi_i\cdot\phi_j)(\phi_k\cdot\phi_i)(\phi_j\cdot\phi_k) \end{aligned} \tag{3.49}$$

where $\dot{\phi}$ stands for $\partial_t\phi$ and ϕ_i for $\partial_i\phi$. We work in (2+1) dimensions: the indices i, j label x and y. The spatial derivative part is identically zero due to redundant labelling in 2 space dimensions. The time-dependent terms

$$\frac{1}{12}L_6 = (\dot{\phi}\cdot\dot{\phi})\left[(\phi_x\cdot\phi_x)^2+(\phi_y\cdot\phi_y)^2-(\phi_x\cdot\phi_y)^2\right]+(\dot{\phi}\cdot\phi_x)(\dot{\phi}\cdot\phi_y)(\phi_x\cdot\phi_y) \\ -(\dot{\phi}\cdot\phi_x)^2(\phi_y\cdot\phi_y)-(\dot{\phi}\cdot\phi_y)^2(\phi_x\cdot\phi_x) \tag{3.50}$$

are the only terms left in the lagrangian. This discovery leads to interesting conclusions and questions. First of all, the energy density of L_6 for a static configuration is identically zero. Static minimal-energy solutions do not depend on the six-order term. For example, if we add L_6 to the baby Skyrme lagrangian, the minimal-energy solutions are exactly the same as for the original baby Skyrme model. However, the scattering behaviour could be different, because time-dependent six-order terms are present in the lagrangian. This model is worth further investigations. It is not too much work to derive the equation of motion, because the spatial part is zero and the number of terms seems manageable. Secondly, we can replace the Skyrme term by L_6. The energy density only contains the σ term and a potential. There do exist time-dependent minimal-energy solutions called Q-balls for such a lagrangian. If we assume a solution

$$W = z(x,y)e^{i\alpha(t)} \tag{3.51}$$

where $z(x,y)$ is a complex function, we get an additional term

$$4\frac{\dot{\alpha}^2|z|^2}{(1+|z|^2)^2} \tag{3.52}$$

in the lagrangian which does not have any derivatives. Hence, we can cancel the term by adding an appropriate potential; the additional term with an opposite sign. This corresponds to a balance between the rotating solution and the potential. Any static solution z of the model has a time-dependent solution associated to it. However, our six-derivatives term destroys

this relationship, because we get additional time-dependent terms that include α and contain derivatives. The potential cannot be modified so to cancel the effect of a solution of the form (3.51). According to Derrick' theorem, any minimal-energy solution is not stable, because we can lower its energy by scaling. However, does the time-dependent six-derivatives term prevent the configuration from collapse? Again, a numerical study should give an answer and we will attempt to do this in the near future.

We believe that the study of higher order terms is interesting and should lead to new behaviour and structure. It is not clear which terms to choose and the motivation for future research seems rather to be of mathematical interest than of physical importance. However, an effective theory should have higher order terms. Finally, we believe that Simulated Annealing will help us in these studies and is better equipped than the Euler-Lagrange equation for minimisation. Work is on progress on a 2D minimisation scheme.

Chapter 4

Quantum Aspects via Numerical Methods

> "... It is truly surprising how little difference all this makes. Most physicists use quantum mechanics every day without needing to worry about the fundamental problem of its interpretation... A year or so ago, while Philip Candelas (of the physics department at Texas) and I were waiting for the elevator, our conversation turned to a young theorist who had then dropped out of sight. I asked Phil what had interfered with the ex-student's research. Phil shock his head sadly and said,"He tried to understand quantum mechanics." "
>
> *(from Weinberg's 'Dreams of a Final Theory')*

In the previous chapter, we have shown how to study classical aspects of solitons using numerical techniques. In this chapter, we discuss how to study the aspects of the quantum nature of solitons, namely their mass correction, using numerical methods.

In our introduction, we explained the difficulties surrounding the quantization of the (3+1)-dimensional Skyrme model. Nappi et al. [ANW83] partially overcame these problems by using

a spinning-top approximation; the minimal-energy solution is radially symmetric and rotating without deformation. Effectively, they only include the rotational zero mode of the 1-skyrmion. This procedure allows to quantise the 1-skyrmion as a nucleon and gives reasonable agreement with experiments. The work by Braaten et al. [BTC90] and Battye and Sutcliffe [BS97] on the structure of classical multi-skyrmions supports further the idea that an appropriate quantization around these minimal-energy solutions for a given topological sector could lead to an effective description of atomic nuclei. However, the calculation of quantum properties of the multi-skyrmions is very difficult, because these minimal-energy solutions are not radially symmetric, for example. This is rather frustrating, for the claim that the Skyrme model descending from a large N-QCD approximation models mesons, baryons and higher nuclei is a very compelling one. There have been various attempts to extract quantum properties, notably by Walet [Wal96] and Leese et al. [LMS95]. A recent zero mode quantization of multi-skyrmions from charge four to nine has been undertaken by Irvine [Irv98]. Reliable quantitative results were not to be expected, but even the correct quantum number for the ground states of some nuclei, skyrmions with odd charge 5, 7 and 9, could not be obtained.

All these attempts rely on theoretical approximations like moduli-space or rational map ansatz and mostly include only zero modes. Barnes, Baskerville and Turok's attempt is notably different. They want to include all lowest modes, not just zero modes, and get more reliable quantitative results. Therefore, they have to use numerical techniques to achieve their goal. In a series of papers, they compute the lowest modes spectrum of $B = 2$ [BBT97a], $B = 4$ [BBT97b] and $B = 7$ [Bas97] numerically. Their numerical results shed further light on normal modes of multi-skyrmions and motivated theoretical studies. In another paper, Barnes and Turok [BT97] compute numerically the mass correction of the (1+1)-dimensional ϕ^4 kink. They wanted to show how to use numerically extracted lowest normal modes to compute the quantum properties in a simple toy model. To achieve this task, they use a trace formula over the normal

modes of the vacuum and the soliton ground-state; derived in [CCG76]. The ϕ^4 kink model proved to be an ideal candidate, for theoretical results are known and can be compared with numerical ones. In his PhD thesis [Bar98], Barnes explains how to extend their scheme to (3+1) dimensions; in principle. However, renormalisation issues and the sheer complexity of their approach in higher dimensions pose serious problems for an implementation. Possibly, one could use another formula from [CCG76] using the phase shifts of the normal modes: see, for example, recent work by Holzwarth and Walliser [HW99]. Whatever way, Barnes et al. have not yet published a description on how to compute quantum properties of the (3+1) dimensional multi-skyrmions from their numerically calculated normal modes.

In this chapter we focus on the computation of the mass correction of (1+1)-dimensional solitonic theories theoretically and numerically. We follow Rajaraman's semi-classical quantisation procedure; another option is via path integrals – see Dashen et al. [DHN75]. Specifically, we are interested in the use of the normal modes to compute the mass correction and the extent to which the lowest modes from both, the soliton and the vacuum, sectors give the leading contribution. We start with a review of the derivation of the first order quantum correction. Then, we derive the trace formula from first principles.[1] We use this formula to re-compute the mass correction and show that the lowest modes are the most important ones. Then, we calculate the lowest modes numerically and hence the leading contribution to the mass correction.

Thus, rather than aiming for higher dimensions, which proves to be very challenging and difficult, we content ourselves with getting a good understanding of the one-dimensional case.

[1] this is not done in [CCG76].

4.1 Mass Quantum Correction: General Idea

We start out with a general lagrangian for a (1+1)-dimensional field theory

$$\mathcal{L} = \frac{1}{2}\dot{\phi}^2 - \frac{1}{2}\phi'^2 - V(\phi) \tag{4.1}$$

for the scalar field $\phi(t,x)$ and with the potential V being positive. The time-independent Euler-Lagrange equation leads to

$$-\phi'' + \frac{dV}{d\phi} = 0. \tag{4.2}$$

We quantise around the minimal-energy static solution $\phi_{st}(x)$ satisfying (4.2), which could be the vacuum or the minimal-energy solution in a non-zero topological sector. The semi-classical expansion states that the quantum field $\hat{\phi}(t,x)$ is the classical static field $\phi_{st}(x)$ plus a quantum correction field $\hat{\epsilon}(t,x)$,

$$\hat{\phi}(t,x) = \phi_{st}(x) + \hat{\epsilon}(t,x) \tag{4.3}$$

where $\hat{}$ reminds us to treat the function as a quantum object, an operator satisfying, possibly non-commuting, commutation relations with other operators. We have to substitute (4.3) into the hamiltonian

$$H(\phi) = \int_{-\infty}^{\infty} dx \left(\frac{1}{2}\dot{\phi}^2 + \frac{1}{2}\phi'^2 + V(\phi)\right) \tag{4.4}$$

and obtain, in orders of ϵ,

$$\hat{\mathcal{H}}(x) = \underbrace{\frac{1}{2}\phi_{st}'^2}_{\text{Classical}} + \hat{\epsilon}\underbrace{\left(-\phi_{st}'' + \left.\frac{dV}{d\phi}\right|_{\phi_{st}}\right)}_{=0\ (4.2)} + \underbrace{\frac{1}{2}\hat{\pi}^2 + \frac{1}{2}\hat{\epsilon}\left(-\frac{d^2}{dx^2} + \left.\frac{d^2V}{d\phi^2}\right|_{\phi_{st}}\right)\hat{\epsilon} + O(\hat{\epsilon}^3)}_{\text{Quantum}} \tag{4.5}$$

where $\hat{\pi}$ is the conjugate momentum of $\hat{\epsilon}$. We have used integration by parts, set the boundary terms to zero and Taylor expanded the potential term in powers of ϵ. We split our hamiltonian into three parts,

$$\hat{H} = H_{Classical} + \hat{H}_{Quantum} + \hat{H}_{HigherOrder}, \tag{4.6}$$

where the classical mass/energy can be found by substituting ϕ_{st} into (4.4). We concentrate on the lowest order quantum energy $\hat{H}_{Quantum}$. This is justified in the framework of a perturbation theory where higher order terms are neglected due to their smallness in comparison to the lowest term. This approximation is justified if the potential is roughly harmonic around the static solution and ϵ^n terms depend on the coupling constant λ in the form λ^n, for example. If these conditions are not fulfilled or a better accuracy is wanted, one can resort to well-known perturbation techniques of standard quantum mechanics. However, let us emphasise that this would considerably complicate our task. Therefore, Barnes et al.'s attempts are already significantly hampered for those multi-skyrmions whose potential does not have a steep valley i.e. are not suitable for a harmonic oscillator approximation. This is the case for $B = 2$, for example.[2]

Our quantum hamiltonian, in the harmonic approximation, has the form

$$2\hat{\mathcal{H}}(t,x) = \hat{\pi}^2(t,x) + \hat{\epsilon}(t,x) \underbrace{\left(-\frac{d^2}{dx^2} + \left.\frac{d^2V}{d\phi^2}\right|_{\phi_{st}} \right)}_{\mathbf{A^2}} \hat{\epsilon}(t,x) \tag{4.7}$$

where A^2 is an operator. If A^2 acts as a number, the hamiltonian has the form of an harmonic oscillator and we know the quantisation procedure. In effect, we have to solve the eigenvalue equation

$$\mathbf{A^2}\hat{\epsilon}(t,x) = \omega^2\hat{\epsilon}(t,x) \tag{4.8}$$

and this is equivalent to the time-independent Schrödinger equation. We have to decompose the quantum field $\hat{\epsilon}$ in terms of a complete set of real and orthonormal eigenfunctions. Therefore,

$$\hat{\epsilon}(t,x) = \sum_n^{\infty} \hat{q}_n(t)\hat{\eta}_n(x) \tag{4.9}$$

with

$$\sum_n \hat{\eta}_n(x)\hat{\eta}_n(y) \;=\; \delta(x-y)$$

[2]private communication from Barnes

$$\int dx \left[\hat{\eta}_n(x)\hat{\eta}_m(x)\right] = \delta_{n,m} \tag{4.10}$$

and

$$\mathbf{A^2}\hat{\eta}_i(x) = \omega_i^2\hat{\eta}_i(x). \tag{4.11}$$

We substitute the decomposition (4.9) into (4.7), integrate over x and use the constraints (4.10) on the eigenfunctions. We are left with

$$2\hat{\mathcal{H}}(t) = \sum_n \left[\hat{p}_n^2(t) + \omega_n^2\hat{q}_n^2(t)\right] \tag{4.12}$$

where $\hat{p}_n$ is the conjugate momentum of $\hat{q}_n$. The hamiltonian is an infinite sum of harmonic oscillators of frequency ω_n. We have reduced our quantum field theory with an infinite number of degrees of freedom to a pseudo particle quantum mechanics with an infinite number of harmonic oscillators. We are now able to use standard particle quantum mechanics. Using the operator method with Heisenberg's commutation relation

$$[\hat{p}_n, \hat{q}_n] = i\hbar, \tag{4.13}$$

we get

$$H = \hbar\sum_n \left(\alpha_n + \frac{1}{2}\right)\omega_n \tag{4.14}$$

where α_n is the αth energy level of the nth oscillator. Naively speaking, we have all the information we need to calculate the mass correction: the classical mass and the quantum correction to first order i.e. the quantum hamiltonian. Unfortunately, if we were to calculate the quantum mass in a specific model, we would quickly realise that the mass is divergent; the infinite number of oscillators, an inherent feature of any quantum field theory, being the cause of this divergent result. In the next section, we describe, using the ϕ^4 model as our example, how to extract a meaningful quantum properties from our naive expression.

4.2 Mass Quantum Correction: Derivation

We follow Rajaraman's procedure. For a very detailed and lucid description, we refer to Rajaraman's book [Raj96, section 5.3]. We have re-done all the calculations by hand and with the use of Maple. Further we have expanded on the discussion of some parts, given more details and corrected some typographical errors.[3]

The hamiltonian of the ϕ^4 kink model is

$$2H = \int dx \left(\dot{\phi}^2 + \phi'^2 - m^2\phi^2 + \frac{\lambda}{2}\phi^4 + \frac{m^4}{2\lambda} \right) \tag{4.15}$$

where m is the mass of the field ϕ and λ the self-coupling constant. In topological charge sector zero, the minimal-energy solution i.e. the vacuum is

$$\phi_{st}(x) = \pm\frac{m}{\sqrt{\lambda}} \tag{4.16}$$

and, in topological charge sector one, the minimal-energy solution i.e. the 1-kink is

$$\phi_{st}(x) = \pm\frac{m}{\sqrt{\lambda}} \tanh\left[\frac{m(x-a)}{\sqrt{2}}\right] \tag{4.17}$$

where a indicates a translational invariance (this will lead to a zero mode). We quantise around the solutions with the positive sign in front which is the soliton – compared with the negative sign in front which is the anti-soliton.

The corresponding eigenvalue equation for the vacuum is

$$\left[-\frac{d^2}{dx^2} + 2m^2\right] \hat{\eta}_i(x) = \omega_{V,i}^2 \, \hat{\eta}_i(x) \; . \tag{4.18}$$

The eigenfunctions and eigenvalues are

$$\hat{\eta}_k(x) = \exp(ikx) \tag{4.19}$$

[3] and probably introduced others.

and

$$\omega_{V,k}^2 = k^2 + 2m^2. \tag{4.20}$$

We use periodic boundary conditions in a box of length L and

$$k_n L = 2\pi n \tag{4.21}$$

where n is an integer. The continuum limit is reached by taking L to infinity and any discrete sum over k_n, or simply n, turns into an integral over k of the form

$$\sum_n \longrightarrow \int dn = \frac{L}{2\pi} \int dk \tag{4.22}$$

using the constraint (4.21) on k_n.

The corresponding eigenvalue equation for the 1-kink is less trivial

$$\left[-\frac{1}{2}\frac{d^2}{dz^2} + (3\tanh^2 z - 1) \right] \hat{\eta}_i(z) = \frac{\omega_{K,i}^2}{m^2}\, \hat{\eta}_i(z), \tag{4.23}$$

where $z \equiv mx/\sqrt{2}$ for convenience. In fact, it belongs to a class of special Schrödinger equations; the Sine-Gordon model being another example.[4] There are two discrete modes; one zero mode

$$\hat{\eta}_0(z) = \cosh^{-2} z \quad \text{with} \quad \omega_{K,0}^2 = 0 \tag{4.24}$$

and a second discrete mode

$$\hat{\eta}_1(z) = \sinh z \, \cosh^{-2} z \quad \text{with} \quad \omega_{K,0}^2 = \frac{3}{2}m^2. \tag{4.25}$$

The continuous eigenmodes, which we label with q, are [5]

$$\hat{\eta}_q(z) = e^{iqz} \left(3\tanh^2 z - 1 - q^2 - 3iq \tanh z \right) \tag{4.26}$$

[4] private communication from Jackiw and see [Jac77, pages 683-684]

[5] the eigenmodes are Jacobi polynomials in $\tanh z$. [Jac77]

with

$$\omega_{K,q}^2 = m^2 \left(\frac{q^2}{2} + 2 \right). \tag{4.27}$$

Imposing periodic boundary conditions becomes more tricky. For $z \to \pm\infty$, we can use the asymptotic form of $\hat{\eta}_q(z)$

$$\begin{aligned} \hat{\eta}_q(z) &\longrightarrow e^{iqz} \left(2 - q^2 \mp 3iq \right) \\ &\longrightarrow \sqrt{(q^2+4)^2(q^2+1)} \exp \left[i(qz \pm \frac{1}{2}\delta(q)) \right] \end{aligned} \tag{4.28}$$

where $\delta(q)$ is the phase shift of the scattering states from the viewpoint of the Schrödinger equation;

$$\delta(q) = -2 \arctan \left[\frac{3q}{2 - q^2} \right]. \tag{4.29}$$

The condition imposed by the periodic boundary is

$$q_n \left(\frac{mL}{\sqrt{2}} \right) + \delta(q_n) = 2\pi n \tag{4.30}$$

and the sum over n becomes an integral over q in the limit where L goes to infinity:

$$\sum_n \longrightarrow \int dn = \frac{1}{2\pi} \int dq \left(\frac{mL}{\sqrt{2}} + \frac{\partial}{\partial q} [\delta(q)] \right) \tag{4.31}$$

using the constraint (4.30) on n. Let us briefly note that the zero mode, which we have found, is nothing else but the manifestation that the 1-kink solution is translationally invariant. We can imagine the infinite-dimensional potential space at its minimal-energy location having a 1-dimensional valley along which we can move our solution by varying a without changing the energy of the system. This zero mode certainly needs to worry us, for our harmonic oscillator approximation assumes steep valleys in all dimensions. However, this is only problematic if the zero mode is coupled with another mode and this does not happen in the computation of the mass correction up to first order. A proper treatment of zero modes is done with collective coordinates: see Rajaraman [Raj96, chapter 8].

We have all the necessary information on the eigenvalues and should naively be able to compute the mass of the 1-kink up to first order quantum corrections. Using (4.6) and the eigenvalues of the 1-kink solution, we get an expression for the energy

$$E_K = \underbrace{\underbrace{\underbrace{\frac{2\sqrt{2}m^3}{3\lambda}}_{Classical} + \underbrace{\hbar m\frac{\sqrt{3}}{2\sqrt{2}}}_{Discrete}}_{Finite} + \underbrace{\frac{1}{2}\hbar m \sum_n \sqrt{\frac{1}{2}q_n^2 + 2}}_{Continuous}}_{Divergent} \tag{4.32}$$

which includes the finite classical energy, no contribution from the zero mode due to its zero frequency, a finite contribution from the second discrete mode and a sum over the continuous modes. Unfortunately, if we were to perform the integral over q using (4.30), we would find it to be divergent. This clearly shows that our naive treatment of quantum field theory is inadequate. To have a finite answer, there are two modifications we have to make.

4.2.1 Energy level difference

Let us write out the expression for the vacuum energy up to first order quantum corrections

$$E_V = \frac{1}{2}\hbar \sum_n \sqrt{k_n^2 + 2m^2}. \tag{4.33}$$

Using (4.22), we get

$$E_V = \frac{\hbar L}{4\pi}\int_{-\infty}^{\infty} dk\sqrt{k^2 + 2m^2} \tag{4.34}$$

which is a quadratically divergent integral. Thus, even the leading quantum contribution to the classical vacuum is not finite. However, we can follow the example of newtonian gravity which defines potential energy as the difference between two states. It makes physical sense to define our naive vacuum energy, even though it is infinite, as the lowest of possible energy states in the theory i.e. to put it equal to zero and hence to subtract it from our naive calculation of the

1-kink energy. We get

$$E_K - E_V = \tilde{E}_K = \underbrace{\frac{2\sqrt{2}m^3}{3\lambda} + \hbar m\frac{\sqrt{3}}{2\sqrt{2}}}_{E_{finite}} + \frac{1}{2}\hbar\sum_n \left(m\sqrt{\frac{1}{2}q_n^2+2} - \sqrt{k_n^2+2m^2}\right) \tag{4.35}$$

and we label all finite terms collectively E_{finite}. We go to the continuum limit and perform the integral over k. Therefore, we re-express q_n in terms of k_n

$$q_n = \frac{\sqrt{2}}{m}\left(k_n - \frac{\delta(q_n)}{L}\right) \tag{4.36}$$

using the boundary conditions (4.30) and (4.21). The expression in the sum takes the form

$$\begin{aligned} m\sqrt{\frac{1}{2}q_n^2+2} - \sqrt{k_n^2+2m^2} &= \sqrt{\left(k_n - \frac{\delta(k_n)}{L}\right)^2 + 2m^2} - \sqrt{k_n^2+2m^2} \\ &= -\frac{k_n\delta(k_n)}{L\sqrt{k_n^2+2m^2}} + O(1/L^2) \\ &= \frac{2}{L}\arctan\left(\frac{3m}{\sqrt{2}}\frac{k_n}{m^2-k_n^2}\right)\frac{k_n}{\sqrt{k_n^2+2m^2}} + O(1/L^2) \end{aligned} \tag{4.37}$$

where we have Taylor expanded the first line, used expression (4.29) and Taylor expanded it. Both Taylor expansions are in $\frac{1}{L}$ and make sense, for we take the box size L to infinity later. Using (4.22), the expression for the energy becomes

$$\tilde{E}_K = E_{finite} + \frac{\hbar}{2\pi}\int dk\ \underbrace{\arctan\left(\frac{3m}{\sqrt{2}}\frac{k}{m^2-k^2}\right)}_{du/dk}\underbrace{\frac{k}{\sqrt{k^2+2m^2}}}_{v} + O(1/L)\ . \tag{4.38}$$

The dependence on the box size goes away for $L \to \infty$ and we are allowed to neglect the $O(1/L)$ and higher terms. As our notation indicates, we perform integration by parts. The boundary term has the form

$$\frac{\hbar}{2\pi}\lim_{\alpha\to\infty}\left[\arctan\left(\frac{3m}{\sqrt{2}}\frac{k}{m^2-k^2}\right)\sqrt{k^2+2m^2}\right]_{k=\alpha}^{k=-\alpha}. \tag{4.39}$$

This limit is ill-defined for trivial substitution of $\alpha = \infty$: the arctan function gives us 0 and the polynomial function ∞. Therefore, we use l'Hôptial's rule and obtain a finite answer

$$\hbar m \frac{3}{\pi\sqrt{2}} \tag{4.40}$$

which we include in our E_{finite}. The integral obtained by integration by parts has the form

$$\frac{3\sqrt{2}m}{2\pi} \int dk \frac{k^2 + m^2}{\sqrt{k^2 + 2m^2}\,(2k^2 + m^2)}. \tag{4.41}$$

We put a cut-off Λ on the k limits and change to the variable $p \equiv k/m$. We get

$$\lim_{\Lambda\to\infty} \int_{\frac{\Lambda}{m}}^{-\frac{\Lambda}{m}} \frac{p^2 + 1}{\sqrt{p^2 + 2}\,(2p^2 + 1)} \tag{4.42}$$

If we perform this integral, we still find a logarithmic divergence plus a finite contribution. We need to cancel the divergence with another term. We need to look closer at the infinities produced by the infinite degrees of freedom of a field theory.

4.2.2 Normal-Ordering and Counter-terms

We have to normal-order the hamiltonian and introduce counter-terms. We do not give a full introduction to all these more complicated ideas and refer to Ryder [Ryd94], for example, for a detailed introduction. We decompose the field ϕ in terms of a complete set of orthonormal eigenfunctions of the vacuum fluctuations

$$\phi(t, x) = \sum_n \left[\frac{e^{-i\omega_n t}}{\sqrt{2\omega_n}} \hat{a}_n \epsilon_n(x) \; + \; \frac{e^{i\omega_n t}}{\sqrt{2\omega_n}} \hat{a}_n^\dagger \epsilon_n^\dagger(x) \right] \tag{4.43}$$

where a is the annihilation and $a^\dagger$ the creation operator (we neglect the $\hat{}$ on them). The hamiltonian (4.7) becomes

$$2\hat{H} = \sum_n \omega_n \left(a_n a_n^\dagger + a_n^\dagger a_n \right) = \sum_n \omega_n \left(2a_n^\dagger a_n + 1 \right) \tag{4.44}$$

using the orthonormality relations of ϵ and the commutation relation between a_n and $a_n^\dagger$. The term $a_n^\dagger a_n$ is viewed as the number operator N_n and gives the number of nth oscillators that are excited. We see that the sum $\sum_n 1$ is divergent and the common procedure is to re-define the hamiltonian. We are free to choose the zero of energy and are allowed to neglect the 1. Phrased differently, we normal-order the hamiltonian by writing all annihilation operators to the right of all creation operators. Thus, we get

$$2 : \hat{H} : \;=\; : \sum_n \omega_n (\underbrace{a_n a_n^\dagger}_{flip} + a_n^\dagger a_n) : \;=\; 2 \sum_n \omega_n a_n^\dagger a_n \tag{4.45}$$

where :: stands for normal-ordering. The relations between a normal-ordered and non-ordered product of the fields are

$$\begin{aligned} : \phi^4 : \;&=\; \phi^4 + \alpha\phi^2 + \beta \\ : \phi^2 : \;&=\; \phi^2 + \delta \end{aligned} \tag{4.46}$$

where α, β and γ are constants. We write the normal-ordered hamiltonian as our non-ordered hamiltonian plus two counter-terms that arise from the relations (4.46)

$$: \hat{H} : \;=\; \hat{H} - \int dx \left(\frac{1}{2} \delta m^2 \phi^2 \;+\; \gamma \right) \tag{4.47}$$

where δm is the mass correction to the field and can be evaluated using the one-loop Feynman diagram. The constant γ is not of any importance, because it will cancel itself out due to its presence in both, the vacuum and the 1-kink, hamiltonian. The additional term to E_{finite} and the divergent term (4.42) come from subtracting the counter-term of the vacuum from the counter-term of the 1-kink and we get

$$E_K^{CT} - E_V^{CT} = \frac{1}{2} \delta m^2 \left(\frac{m^2}{\lambda} \right) \int dx \left[1 - \;\tanh^2 \left(\frac{mx}{\sqrt{2}} \right) \right] = \frac{\sqrt{2} m}{\lambda} \delta m^2 \tag{4.48}$$

We evaluate δm^2 by using the equivalent expression in ϕ^4 theory. We refer to Ryder [Ryd94, section 6.4] for a detailed discussion. The standard formula (Ryder: eq 6.95) in perturbation

theory for the ϕ^4 model is

$$\delta m^2 = \frac{1}{2} i g \Delta_F(0) \tag{4.49}$$

where g is the coupling and $\Delta_F(0)$ the free particle propagator of a loop diagram i.e $\Delta_F(x-x)$. We have to be careful when adapting the result to our case. Three modifications to ϕ^4 (Ryder eq 6.65) are necessary:

- $g/4! = \lambda/4$ and $g = 6\lambda$.
- The theory should be in (1+1) dimensions.
- There is only one vacuum. The vacuum eigenvalues are $k^2 + \tilde{m}^2$ and those of our ϕ^4 kink theory are $k^2 + 2m^2$. Therefore, we need to change the mass $\tilde{m}^2$ to $2m^2$.

The (1+1) dimensional free particle loop propagator (Ryder: eq 6.14) with modified mass $2m^2$ has the form

$$\Delta_F(0) = \frac{\hbar}{(2\pi)^2} \int \frac{d\mathbf{k}^2}{\mathbf{k}^2 - 2m^2} \tag{4.50}$$

where we have a pole at $\mathbf{k}^2 = 2m^2$ and the two-vector $\mathbf{k}$ equals $(E, -k)$. We evaluate the double integral further

$$\begin{aligned} \frac{4\pi^2}{\hbar} \Delta_F(0) &= \int dk \int \frac{dE}{E^2 - (k^2 + 2m^2)} \\ &= -i \int \frac{dk}{\sqrt{k^2 + 2m^2}} \end{aligned} \tag{4.51}$$

where we have integrated over E. We change to the variable $p \equiv k/m$ and put a cut-off Λ on p. Substituting everything into (4.49), we get

$$\delta m^2 = \frac{3\lambda\hbar}{4\pi} \lim_{\Lambda \to \infty} \int_{-\frac{\Lambda}{m}}^{\frac{\Lambda}{m}} \frac{dp}{\sqrt{p^2 + 2}} \tag{4.52}$$

which we substitute into the additional term (4.48).

4.2.3 Finite Mass Correction

Finally, we are able to write the quantum mass of the 1-kink as

$$M = \tilde{E}_K + \tilde{E}^{CT} = E_{finite} + \hbar m \frac{3\sqrt{2}}{4\pi} \lim_{\Lambda\to\infty} \int_{-\frac{\Lambda}{m}}^{\frac{\Lambda}{m}} \left[\frac{dp}{\sqrt{p^2+2}} - \frac{2(p^2+1)}{\sqrt{p^2+2}\,(2p^2+1)} \right]. \tag{4.53}$$

We have done the integral using a cut-off Λ with Maple. Both terms produce the same logarithmic divergent term which cancel each other out. Taking the cut-off to infinity, we get the final answer for the mass of a 1-kink up to first order quantum corrections

$$M = \left(\frac{2\sqrt{2}}{3}\right) \frac{m^3}{\lambda} + \hbar m \left[\frac{1}{6}\sqrt{\frac{3}{2}} - \frac{3}{\pi\sqrt{2}} \right] \tag{4.54}$$

where we have written E_{finite} out explicitly. The first term is just the total energy of the classical 1-kink solution. Note that the presence of $1/\lambda$ indicates the non-perturbative nature of the solution. To zeroth order in λ and first order in $\hbar$, we have the first quantum correction. It is only valid in the weak-coupling limit. The next term of the quantum correction would be of order $\lambda\hbar^2$. Rajaraman [Raj96, section 5.4-5.6] gives a detailed interpretation of the result and also explains why the effect of the counter-terms on the kink solution and the zero mode are effects of order λ.

This concludes our derivation of the quantum mass. In the next section, we show that it is possible to get a formula for the mass correction which allows us to quantify the contribution of the different modes and compute the mass correction numerically by using numerically computed lowest eigenmodes.

4.3 Trace formula: Derivation

The trace formula has been first published by Cahill et al. [CCG76], but an explicit derivation has not been given in their paper. We derive the formula in this section[6]. We start by writing

[6] private communication by Barnes

out the hamiltonian (4.7)

$$2\hat{\mathcal{H}}(t,x) = \hat{\pi}^2(t,x) + \hat{\epsilon}(t,x)\mathbf{A^2}\hat{\epsilon}(t,x) \tag{4.55}$$

and the equation of motion of the normal modes is

$$\ddot{\epsilon}(t,x) = -\omega^2\epsilon(t,x) \tag{4.56}$$

with the eigenvalue equation

$$\mathbf{A^2}\ \epsilon_i(x) = \omega_i^2\ \epsilon_i(x) \tag{4.57}$$

where we ignore the $\hat{}$ on the quantum field. A^2 depends on the static solution around which we expand. We label A_V^2 the operator for the vacuum and A_K^2 the operator for the kink. We expand the quantum fluctuation $\epsilon(t,x)$ in terms of the normal modes of the vacuum, which we label $\epsilon_K(t,x)$, and the 1-kink, which we label $\epsilon_V(t,x)$. In terms of the plane waves of the mesons with eigenvalue ω_k,

$$\epsilon_V(t,x) = \sum_n \left[\frac{e^{-i\omega_k t}}{\sqrt{2\omega_k}}a(k)e^{ikx} + \frac{e^{i\omega_k t}}{\sqrt{2\omega_k}}a^\dagger(k)e^{-ikx}\right] \tag{4.58}$$

and, in terms of the normal modes of the 1-kink with eigenvalue ω_n,

$$\epsilon_K(t,x) = \sum_n \left[\frac{e^{-i\omega_n t}}{\sqrt{2\omega_n}}a_n\epsilon_n(x) + \frac{e^{i\omega_n t}}{\sqrt{2\omega_n}}a_n^\dagger\epsilon_n^\dagger(x)\right] \tag{4.59}$$

where the plane waves $\exp(ikx)$ and the normal modes ϵ_n are orthonormal eigenfunctions. The next step involves writing the annihilation and creation operators of the eigenmodes in terms of the creation and annihilation operators of the planes waves. By definition,

$$\epsilon_K(t,x) = \epsilon_V(t,x) \tag{4.60}$$

$$\dot{\epsilon}_K(t,x) = \dot{\epsilon}_V(t,x). \tag{4.61}$$

We then integrate over both equations with x, use the fact that the eigenmodes are a complete orthonormal set (4.10) and solve the set of two equations for a_n and $a_n^\dagger$. We obtain

$$a_n^\dagger = \frac{1}{2}\sum_k \left[a^\dagger(k)\tilde{\epsilon}_n(-k)\left(\sqrt{\frac{\omega_n}{\omega_k}}+\sqrt{\frac{\omega_k}{\omega_n}}\right)+a^\dagger(k)\tilde{\epsilon}_n(k)\left(\sqrt{\frac{\omega_n}{\omega_k}}-\sqrt{\frac{\omega_k}{\omega_n}}\right)\right] \tag{4.62}$$

$$a_n = \frac{1}{2}\sum_k \left[a^\dagger(k)\tilde{\epsilon}_n(-k)\left(\sqrt{\frac{\omega_n}{\omega_k}}-\sqrt{\frac{\omega_k}{\omega_n}}\right)+a^\dagger(k)\tilde{\epsilon}_n(k)\left(\sqrt{\frac{\omega_n}{\omega_k}}+\sqrt{\frac{\omega_k}{\omega_n}}\right)\right] \tag{4.63}$$

where $\tilde{\epsilon}_n(k)$ is the exponential Fourier transform, $\int dx \exp(ikx)\epsilon_n(x)$, of $\epsilon_n(x)$. We calculate the hamiltonian in terms of soliton normal modes annihilation and creation operators in the last section (4.45) and expand the term in terms of the annihilation and creation operators of the vacuum. We get

$$\begin{aligned}
\omega_n a_n^\dagger a_n &= \text{'terms with } a^\dagger a,\ aa \text{ and } a^\dagger a^\dagger\text{'} \\
&+ \frac{1}{4}\omega_n \sum_{k,l} a(k)\tilde{\epsilon}_n(k)\left(\sqrt{\frac{\omega_n}{\omega_k}}-\sqrt{\frac{\omega_k}{\omega_n}}\right)a^\dagger(l)\tilde{\epsilon}_n(-l)\left(\sqrt{\frac{\omega_n}{\omega_l}}-\sqrt{\frac{\omega_l}{\omega_n}}\right) \\
&= \text{'terms with } a^\dagger a,\ aa \text{ and } a^\dagger a^\dagger\text{'} \\
&+ \frac{1}{4}\sum_k \tilde{\epsilon}_n(k)\tilde{\epsilon}_n(-k)\left[\frac{\omega_n}{\omega_k}+\frac{\omega_k}{\omega_n}-2\right]\omega_n
\end{aligned} \tag{4.64}$$

where we have used the commutation relation between operators $[a(k), a^\dagger(l)] = \delta_{k,l}$ and merged the resulting $a^\dagger a$ term into the 'collective' term. Finally, we can express the un-ordered term as the normal-ordered term i.e. all the terms with $a^\dagger a$, aa and $a^\dagger a^\dagger$ and an extra term:

$$\omega_n a_n^\dagger a_n = :\omega_n a_n^\dagger a_n: + \frac{1}{4}\sum_k \tilde{\epsilon}_n(k)\tilde{\epsilon}_n(-k)\frac{(\omega_n-\omega_k)^2}{\omega_k} \tag{4.65}$$

which leads us to the final answer

$$:H: = :\omega_n a_n^\dagger a_n: = \omega_n a_n^\dagger a_n + \delta m. \tag{4.66}$$

The mass correction δm can be expressed as a trace over any complete set of orthonormal states,

$$\delta m = -\frac{1}{4}Tr\left[\frac{(A_K - A_V)^2}{A_V}\right] \tag{4.67}$$

where A_V^2 is the operator of the vacuum and A_K^2 is the operator of the kink perturbations. This trace formula is finite. Further further discussions see [BT97] and [Bar98].

4.4 Trace formula: Theoretical Result

We use the trace formula to calculate the contribution of the lowest discrete modes to the mass correction. Cahill et al. only quote the results in their paper [CCG76].[7] We can re-write the trace formula (4.67) in the following way

$$\delta m = -\frac{1}{4}\sum_n \int_{-\infty}^{\infty} dk \; |\eta_{K,n}(x)\eta_{V,k}(x)|^2 \; \left[\omega_n^2\omega_k^{-1} - 2\omega_n + \omega_k\right] \tag{4.68}$$

which reduces for the special case of the zero mode mass correction to

$$\delta m_0 = -\frac{1}{4}\int_{-\infty}^{\infty} dk \; |\eta_{K,0}(x)\eta_{V,k}(x)|^2 \; \omega_k \tag{4.69}$$

where $\eta_{K,n}$ are the eigenmodes of the kink and $\eta_{V,k}$ the eigenmodes of the vacuum. Finding the appropriate Fourier transform is the main technical difficulty in solving these kinds of integrals. We have used the Maple library *inttrans* to find Fourier exponential, cos and sin transforms and the book on integral tables by Erdelyi et al. [EMOT54].

4.4.1 ϕ^4 kink model

We have seen that the ϕ^4-kink has two discrete modes (4.24). The zero mode

$$\eta_{K,0}(x) = \sqrt{\frac{3m}{4\sqrt{2}}}\cosh^{-2}\left(\frac{mx}{\sqrt{2}}\right) \tag{4.70}$$

with $\omega_{K,0}^2 = 0$ and the second discrete mode

$$\eta_{K,1}(x) = \sqrt{\frac{3m}{2\sqrt{2}}}\sinh\left(\frac{mx}{\sqrt{2}}\right)\cosh^{-2}\left(\frac{mx}{\sqrt{2}}\right) \tag{4.71}$$

[7] see also [Hol92] for explicit calculations

with $\omega_{K,1}^2 = \frac{3}{2}m^2$ are here given in their normalised form i.e. integration of the mode squared over x gives one. The normalised eigenmodes of the vacuum fluctuations are

$$\eta_{V,k}(x) = \frac{1}{\sqrt{2\pi}} e^{ikx} \tag{4.72}$$

with eigenvalues $\omega_{V,k} = k^2 + 2m^2$. Using (4.69), we obtain the following integral

$$\delta m = (\ldots) \int_{-\infty}^{\infty} dk \, \sqrt{k^2+2m^2} \left[\int dx \frac{e^{ikx}}{\cosh^2\left(\frac{mx}{\sqrt{2}}\right)} \right] \left[\int dy \frac{e^{-iky}}{\cosh^2\left(\frac{my}{\sqrt{2}}\right)} \right] \tag{4.73}$$

which we simplify to

$$\begin{aligned} \delta m_0 &= (\ldots) \int_{-\infty}^{\infty} dk \, \sqrt{k^2+2m^2} \left[\int_0^{\infty} dx \frac{\cos(kx)}{\cosh^2\left(\frac{mx}{\sqrt{2}}\right)} \right]^2 = (\ldots) \int_{-\infty}^{\infty} dk \, \frac{\sqrt{k^2+2m^2}\, k^2}{\sinh^2\left(\frac{k\pi}{\sqrt{2}m}\right)} \\ &= -\frac{3m}{2\sqrt{2}\pi^3} \underbrace{\int_{-\infty}^{\infty} dq \, \frac{q^2\sqrt{q^2+\pi^2}}{\sinh^2 q}}_{I_0} \end{aligned} \tag{4.74}$$

where we have used Euler's formula, the Fourier cos transform of $\cosh^{-2}$ and changed to the variable $q \equiv \frac{k\pi}{\sqrt{2}m}$. Using (4.68), we obtain the correction to the mass from the second discrete mode

$$\begin{aligned} \delta m_1 &= (\ldots) \int_{-\infty}^{\infty} dk \left(\frac{3m^2}{2}(k^2+2m^2)^{-\frac{1}{2}} - 3m^2 + \sqrt{k^2+2m^2} \right) \left[\int_0^{\infty} dx \sin(kx) \frac{\sinh\left(\frac{mx}{\sqrt{2}}\right)}{\cosh^2\left(\frac{mx}{\sqrt{2}}\right)} \right]^2 \\ &= (\ldots) \int_{-\infty}^{\infty} dk \, (\ldots) \, \frac{k^2 \cosh^2\left(\frac{mx}{\sqrt{2}}\right)}{\left(1+\cosh^2\left(\frac{mx}{\sqrt{2}}\right)\right)} \\ &= -\left(\frac{1}{4}\right) \frac{3m}{2\sqrt{2}\pi^3} \underbrace{\int_{-\infty}^{\infty} dq \, \left(\frac{(\sqrt{q^2+4\pi} - \sqrt{3\pi^2})^2}{\sqrt{q^2+4\pi^2}} \right) \frac{q^2}{[1+\cosh q]^2}}_{I_1} \end{aligned} \tag{4.75}$$

where we have used Euler's formula, the Fourier sin transform of $\sinh\cosh^{-2}$ and changed to the variable $q \equiv \frac{k\pi}{\sqrt{2}m}$.

We have evaluated I_0 and I_1 numerically with Maple and obtain

$$I_0 = 11.247$$
$$\frac{1}{4}I_1 = 0.827$$

and the contributions to the mass correction are

$$\delta m_0 + \delta m_1 \;=\; (-0.384 - 0.0283)m \;=\; -0.413m \tag{4.76}$$

compared to the full quantum correction (4.54)

$$\delta m \;=\; -0.471m \tag{4.77}$$

where we have set $\hbar$ to one. Finally, we find that the zero mode contributes 81.5% and the second discrete mode 6%, thus in total 87.5%, to the total mass correction.

We are also interested to what value of k the normal modes of the vacuum fluctuations have to go to give a reliable answer to the mass correction. Intuitively, the zero and second discrete mode are localised and its norm with the long wavelength vacuum modes should become very small. We have put a cut-off Λ on our integral I_0 and $\frac{1}{4}I_1$ and evaluated the integrals as a function of the cut-off. We have done this numerically with Maple. Figure 4.1 shows that we only need to go up to a cut-off of around $q = 5$ for the zero mode and of around $q = 15$ for the second discrete mode. (k$\equiv \frac{\sqrt{2m}}{\pi}q$) This is good news, for we can ignore long wavelength vacuum modes.

4.4.2 Sine-Gordon model

We do the same for the Sine-Gordon model. There is only one discrete mode, the zero mode of translation: see section 4.2 and [Jac77]. The normalised zero mode has the form

$$\eta_{K,0}(x) = \sqrt{\frac{m}{2}}\cosh^{-1}(mx) \tag{4.78}$$

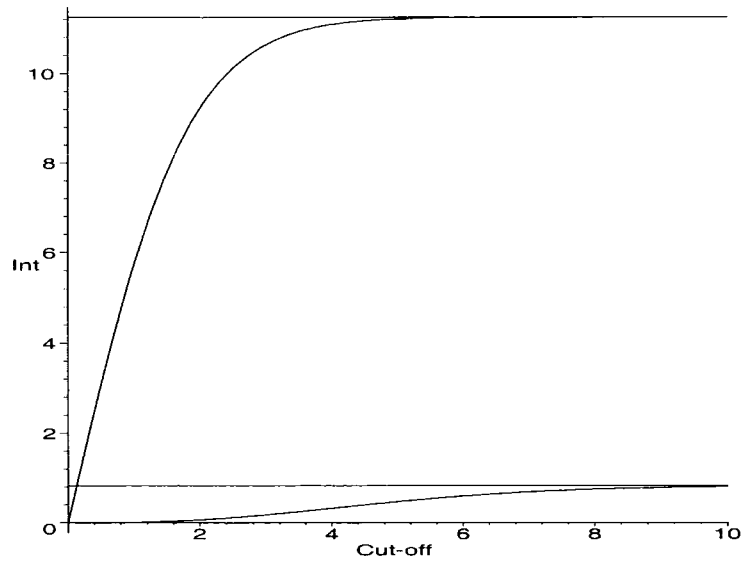

Figure 4.1: Value of I_0 (upper curve) and I_1 (lower curve) as a function of their cut-off Λ for q

with eigenvalue $\omega_{K,0} = 0$. The eigenmodes of the vacuum fluctuations are the same as before, but the eigenvalues change to $\omega_{V,k} = k^2 + m^2$. The mass correction takes the form

$$\begin{aligned} \delta m_0 &= (\ldots) \int dk \sqrt{k^2+m^2} \left[\int dx \cos(kx) \cosh^{-1}(mx) \right]^2 \\ &= (\ldots) \int dk \sqrt{k^2+m^2} \cosh^{-2}\left(\frac{\pi k}{2m}\right) \\ &= -\frac{m}{4\pi} \int dq \frac{\sqrt{q^2+\left(\frac{\pi}{2}\right)^2}}{\cosh^2 q} \end{aligned} \tag{4.79}$$

where we have used Euler's formula, the Fourier cos transform of $\cosh^{-1}$ and changed to the variable $q \equiv \frac{k\pi}{2m}$.

We have evaluated the integral numerically with Maple and obtain

$$\delta m_0 = -3.572\frac{m}{4\pi} = -0.893\,\frac{m}{\pi} = -0.284\,m \tag{4.80}$$

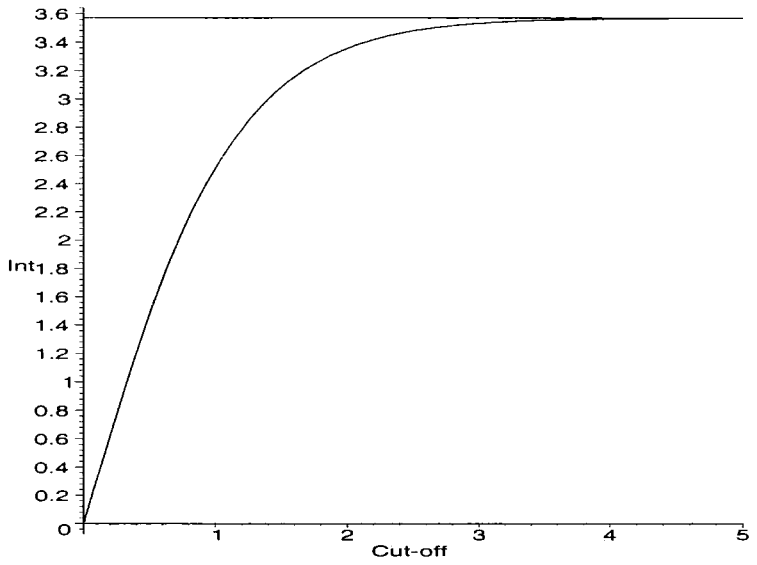

Figure 4.2: The value of the integral versus its cut-off Λ for q

compared to the full quantum correction ([DHN75], [Raj96])

$$\delta m = -\frac{m}{\pi} = -0.318\, m \tag{4.81}$$

where we have set $\hbar$ to one. Finally, we find that the zero mode contributes 89.3% to the total mass correction.

Again, we are interested to what value of k the normal modes of the vacuum fluctuations have to go to give a reliable answer to the mass correction. We have put a cut-off Λ on the integral and evaluated the integral as a function of the cut-off. We have done this numerically with Maple. Figure 4.2 shows that we only need to go up to a cut-off of around $q = 5$ for the zero mode. We do not need to include long wavelengths vacuum modes.

4.5 Trace formula: Numerical Result

In the last section, we have applied the trace formula to the ϕ^4 kink and the Sine-Gordon model. The results are clear-cut. The contribution from the discrete modes to the quantum mass correction is dominant (more than 80%). Further, we do not need to probe our discrete modes for long wavelength of the vacuum mode. This is good news for numerical methods and we can limit ourselves to the lowest normal modes of fluctuations in both the vacuum and the kink sector. Moreover, in (1+1) dimension, we are not restricted by memory or computational needs and can include all the vacuum and kink modes.

4.5.1 Preparation

We calculate the mass correction for the ϕ^4 kink and Sine-Gordon model. We have set the mass $m = 1$ and coupling $\lambda = 1$ for simplicity. The energy functional has the form

$$E = \int dx \left[\frac{1}{2}\dot{\phi}^2 + \frac{1}{2}\phi'^2 + \frac{1}{4}(\phi^2 - 1)^2\right] \tag{4.82}$$

for the ϕ^4 kink and

$$E = \int dx \left[\frac{1}{2}\dot{\phi}^2 + \frac{1}{2}\phi'^2 + (1 - \cos\phi)\right] \tag{4.83}$$

for the Sine-Gordon model; where $\phi' = \frac{d\phi}{dx}$ and $\dot{\phi} = \frac{d\phi}{dt}$. Using appropriate boundary conditions, we find the minimal-energy configuration, which we call ϕ_{st}, for both models in the topological charge sector one. We use the Gauss-Seidel overrelaxation method. Our box size is $L = 40$ from -20 to 20 and we use 1600 points. Thus, the lattice spacing is $dx = 0.025$.

The corresponding eigenvalue vacuum and kink operators in terms of the static solution (see 4.7) are

$$\begin{aligned} A_V^2 &= -\frac{d^2}{dx^2} + 2 \\ A_K^2 &= -\frac{d^2}{dx^2} + 1 - 3\phi_{st}^2 \end{aligned} \tag{4.84}$$

for the ϕ^4 kink and

$$\begin{aligned} A_V^2 &= -\frac{d^2}{dx^2} + 1 \\ A_K^2 &= -\frac{d^2}{dx^2} + \cos\phi_{st} \end{aligned} \tag{4.85}$$

for the Sine-Gordon model. In *Numerical Techniques*, we describe three different methods that solve the discrete eigenvalue problem. The trivial matrix diagonalisation is the more accurate and simplest one. However, we have to admit that the computational time grows as the cube of the number of points and the technique cannot be used in two or more dimensions. We substitute the value of the numerically minimised field[8] into the discretised eigenvalue equation and diagonalise the resulting matrix with periodic boundary conditions.

Figure 4.3 shows the first four normal modes of the ϕ^4 kink. The numerical eigenvalues are $-5.78\ 10^{-8}$, 1.49998, 2 and 2.03072 compared to the exact eigenvalues 0 (zero mode), 1.5 (first mode) and 2 (start of 'continuous' modes). Figure 4.4 shows the first four normal modes of the Sine-Gordon soliton. The numerical eigenvalues are $5.12\ 10^{-8}$, 1.00682, 1.00682 and 1.06128 compared to the exact eigenvalues 0 (zero mode) and 1 (start of 'continuous' modes).

4.5.2 Results

We have all the information needed to compute the mass correction. The trace formula has the form

$$\delta m = -\frac{1}{4}\sum_{n,k}\left(\sum_i \eta_{K,n}(x_i)\eta_{V,k}(x_i)\right)^2 \left[\omega_n^2\omega_k^{-1} - 2\omega_n + \omega_k\right] \tag{4.86}$$

which is similar to (4.68). $\eta_{K,n}(x_i)$ refers to the nth eigenmode of the kink, $\eta_{V,k}(x_i)$ refers to the kth eigenmode of the vacuum and x_i to the position of the ith lattice point.

We start with the ϕ^4 kink. We sum up the contributions to the mass correction, mode by mode. Figure 4.5 shows that the mass correction approaches an asymptotic limit. The first

[8] we used the relaxation method described in *Numerical Methods*

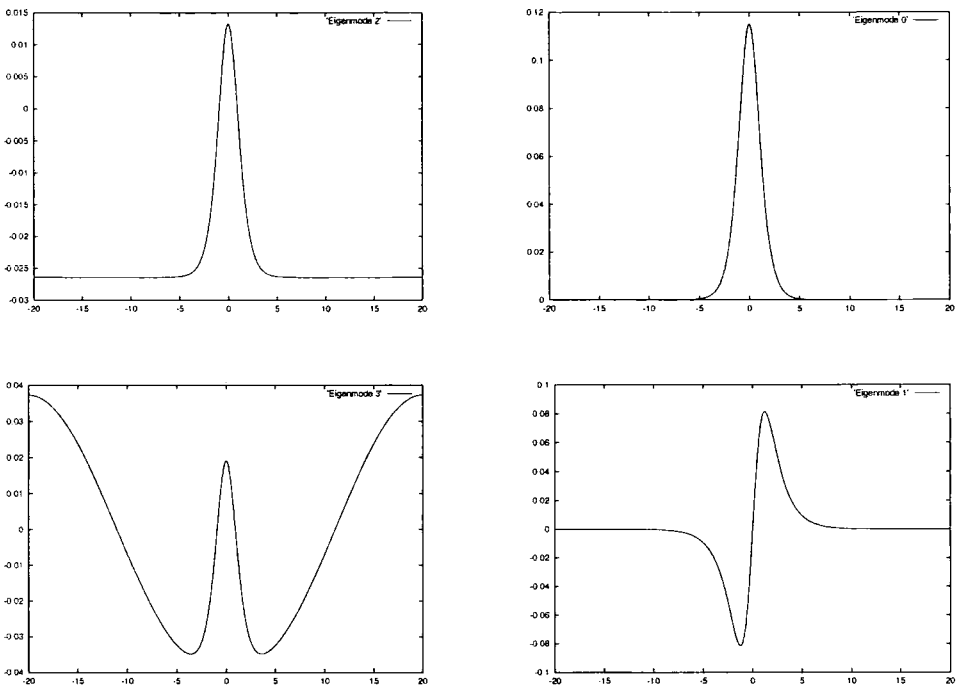

Figure 4.3: The ϕ^4 Kink eigenmodes from zero to three

few mode contributions are the most important ones. We only include mode contributions up to mode 200. Figure 4.6 shows that the norm is mostly zero and peaks for the norm between the nth kink mode and the nth vacuum mode. For the lowest kink mode contribution, only the lowest vacuum modes are important. For the highest kink mode contributions, only the highest vacuum modes are important. The discrete mode corrections are

$$\begin{aligned} \delta m_0 &= -0.384626 \\ \delta m_1 &= -0.0282964 \end{aligned} \tag{4.87}$$

which are very close to their exact values (4.76). The numerical value of the mass correction is

$$\delta m = -0.471097 \tag{4.88}$$

compared to the exact value of -0.471113 and is 99.997% accurate. This is a very satisfactory result.

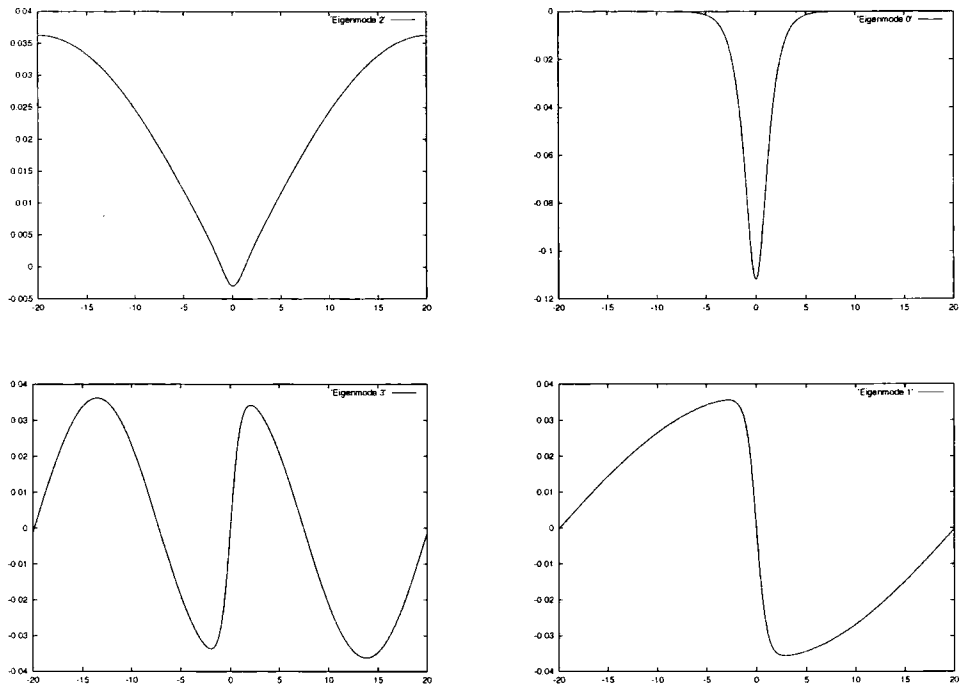

Figure 4.4: The Sine-Gordon eigenmodes from zero to three

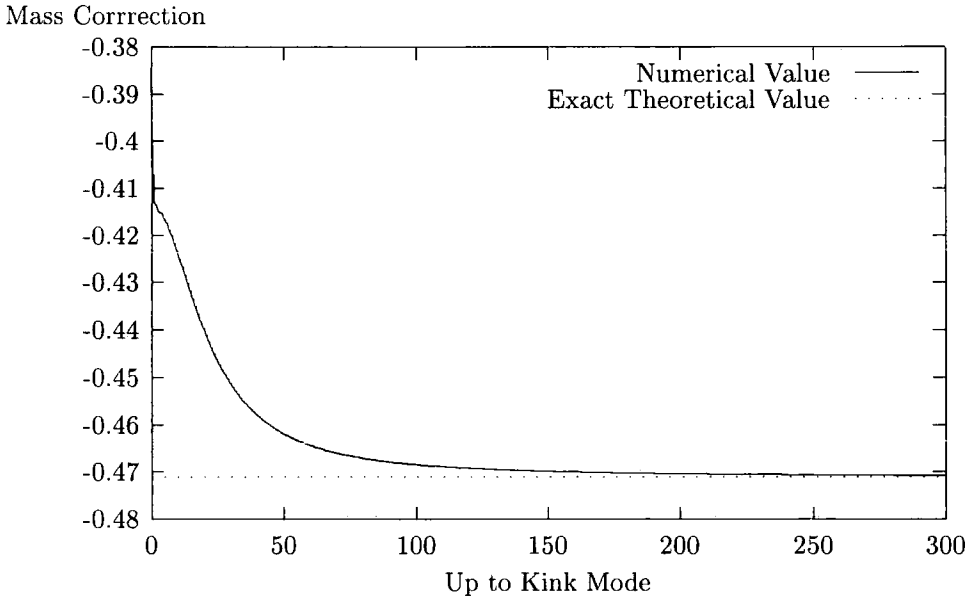

Figure 4.5: The total contribution to the mass correction mode by mode

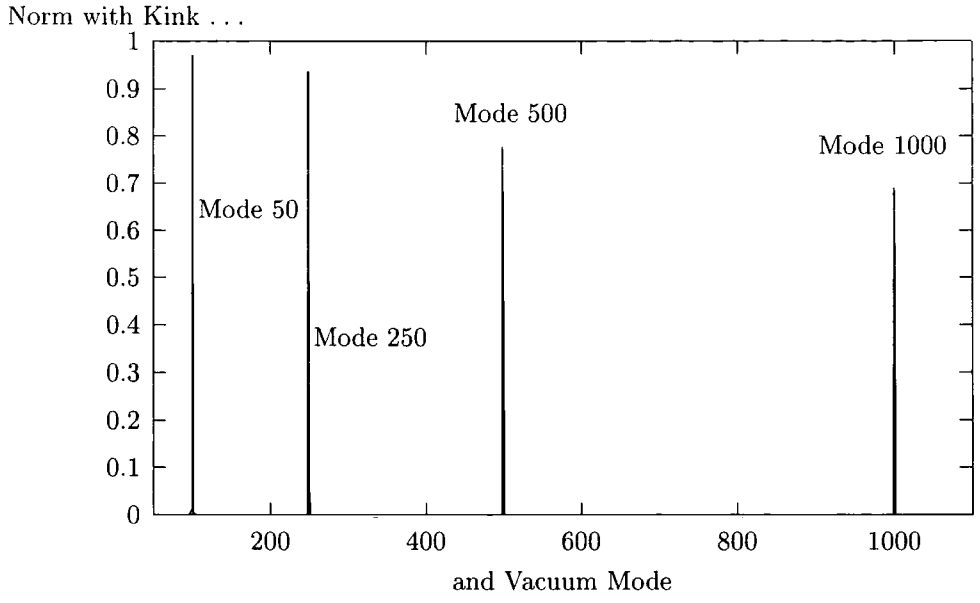

Figure 4.6: Norm between four kink modes and the vacuum modes

We turn our attention to the Sine-Gordon kink. We sum up the contributions to the mass correction mode by mode. Figure 4.7 shows that the mass correction approaches an asymptotic limit. The first few mode contributions are the most important ones. Figure 4.8 shows the contribution of the first mode for each vacuum mode. Note that some contributions are zero, because the first mode is an odd function and some of the vacuum modes are even functions. The discrete mode i.e. zero mode correction of the Sine-Gordon kink is

$$\delta m_0 = -0.28402 \tag{4.89}$$

which is very close to the exact value (4.80). The numerical value of the mass correction is

$$\delta m = -0.318144 \tag{4.90}$$

compared to the exact value of -0.318309 and is 99.95% accurate. This is a very satisfactory result.

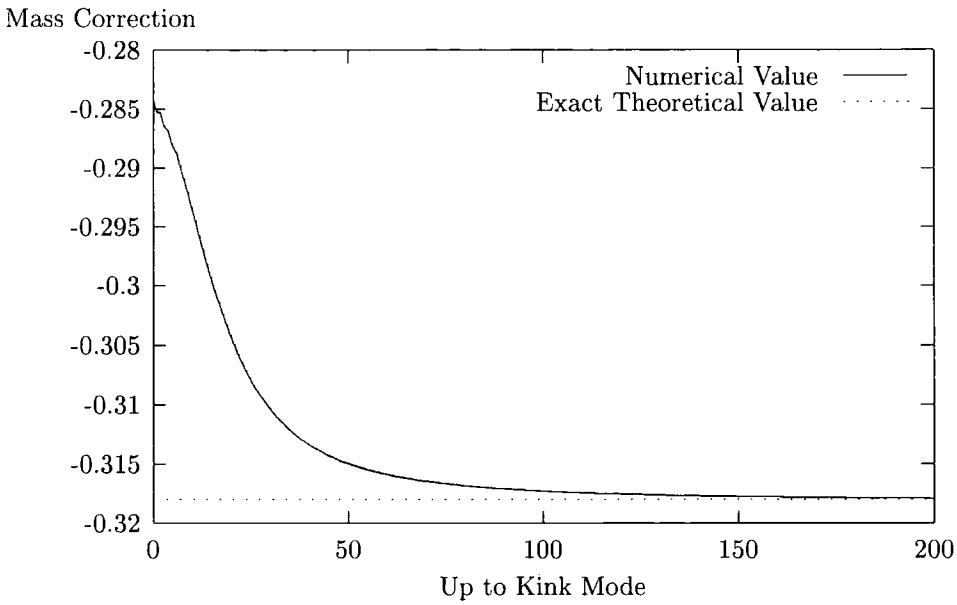

Figure 4.7: The total contribution to the mass correction mode by mode

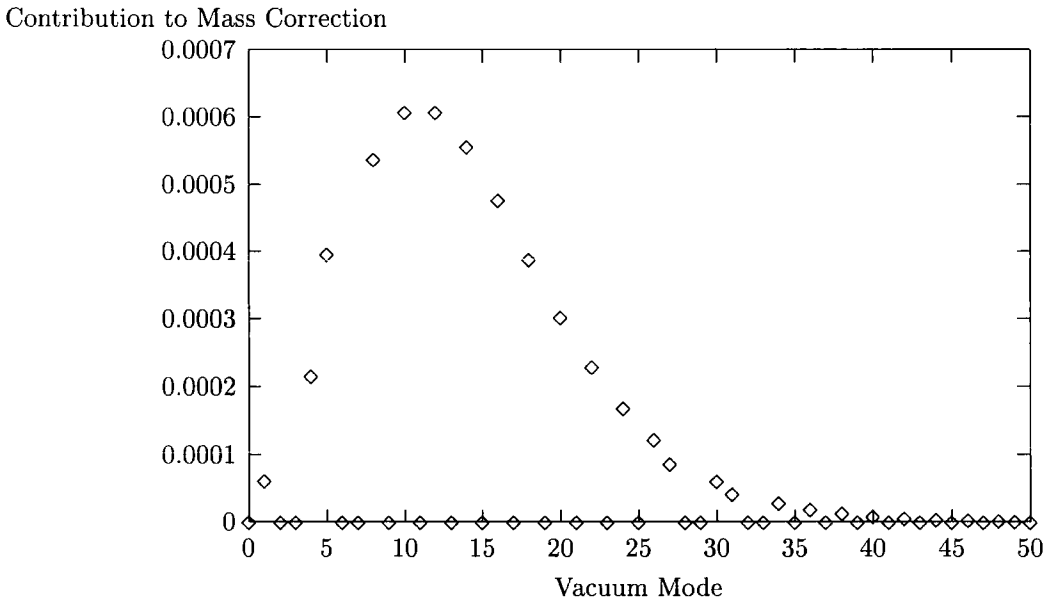

Figure 4.8: Mass correction of the first kink mode versus the vacuum modes

4.6 Conclusion

We have shown that the trace formula works very well in (1+1) dimensions for the Sine-Gordon and the ϕ^4 kink model. The numerical quantum mass correction is very close to the exact one. Our technique can be applied with ease to any (1+1) dimensional theory. This allows us to calculate the mass correction to *non-integrable* solitonic systems, for example. Specifically, we are interested in the Sine-Skyrme model [PPZ93] and plan to study the mass correction numerically. Or, we can look at the mass correction of multi-skyrmions, for example.

There are two drawbacks. We have used a brute force matrix diagonalisation to find the eigenvalues. It works very well and is reasonably fast in (1+1) dimensions. However, if you are to implement the trace formula in higher dimensions, you will have to use a different technique. Barnes and Turok in [BT97] have used a diffusion equation method; as discussed in the chapter on numerical methods. They compute the zero mode, then project it out of the initial configuration, get the next mode and so on. Only the first modes are accurate, because the errors are summing up. Computational restrictions also limit the calculations to the first few modes.

Chapter 5

Conclusion

> "We have found that where science has progressed the farthest, the mind has but regained from nature that which mind has put into nature. We have found a strange foot-print on the shores of the unknown. We have devised profound theories, one after another, to account for its origin. At last, we have succeeded in reconstructing the creature that made the foot-print. And Lo! It is our own."
> *(the English physicist Eddington)*

Firstly, we have clearly shown that numerical techniques can study classical and quantum aspects. The computer codes we had to produce and the methods we had to understand provide the author with all the essential tools to further investigate solitonic or other systems requiring numerical methods. In the future, much less time will be spent on preparing the grounds. Secondly, we were able to confirm previous work by Piette et al. on multi-skyrmions and show the variety of multi-skyrmion structure in different baby Skyrme models. We succeeded in computing the quantum mass corrections of (1+1) dimensional models numerically by using a trace formula. We also implemented the Simulated Annealing scheme to solitonic systems and show that it handles higher order terms better. Thirdly, our work triggered new research ideas

which we intend to pursue. We list the most interesting ones:

- to implement the Simulated Annealing scheme for 2 dimensions. This would allow us to systematically look at multi-skyrmion structure for different potentials and for higher order terms. It is hard to see how the conventional approach could study higher order terms.
- to do the same in 3 dimensions if possible.
- to study the scattering behaviour in the baby Skyrme model with a six-derivatives term. The equation of motion will be extensive, but probably just manageable.
- to study the mass correction for different theories. Especially the Sine-Skyrme model, a 1-dimensional analogue to the baby Skyrme model, would be an interesting starting point. We also intend to look at the mass correction of the multi-skyrmions in (1+1) dimensional models.
- to apply the trace formula to the baby Skyrme models.
- to look at the baby Skyrme models with potentials with more than one vacuum and see if their multi-skyrmions are all radially symmetric.

Final Thoughts

We have studied classical and quantum properties of solitons. The baby Skyrme models are not integrable and no exact solutions are known in general. We could only achieve this study by using numerical methods. Our approach is symptomatic for the increased use of computers in extracting valuable information from theories untrackable by mathematical tools. Lattice QCD, structure formation and black hole simulations are further examples. Certainly, the

exponential increase of CPU power and its decrease in price will further enhance this approach and 'numerical experiments' will become a well established area between 'real' experiments and pure theory.

Physicists have two ways of thinking about physical systems; in terms of waves or particles. Solitons combine both fundamental concepts and are waves with particle behaviour. This new concept is exciting and very appealing to theorists in all domains – a new tool to use. Promising research in real industrial applications is underway in the area of telecommunication and DNA, for example. On the fundamental level, solitons have been discovered in quantum field theory, too. Monopoles, instantons and skyrmions are now well established and if physical intuition 'What can happen, will happen' is valid, experimental verification will follow. Solitons also play an important role in the most likely TOE, M-theory in 11 dimensions: see Duff's review [Duf98, section 8]. Briefly, the Olive-Montonen conjecture suggests a duality between elementary particles carrying Noether charges and solitons carrying a topological charge. If you interchange the particles/solitons and invert their coupling, the theory gives the same predictions. This idea later led to the emergence of S-duality which plays a crucial role in linking the five string theories together. M-theory is compactified by hand down to the 4 dimensional standard model. A sensible compactification scheme must arise from the M-theory lagrangian itself. Solitons could play this role. Actually, some researchers believe that a newly found object in string-M theory, a Dirichlet brane (D-brane) which can be viewed as a soliton with extra degrees of freedom, could take over the compactification role. We can even think of dynamical compactification in the baby Skyrme model in (2+1) dimensions as a very simple toy model! We start out with a high temperature configuration of topological charge one. This is our early universe with many fluctuations of skyrmion and anti-skyrmion pairs–the dynamics is two-dimensional. We cool the configuration and it will eventually condensate to a 1-skyrmion. Now, the dynamics of the field is effectively described by an 1-dimensional field theory of the

1-skyrmion. Or we think of a high-temperature new Baby Skyrme configuration with charge five. Cooling reduces the dynamics to a one-dimensional ring: see figure 3.9.

The author is in no doubt that solitons will play an increasingly important role in industrial application and fundamental physics.

Bibliography

[AC91] M J Ablowitz and P A Clarkson. *Solitons, Nonlinear Evolution Equations and Inverse Scattering.* Cambridge University Press, 1991.

[Ame77] W Ames. *Numerical Methods for Partial Differential Equations.* Acadamic Press, 1977.

[ANW83] G Adkins, C Nappi, and E Witten. Static properties of nucleons in the skyrme model. *Nuclear Physics B*, 228:552–566, 1983.

[Bar98] C Barnes. *PhD Thesis.* PhD thesis, Princeton, 1998.

[Bas97] K Baskerville. Normal modes of the $b = 7$ skyrme soliton. *hep-th/9704012*, 1997.

[BBT97a] C Barnes, K Baskerville, and N Turok. Normal mode spectrum of the deuteron in the skyrme model. *Physics Letters*, B411:180–186, 1997.

[BBT97b] C Barnes, K Baskerville, and N Turok. Normal modes of the $b = 4$ skyrme soliton. *Physics Review Letters*, 79:367–370, 1997.

[BFR78] R L Burden, J D Faires, and A C Reynolds. *Numerical Analysis.* PWS Publisher, 1978.

[Bow] P Bowcock. Integrable solitons. Lecture Notes, University of Durham.

[Boy89] J P Boyd. *Chebyshev & Fourier Spectral Methods.* Springer verlag, 1989.

[BS97] R A Battye and P M Sutcliffe. Symmetric skyrmions. *Physical Review Letters B*, 79:363–366, 1997.

[BT97] C Barnes and N Turok. A technique for calculating quantum corrections to solitons. *hep-th/9711071*, 1997.

[BTC90] E Braaten, S Townend, and L Carson. Novel structure os static multi-soliton solutions in the skyrme model. *Physics Letters B*, B(235):147–152, 1990.

[CCG76] K Cahill, A Comtet, and R J Glauber. Mass formulas for static solutions. *Physics Letters*, 64B(3):283–285, September 1976.

[DHN75] R F Dashen, B Hasslacher, and A Neveu. Particle spectrum in model field theory from semiclassical functional integral techniques. *Physical Review D*, 11(12):3424–3450, June 1975.

[DJ96] P G Drazin and R S Johnson. *Solitons: an introduction.* Cambridge University Press, 1996.

[Duf98] M Duff. A laymen's guide to m-theory. *hep-th/9805177*, 1998.

[EMOT54] Erdélyi, Magnus, Oberhettinger, and Tricomi. *Tables of Integral Transforms.* McGraw-Hill, 1954.

[FPU55] E Fermi, J R Pasta, and S M Ulam. Studies of nonlinear problems. *Los Alamos Sci., Lib. Rep.*, LA-1940, 1955.

[Hol92] G Holzwarth. Quantum correction to nucleon and delta mass in the skyrme model. *Physics Letters B*, 291:218–222, 1992.

[HS86] G Holzwarth and B Schwesinger. Baryons in the skyrme model. *Rep. Prog. Phys.*, 49:825–871, 1986.

[HW99] G Holzwarth and H Walliser. The casimir energy of skyrmions in the 2+1-dimensional o(3)-model. *hep-ph/9907492*, 1999.

[Irv98] P Irvine. Zero mode quantizaton of multi-skyrmions. *hep-th/9804142*, 1998.

[Jac77] R Jackiw. Quantum meaning of classical field theory. *Reviews of Modern Physics*, 49(3):681–706, July 1977.

[JJGB85] A Jackson, A D Jackson, A S Goldhaber, and G E Brown. A modified skyrmion. *Physics Letters B*, 154:101–106, April 1985.

[KPZ98] A Kudryavtsev, B M A G Piette, and W J Zakrzewski. Skyrmions and domain walls in (2+1) dimensions. *Nonlinearity*, 11:783–795, 1998.

[LMS95] R A Leese, N S Manton, and B J Schoers. Attractive channel skyrmions and the deuteron. *Nuclear Physics*, B442:228–267, 1995.

[LPZ90] R A Leese, M Peyrard, and W J Zakrzewski. Soliton scattering in some relativistic models in (2+1) dimensions. *Nonlinearity*, 3:773–807, 1990.

[Mar90] L Marleau. The skyrme model and higher order terms. *Physics Letters B*, 235(1,2):141–146, January 1990.

[MGK68] R M Miura, C S Gardner, and M D Kruskal. Korteweg-devries equations and generalizations. ii. existence of conservation laws and constants of motion. *J. Math. Phys.*, 9:1204–1209, 1968.

[Miu68] R M Miura. Korteweg-devries equations and generalizations i. a remarkable explicit non-linear transformation. *J. Math. Phys.*, 9:1202–1204, 1968.

[MRS93] V G Makhankov, Y P Rubakov, and V I Sanyuk. *The Skyrme Model.* Springer Verlag, 1993.

[Pie96] B M A G Piette. Ordinary and partial differential equations. Lectures notes given at Bharathidasan University, 1996.

[PMKTZ94] B M A G Piette, H J W Mueller-Kirsten, D H Tchrakian, and W J Zakrzewski. A modified mottola-wipf model with sphaleron and instanton fields. *Phys. Lett. B*, 320:294–298, 1994.

[PPZ93] M Peyrard, B Piette, and W Zakrzewski. Soliton like behaviour in a modified sine-gordon model. *Physica D*, 64:335–364, 1993.

[PS62] J K Perring and T H R Skyrme. A model unified field equation. *Nucl. Phys.*, page 550, 1962.

[PSZ95a] B M A G Piette, B J Schoers, and W J Zakrzewski. Dynamics of baby skyrmions. *Nuclear Physics B*, 439:205–235, 1995.

[PSZ95b] B M A G Piette, B J Schoers, and W J Zakrzewski. Multisolitons in two-dimensional skyrme model. *Z. Phys. C*, 65:165–174, 1995.

[PTVF92] W H Press, S A Teukolsky, W T Vetterling, and B P Flannery. *Numerical Recipes in C.* Cambridge University Press, 1992.

[PZ95] B M A G Piette and W J Zakrzewski. Skyrmion dynamics in (2+1) dimension. *Chaos, Solitons and Fractals*, 5:2495–2508, 1995.

[PZ98] B M A G Piette and W J Zakrzewski. Numerical integration of (2+1)d pdes for s^2 valued functions. *J. Comp. Phys.*, 145:359–381, 1998.

[Raj96] R Rajarman. *Solitons and Instantons.* North-Holland, 1996.

[RS84] C Rebbi and G Soliani. *Solitons and Particles.* World Scientific, 1984.

[Rus45] J Scott Russell. Report on waves. *Proc. of the British Association for the Advancement of Science, London*, page page 311, 1845.

[Ryd94] L H Ryder. *Quantum Field Theory.* Cambridge University Press, 1994. chapter 10.

[Sky61] T H R Skyrme. A nonlinear field theory. *Proc. Roy. Soc. A*, 260:127–138, 1961.

[Sut91] P Sutcliffe. The interaction of skyrme-like lumps in (2+1) dimensions. *Nonlinearity*, 4:1109–1121, 1991.

[tH73] G 't Hooft. A planar diagram theory for strong interaction. *Nuclear Physics B*, 72:461–473, 1973.

[tH74] G 't Hooft. A two-dimensional model for mesons. *Nuclear Physics B*, 75:461–470, 1974.

[vLA87] P J M van Laarhoven and E H L Aarts. *Simulated Annealing: Theory and Applications.* D. Reidel Publishing Company, 1987.

[Wal96] N Walet. Quantising the $b = 2$ and $b = 3$ skyrmion systems. *Nuclear Physics*, A606:429–458, 1996.

[Wit79] E Witten. Baryons in the 1/n expansion. *Nuclear Physics B*, 160:55–115, 1979.

[ZK65] N J Zabusky and M D Kruskal. Interaction of "solitons" in a collisionless plasma and the recurrence of initial states. *Phys. Rev. Lett.*, 15(6):240–243, August 1965.

Appendix A

This is the part of the software code used for the time-evolution of configuration in the holomorphic baby Skyrme model.

```
/* Caculate the free-indices expressions */

 for(j=0 ; j<3 ;j++)
 {
     fx[j]  =  (Field[RIGHT+j] - Field[LEFT+j])/(2*pde->dx);

     fy[j]  =  (Field[TOP+j] - Field[BOTTOM+j])/(2*pde->dy);

     fxt[j]  =  (Field[RIGHT+j+3] - Field[LEFT+j+3])/(2*pde->dx);

     fyt[j]  =  (Field[TOP+j+3] - Field[BOTTOM+j+3])/(2*pde->dy);

     fxy[j] =   ( Field[TOP_RIGHT+j] - Field[TOP_LEFT+j]
                -Field[BOTTOM_RIGHT+j] + Field[BOTTOM_LEFT+j] )
              /(4*pde->dx*pde->dy) ;

     fxx[j] =   ( Field[(RIGHT+j)] - 2*Field[j] + Field[(LEFT+j)] )
             / (4*pde->dx*pde->dx) ;

     fyy[j] =   ( Field[(TOP+j)] - 2*Field[j] + Field[(BOTTOM+j)] )
             / (4*pde->dy*pde->dy) ;

     Lapl[j] = (  4*(Field[LEFT+j] + Field[RIGHT+j] +
                     Field[TOP+j]  + Field[BOTTOM+j])
                +
                 ( Field[TOP_LEFT+j]    + Field[TOP_RIGHT+j] +
                  +Field[BOTTOM_LEFT+j] + Field[BOTTOM_RIGHT+j])
                -
                 20*Field[j]  )
               /
               (6*pde->dx*pde->dx);
 }
```

```
/* Calculate the summed-over-free-indices expressions */

xyaxa=0;xyaya=0;xxaya=0;yyaxa=0;
xaxa=0;yaya=0;xaya=0;
tata=0;xata=0;yata=0;
xtata=0;ytata=0;
xtaxa=0;ytaya=0;
xxata=0;yyata=0;
assa=0;ssata=0;

for(j=0;j<3;j++)
{
      xyaxa += fxy[j] * fx[j];
      xyaya += fxy[j] * fy[j];
      xxaya += fxx[j] * fy[j];
      yyaxa += fyy[j] * fx[j];

      xaxa += fx[j] * fx[j];
      yaya += fy[j] * fy[j];
      xaya += fx[j] * fy[j];

      tata += Field[3+j] * Field[3+j];
      xata += fx[j] * Field[3+j];
      yata += fy[j] * Field[3+j];

      xtata += fxt[j] * Field[3+j];
      ytata += fyt[j] * Field[3+j];

      xtaxa += fxt[j] * fx[j];
      ytaya += fyt[j] * fy[j];

      xxata += fxx[j] * Field[3+j];
      yyata += fyy[j] * Field[3+j];

      assa += Field[j] * Lapl[j];
      ssata += Lapl[j] * Field[3+j];
```

```
}

  /* calculate the scalar expressions */

  beta = 1 - 2 * theta1 * assa;

  det =  ( beta - 2*theta1*(fx[0]*fx[0]+fy[0]*fy[0]) )*
         ( beta - 2*theta1*(fx[1]*fx[1]+fy[1]*fy[1]) )*
         ( beta - 2*theta1*(fx[2]*fx[2]+fy[2]*fy[2]) )
        -
         4*theta1*theta1*
        (fx[1]*fx[2]+fy[1]*fy[2])*(fx[1]*fx[2]+fy[1]*fy[2])*
         ( beta - 2*theta1*(fx[0]*fx[0]+fy[0]*fy[0]) )
        -
         4*theta1*theta1*
        (fx[0]*fx[1]+fy[0]*fy[1])*(fx[0]*fx[1]+fy[0]*fy[1])*
         ( beta - 2*theta1*(fx[2]*fx[2]+fy[2]*fy[2]) )
        -
         4*theta1*theta1*
        (fx[0]*fx[2]+fy[0]*fy[2])*(fx[0]*fx[2]+fy[0]*fy[2])*
         ( beta - 2*theta1*(fx[1]*fx[1]+fy[1]*fy[1]) )
        -
         16*theta1*theta1*theta1*
        (fx[0]*fx[2]+fy[0]*fy[2])*(fx[0]*fx[1]+fy[0]*fy[1])*
        (fx[1]*fx[2]+fy[1]*fy[2]);


  M[0][0] = ( (fx[1]*fx[1]+fy[1]*fy[1]) * (fx[2]*fx[2]+fy[2]*fy[2]) )
           -( (fx[1]*fx[2]+fy[1]*fy[2]) * (fx[1]*fx[2]+fy[1]*fy[2]) );

  M[1][1] = ( (fx[0]*fx[0]+fy[0]*fy[0]) * (fx[2]*fx[2]+fy[2]*fy[2]) )
           -( (fx[0]*fx[2]+fy[0]*fy[2]) * (fx[0]*fx[2]+fy[0]*fy[2]) );

  M[2][2] = ( (fx[0]*fx[0]+fy[0]*fy[0]) * (fx[1]*fx[1]+fy[1]*fy[1]) )
           -( (fx[0]*fx[1]+fy[0]*fy[1]) * (fx[0]*fx[1]+fy[0]*fy[1]) );

  M[0][1] = ( (fx[1]*fx[2]+fy[1]*fy[2]) * (fx[0]*fx[2]+fy[0]*fy[2]) )
           -( (fx[0]*fx[1]+fy[0]*fy[1]) * (fx[2]*fx[2]+fy[2]*fy[2]) );
```

```
M[1][0] = M[0][1];

M[0][2] = ( (fx[0]*fx[1]+fy[0]*fy[1]) * (fx[1]*fx[2]+fy[1]*fy[2]) )
         -( (fx[0]*fx[2]+fy[0]*fy[2]) * (fx[1]*fx[1]+fy[1]*fy[1]) );

M[2][0] = M[0][2];

M[1][2] = ( (fx[0]*fx[1]+fy[0]*fy[1]) * (fx[0]*fx[2]+fy[0]*fy[2]) )
         -( (fx[0]*fx[0]+fy[0]*fy[0]) * (fx[1]*fx[2]+fy[1]*fy[2]) );

M[2][1] =  M[1][2];


/* Caculate the right-hand side (one free indice)  */

for(j=0;j<3;j++)
{
  term1[j] =  Lapl[j]
              +
              2 * theta1 *
              (
               -tata * Lapl[j]
              +
               fxx[j] * yaya
              +
               fyy[j] * xaxa
              -
               2 * fxy[j] * xaya
              +
               fx[j] * ( xyaya - yyaxa - xtata )
              +
               fy[j] * ( xyaxa - xxaya - ytata )
              +
               Field[3+j] * (  ssata
                             - xtaxa - ytaya )
              +
               2 * fxt[j] * xata
```

```
                +
                 2 * fyt[j] * yata
                )
              -
                 theta2 * (1+Field[2])*(1+Field[2])*(1+Field[2])
                  * (j-0)*(j-1);

    term2[j] =  Field[j]
              *
               ( -tata - assa
                +
                 2 * theta1 *
                 (  2*xaxa*yaya
                  - 2*xaya*xaya
                  + 2*assa* tata
                  + 2*xata*xata
                  + 2*yata*yata)
                +
                 2 * theta2 * (1+Field[2])*(1+Field[2])*(1+Field[2])
                   * Field[2]
               );
}


   /* multiply Matrix inverse with right-hand side */

   for(j=0;j<3;j++)
   {
     term3 =  beta*( term1[j] + term2[j] );

     for(i=0;i<3;i++)
     {
       term3 +=  beta*2*theta1*( fx[j] * fx[i] + fy[j] * fy[i] ) *term1[i];

       term3 +=  4*theta1*theta1*M[j][i] * (term1[i]+term2[i]);
     }

     Force[j+3] = term3/det ;
```

Appendix B

This is the computer code using the Simulated Annealing scheme to minimise one dimensional functionals. See chapter on numerical techniques for more details. We do not include the random number generator routine due to copyright reasons. The interested reader can consult Numerical Recipes [PTVF92]. It's important to use a good random generator ergo the standard C routines are not recommended. Their period of random numbers is very short, 32'767, and one Simulated Annealing run needs many ten thousand random numbers.

```
/*********************************************/
/* Minimisation of one-dimensional functional */
/* using the Simulated Annealing algorithm    */
/*                                            */
/* Version : July 1999 (Durham, CPT)          */
/* Authors : Mark Hale & Tom Weidig           */
/*********************************************/


/* include standard libraries */

#include <math.h>
#include <time.h>
#include <stdio.h>


/* define setup of program */

#ifndef __IBMC__
   #define _Inline static
#endif

#define PI 3.14159265358979

#define BABY 1
```

```
   #define OLD 1
   #define NEW 2
#define SINE_GORDON 2
#define SKYRME 3
#define HOSKYRME 4

#define MODEL      HOSKYRME          /* model */
#define SUB_MODEL  NEW               /* model sub-type */
#define N          401               /* number of points */
#define L          15.0              /* lattice length */
#define dr         L/(N-1)           /* lattice spacing */
#define T_INIT     1000.0            /* initial temperature */
#define THERMAL
#ifdef THERMAL
   #define K       1.0e-6            /* Boltzmann constant */
#endif
#define COOL_ITER  500               /* number of cooling iterations */
#define EQM_ITER   1000*N            /* number of thermal eqm iterations */

#define n          1                 /* topological charge */
#define theta_v    0.08873           /* potential coefficient */
#define theta_6    0.0               /* coefficient of higher order term */

/* function prototypes */

int main(int,char *[]);
_Inline double energyOfPoint(double [],const int);
_Inline double totalEnergy(double []);
_Inline double rCoord(const int);
_Inline void loadData(char *,double [],double []);
_Inline void saveData(double [],double [],const double);
_Inline double myRandom(long *);


/************************************************/
/* Main Program with Simulated Annealing Routine */
/************************************************/
```

```
int main(int argc,char *argv[]) {
   int i,j,pos;
   double func[N],energy[N],newEnergy[3];
   double deltaFunc,deltaEnergy,temp=T_INIT;
   int upSteps,downSteps,noSteps;          /* statistics */
   long idum=-time(NULL);                  /* random seed */


   /*** INITIAL CONDITIONS ***/

/* parse cmd line arguments */
   if(argc==2) {
      loadData(argv[1],func,energy);
   } else {
   /* initial function  */
      for(i=0;i<N-1;i++) {
         #if MODEL==BABY
            func[i]=PI*exp(-10.0*i*dr/L);
         #elif (MODEL==SKYRME || MODEL==HOSKYRME)
            func[i]=PI*exp(-10.0*i*dr/L);
         #elif MODEL==SINE_GORDON
            func[i]=2*PI*i*dr/L;
         #endif
      }
   /* boundary conditions */
      #if MODEL==BABY
         func[N-1]=0.0;
      #elif (MODEL==SKYRME || MODEL==HOSKYRME)
         func[N-1]=0.0;
      #elif MODEL==SINE_GORDON
         func[N-1]=2*PI;
      #endif
   /* initial energy */
      for(i=0;i<N;i++)
         energy[i]=energyOfPoint(func,i);
   }
```

```
/*** COOLING SCHEDULE ***/

for(i=0;i<COOL_ITER;i++) {
   do {
      upSteps=downSteps=noSteps=0;
      for(j=0;j<EQM_ITER;j++) {

      /* fluctuate */
         pos=(int)(myRandom(&idum)*(N-2))+1;
         /* deltaFunc=(2.0*myRandom(&idum)-1.0)*dr*temp/1000.0; */
            deltaFunc=(2.0*myRandom(&idum)-1.0)
                     *2*K*temp*10.0;
         func[pos]+=deltaFunc;
         newEnergy[0]=energyOfPoint(func,pos-1);
         newEnergy[1]=energyOfPoint(func,pos);
         newEnergy[2]=energyOfPoint(func,pos+1);

      /* Metropolis */
         deltaEnergy=energy[pos-1]+energy[pos]+energy[pos+1]
                     -newEnergy[0]-newEnergy[1]-newEnergy[2];
      #ifdef THERMAL
         if(deltaEnergy>0.0 || exp(deltaEnergy/(K*temp))>myRandom(&idum)) {
      #else
         if(deltaEnergy>0.0) {
      #endif
            if(deltaEnergy>0.0)
               downSteps++;
            else
               upSteps++;
            energy[pos-1]=newEnergy[0];
            energy[pos]=newEnergy[1];
            energy[pos+1]=newEnergy[2];
         } else {
            noSteps++;
            func[pos]-=deltaFunc;
         }
      }
```

```
   #ifdef THERMAL
      } while(upSteps<downSteps);
   #else
      } while(noSteps<downSteps);
   #endif
      temp*=((double)(COOL_ITER-i))/((double)COOL_ITER);
      saveData(func,energy,temp);
   }

   return 0;
}



/***********************************************/
/* Compute the energy density at lattice point */
/***********************************************/

double energyOfPoint(double f[],const int pos) {
   const double r=rCoord(pos);
   const double n_r=n/r;
   const double sinf=sin(f[pos]);
   double density,derivSqr;
   if(pos==0) {
      /* Calculate derivatives */
      derivSqr=(f[1]*f[1]+f[0]*f[0]-2.0*f[0]*f[1])/(dr*dr);
   } else if(pos==N-1) {
      derivSqr=(f[N-1]*f[N-1]+f[N-2]*f[N-2]-2.0*f[N-1]*f[N-2])/(dr*dr);
   } else {
   /* D^2 = average of <d>^2 and <d^2>
      Note: D^2 = <d>^2 = <d^2> when variance (<d^2>-<d>^2) = 0 */
      derivSqr=(3.0*(f[pos+1]*f[pos+1]+f[pos-1]*f[pos-1])
               -2.0*f[pos-1]*f[pos+1]-4.0*f[pos]*(f[pos-1]
               -f[pos]+f[pos+1]))/(8.0*dr*dr);
   }
   #if MODEL==BABY
      #if SUB_MODEL==OLD
         density=r*(derivSqr+sinf*sinf*(n_r*n_r*(1.0+derivSqr))
```

```
                +2.0*theta_v*(1.0-cos(f[pos])))/4.0;
      #elif SUB_MODEL==NEW
         density=r*(derivSqr+sinf*sinf*(n_r*n_r*(1.0+derivSqr)
                +2.0*theta_v))/4.0;
      #endif
   #elif MODEL==SKYRME
      density=PI*( derivSqr* (r*r/2+4*sinf*sinf)
                  +sinf*sinf+2*sinf*sinf*sinf*sinf/(r*r) );
   #elif MODEL==HOSKYRME
      density=PI*( derivSqr* (r*r/2+4*sinf*sinf
                        +theta_6*sinf*sinf*sinf*sinf/(r*r) )
                  +sinf*sinf+2*sinf*sinf*sinf*sinf/(r*r) );


   #elif MODEL==SINE_GORDON
      density=derivSqr/2.0 - (cos(f[pos])-1);
   #endif
   return density*dr;
}


/*************************/
/* Sum up energy density */
/*************************/

double totalEnergy(double e[]) {
   int i;
   double total=0.0;
   for(i=0;i<N;i++)
      total+=e[i];
   return total;
}


/*********************************/
/* Deals with singularity at r=0 */
/*********************************/
```

```
double rCoord(const int pos) {
   double r;
   if(pos==0)
      r=dr/N;
   else
      r=pos*dr;
   return r;
}


/*****************************/
/* Load Initial Configuration */
/*****************************/

void loadData(char *filename,double f[],double e[]) {
/* load binary data */
   FILE *fp=fopen(filename,"rb");
   fread(f,sizeof(double),N,fp);
   fread(e,sizeof(double),N,fp);
   fclose(fp);
}


/**********************/
/* saves data in file */
/**********************/

void saveData(double f[],double e[],double temp) {
   int i;
   FILE *fp;

/* save binary data */
   fp=fopen("_function.bin","wb");
   fwrite(f,sizeof(double),N,fp);
   fwrite(e,sizeof(double),N,fp);
   fclose(fp);

/* save text data */
```

```
   fp=fopen("_energy_func.dat","w");
   for(i=0;i<N;i++)
      fprintf(fp,"%f %f %f\n",rCoord(i),e[i],f[i]);
   fclose(fp);

/* save energy */
   fp=fopen("_tmp_energy.dat","a");
   fprintf(fp,"%f %f\n",temp,totalEnergy(e));
   fclose(fp);
}



/*********************************/
/* Generates random number [0,1] */
/* (copyright Numerical Recipes) */
/* standard C routine is useless */
/*********************************/

double myRandom(long *idum) {

SEE NUMERICAL RECIPES: routine ran2

}
```